Advances in Fuzzy Systems

Fuzzy Logic Applications in Control Theory and Systems Biology

Guest Editors: Sendren Sheng-Dong Xu, Hao Ying, Pablo Carbonell, Ching-Hung Lee, and Wei-Sheng Wu

Fuzzy Logic Applications in Control Theory and Systems Biology

Advances in Fuzzy Systems

Fuzzy Logic Applications in Control Theory and Systems Biology

Guest Editors: Sendren Sheng-Dong Xu, Hao Ying, Pablo Carbonell, Ching-Hung Lee, and Wei-Sheng Wu

Editorial Board

Contents

Hindawi Publishing Corporation
Advances in Fuzzy Systems
Volume 2013, Article ID 504728, 1 page
http://dx.doi.org/10.1155/2013/504728

Editorial
Fuzzy Logic Applications in Control Theory and Systems Biology

Sendren Sheng-Dong Xu,[1] Hao Ying,[2] Pablo Carbonell,[3] Ching-Hung Lee,[4] and Wei-Sheng Wu[5]

[1] *Graduate Institute of Automation and Control, National Taiwan University of Science and Technology, Taipei 10607, Taiwan*
[2] *Department of Electrical and Computer Engineering, Wayne State University, Detroit, MI 48202, USA*
[3] *University of Evry, iSSB, 91000 Evry, France*
[4] *Department of Mechanical Engineering, National Chung Hsing University, Taichung 402, Taiwan*
[5] *Department of Electrical Engineering, National Cheng Kung University, Tainan 701, Taiwan*

Correspondence should be addressed to Sendren Sheng-Dong Xu; sdxu@mail.ntust.edu.tw

Received 2 May 2013; Accepted 2 May 2013

Fuzzy logic has shown itself to be a powerful design and analysis methodology in control theory, enabling the implementation of advanced knowledge-based control strategies for complex dynamic systems such as those emerging applications for systems and synthetic biology. This special issue on advanced fuzzy logic applications compiles seven exciting manuscripts. Four of the manuscripts discuss the effectiveness in applying fuzzy logic to solving control issues. The other three papers discuss the fuzzy retractions, fuzzification, and the fuzzy application in transportation systems.

S. Simani proposes the application of a data-driven fuzzy control design to a wind turbine benchmark model. The author discusses the fuzzy modeling and identification and suggests a fuzzy control approach for the adjustment of both the wind turbine blade pitch angle and the generator torque. H. Benítez-Pérez, A. Benítez-Pérez, J. Ortega-Arjona, and O. Esquivel-Flores discuss a way to tackle multiple time delays that are bounded and the dynamic response from real-time scheduling approximation. D. Krokavec and A. Filasová explore the new conditions suitable for design of a stabilizing output controller for a class of continuous-time Takagi-Sugeno nonlinear systems. N. V. Kolesov discusses the fault diagnosis using fuzzy interacting observers. Three different models of faults are considered, including structural changes, faults in the signal space, and faults in the parameter space. A. Paz, P. Maheshwari, P. Kachroo, and S. Ahmad discuss the estimation of performance indices for the planning of sustainable transportation systems by fuzzy logic. A. E. El-Ahmady and A. S. Al-Luhaybi study new types of fuzzy retractions of fuzzy open flat Robertson-Walker space. Finally, H. V. Kumbhojkar discusses the fuzzification of prime ideals of hemirings. Minimum imperative for proper fuzzification is suggested.

By compiling these articles, we hope to enrich our readers and researchers with respect to these particularly relevant, yet usually highly treatable, fuzzy logic applications.

Sendren Sheng-Dong Xu
Hao Ying
Pablo Carbonell
Ching-Hung Lee
Wei-Sheng Wu

Hindawi Publishing Corporation
Advances in Fuzzy Systems
Volume 2013, Article ID 874393, 9 pages
http://dx.doi.org/10.1155/2013/874393

Research Article

Fault Diagnosis in Dynamic Systems Using Fuzzy Interacting Observers

N. V. Kolesov

Concern Central Scientific and Research Institute ELEKTROPRIBOR, JSC, State Research Center of the Russian Federation, 30 Malaya Posadskaya Street, Saint Petersburg 197046, Russia

Correspondence should be addressed to N. V. Kolesov; kolesovnv@mail.ru

Received 12 September 2012; Accepted 1 January 2013

Academic Editor: Sendren Sheng-Dong Xu

A method of fault diagnosis in dynamic systems based on a fuzzy approach is proposed. The new method possesses two basic specific features which distinguish it from the other known fuzzy methods based on the application of fuzzy logic and a bank of state observers. First, this method uses a bank of interacting observers instead of traditional independent observers. The second specific feature of the proposed method is the assumption that there is no strict boundary between the serviceable and disabled technical states of the system, which makes it possible to specify a decision making rule for fault diagnosis.

1. Introduction

A dynamic system model is widely used to describe technical systems in solving various problems of analysis and synthesis, including diagnosis, as applied to these systems. Although the literature on problems of diagnosis is abundant, the interest to them still persists and the investigations are continuing. The problems of how to increase accuracy, or diagnostic depth, and how to take into account different uncertainties that are inherent in the solution of diagnosis problems are conventionally central to the studies of fault diagnosis. It is to these problems that this paper is devoted, wherein the technical states of the system are assumed uncertain.

In the literature, the diagnosis problem is considered in different formulations, depending primarily on the models used to describe a system: deterministic [1–8], stochastic [9, 10], fuzzy [11–13], and so forth. The choice of a formulation is determined, as a rule, by the application and the problem to be solved by the dynamic system, as well as a priori information on the properties of the system and its possible faults available to developers of diagnostic tools. Thus, if a developer possesses statistical information on the system behavior and faults, it makes sense to use the stochastic approach. If such information is unavailable, the deterministic approach is preferential because in this case, information on uncertainties is minimal. The fuzzy approach complements the tools of the deterministic approach with the rules of analysis and fault decision making based on fuzzy logic. These rules formalize the empirical knowledge of the developer about the nominal and anomalous (in the case of faults) behavior of a system and uncertainties inherent in this problem by introducing fuzzy sets. Of course, there is a certain analogy between the methods that belong to different approaches. It is a consequence of mutual penetration and enrichment of the existing approaches. In this sense, the material presented later is not an exception.

Each of the afore mentioned approaches fits different lines of investigations. Among the most efficient of them is the one that relies on the models of the diagnosed system for synthesis of diagnostic tools. This line is developed in the framework of all approaches and is realized by application of either single state observers [3–5] (stochastic approach—Kalman and Wiener filters [9, 10]) or output observers [2, 3], or their sets (banks) [7–13] as parts of diagnostic tools. If we use banks, each of the observers O_i (Figure 1) is adjusted to one of the technical states of the system (serviceable $S_0 - O_0$, disabled S_1 with the first fault O_1, disabled S_2 with the second fault O_2, etc.). In the general case, vector residuals (difference signals) $\nu_0, \nu_1, \ldots, \nu_N$ between the real output of the dynamic system and the output of each of the observers are formed,

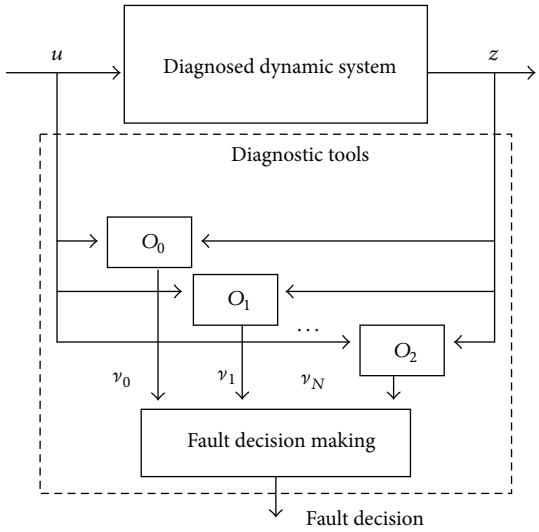

Figure 1: Structure of the diagnostic system.

which is followed by a decision making on the technical state of the diagnosed system.

In this study, we propose a method for diagnosing dynamic systems in the framework of a fuzzy approach. The new method possesses two basic specific features which distinguish it from the other known fuzzy methods based on the application of fuzzy logic and a bank of state observers. First, unlike the approaches in which observers are independent of each other, in this method, we consider a bank of interacting observers. The second specific feature of the proposed method is an assumption that there is no strict boundary between the serviceable and disabled technical states of the system and its elements, which makes it possible to specify a decision making rule for fault diagnosis.

2. Preliminary Definitions and Remarks

First of all, let us discuss the notion of a "fuzzy" technical state and, as a consequence, "fuzzy" fault, which is understood as a transition from the serviceable technical state to the disabled one. The notion of a fuzzy technical state used later seems to be quite adequate to describe the existing engineering approach. Indeed, judging from the value of the parameter which indicates the technical state of an object, an engineer can conclude that the object is either serviceable or disabled. Depending on a particular value of this parameter, the engineer can conclude that the object is serviceable or, correspondingly, disabled to a certain extent.

We define a *fuzzy technical state of an object* with respect to parameter Θ as a linguistic variable characterized, for example, by two terms (fuzzy sets)—serviceable and disabled technical states described by the corresponding membership functions μ_i^0 and μ_i^1.

Figure 2 illustrates the notions of "crisp" (a) and "fuzzy" (b) technical states of an object. In the first case, the domains of values of the key parameter Θ corresponding to the serviceable and disabled technical states of an object (denoted by rectangles of different colors) are separated by a strict boundary. In the second case, these domains intersect (shaded area), and they are determined by the corresponding membership functions with parameters a and b. As a result, for any value of $\Theta = \Theta'$, the technical state of the object can be related both with a fuzzy set of serviceable ($\mu_i^0 = 0.8$) and a fuzzy set of disabled ($\mu_i^1 = 0.3$) states. Note that in this paper, we only consider trapezoidal membership functions:

$$\mu_i^0 = \begin{cases} 1, & 0 \le \Theta_i \le a, \\ \dfrac{b - \Theta_i}{b - a}, & a \le \Theta_i \le b, \\ 0, & \text{otherwise}, \end{cases}$$
$$\mu_i^1 = \begin{cases} 0, & 0 \le \Theta_i \le a, \\ \dfrac{\Theta_i - a}{b - a}, & a \le \Theta_i \le b, \\ 1, & \text{otherwise}. \end{cases} \tag{1}$$

We should also make two more remarks concerning the problems touched upon in this paper. First, for simplicity, we assume that there are no perturbations in the considered model of the system. Second, we do not discuss the already known procedures of synthesis of stable observers [14].

3. Decision Making Rule on Fault Occurrence

The rule is based on the notion of the confidence coefficient K_i of the ith technical state introduced later. It requires that the confidence coefficient K_i should reach a specified level $A$for a technical state with the dominant value of this coefficient; that is, the following condition should be satisfied:

$$K^* = \max_i \{K_i\} \ge A. \tag{2}$$

Let us clarify the procedure of calculation of confidence coefficient. It is based on two groups of parameters that define the technical state of a dynamic system: the residuals ν_i, $i = \overline{0, N}$ obtained as a result of comparison of the system outputs with the outputs of the observers and the estimates $\widehat{\delta}_i$, $\widehat{\Delta}_i$, $i = \overline{0, N}$ of the levels of the faults in the diagnosis in the signal space and parameter space, respectively. It is assumed that the residual ν_i, $i = \overline{0, N}$ formed as a result of comparison of the system outputs with the ith observer can be represented by a linguistic variable, for example, with two terms, "small" and "large," for which the membership functions $\mu_{\nu_i}^0$ and $\mu_{\nu_i}^1$, $i = \overline{0, N}$ are defined. The term "small' corresponds to the situation in which the model used in the observer synthesis is adequate to the current technical state of the diagnosed system. The occurrence of a small, as it is, but nonzero value of this residual is due to the transient processes accompanying the estimation, the lack of complete adequacy of the model of the diagnosed system used for the observer synthesis, and neglected perturbations of its dynamics and output. The term "large" corresponds to the situation in which the model used in the observer synthesis is essentially inadequate to the current technical state of the diagnosed system. This is the case when, for example, a diagnosed system is in the ith

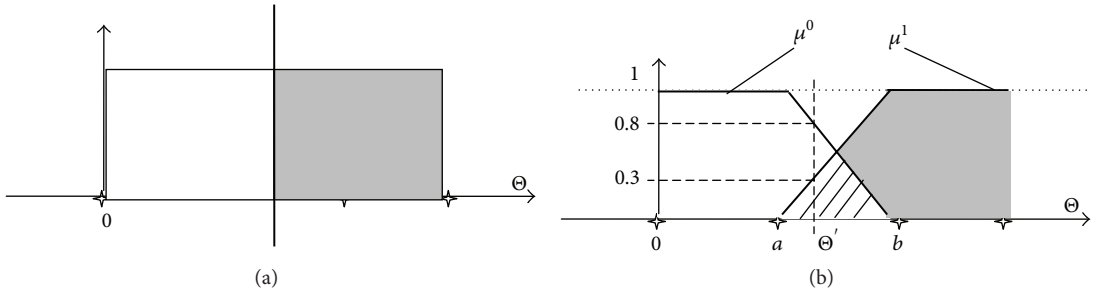

Figure 2: Illustration of the ideas of "crisp" and "fuzzy" technical states.

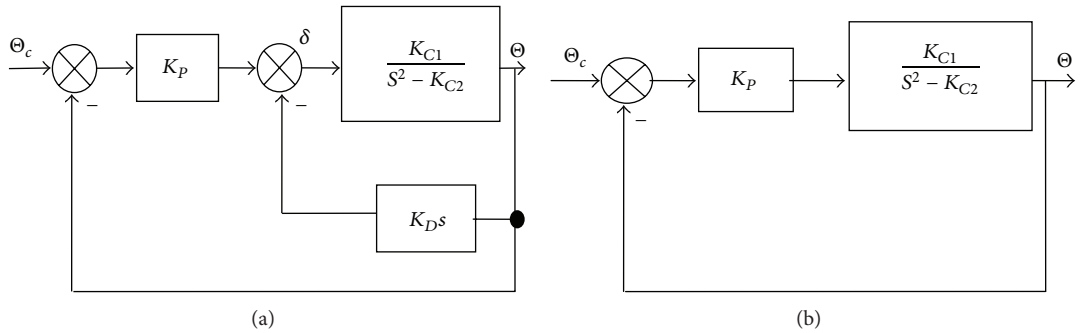

Figure 3: Structure of an attitude control system of a space launch vehicle (a) and an example of structural changes (b).

technical state, whereas the observer is adjusted for the jth technical state. In this case, parameters $\{a_i, b_i \mid i = \overline{0,N}\}$ of the membership functions are determined by the equalities:

$$a_i = \min_i \left\{\nu_i \mid S_j, j \neq i\right\}, \qquad b_i = \max_i \left\{\nu_i \mid S_j, j = i\right\}. \quad (3)$$

As for the variables $\widehat{\delta}_i$, $\widehat{\Delta}_i$, $i = \overline{0,N}$ simulating a fault, we also assume that they are described by linguistic variables with two terms, "serviceable" and "disabled," with the membership functions $\mu^0_{\widehat{\delta}_i}$ and $\mu^1_{\widehat{\delta}_i}$, $i = \overline{1,N}$, or $\mu^0_{\widehat{\Delta}_i}$ and $\mu^1_{\widehat{\Delta}_i}$, $i = \overline{1,N}$, respectively, specified for them.

In order to obtain the confidence coefficients $\{K_i \mid i = \overline{0,N}\}$, first, we determine the characteristics called generalized membership degrees $\{\widetilde{\mu}_i \mid i = \overline{0,N}\}$ of the technical state of the diagnosed system to each of the possible fuzzy technical states. These characteristics generalize the information on the technical state of the system with respect to all observers and are formed based on the set of values $\{\nu_i \mid i = \overline{0,N}\}$. The value of the generalized membership degree is formed in accordance with the following expression:

$$\widetilde{\mu}_i = \mu^0_{\nu_i} \mu^1_{\widehat{\delta}_i} \prod_{\substack{j=0 \\ j \neq i}}^{N} \mu^1_{\nu_j}. \quad (4)$$

The explanation of this expression is obvious. Indeed, the observer adequate to the technical state of the system forms a small residual, whereas the others form large residuals. This being so, we may say that a fault does exist if δ_i is large. We do not consider the situations including equivalent or poorly distinguishable faults.

Then, the confidence coefficient K_i for each technical state S_i is calculated in accordance with the rule of "weighting coefficients" by determining the contribution of the generalized membership degree $\widetilde{\mu}_i$ to the sum of these degrees for all states. Consider

$$K_i = \frac{\widetilde{\mu}_i}{\sum_{j=0}^{N} \widetilde{\mu}_j}. \quad (5)$$

4. Diagnosis of Structural Changes

In this paper, we consider successively three different models of fault: structural changes, faults in the signal space, and faults in the parameter space. In so doing, we study various structures of diagnostic tools different in the organization of the banks of the state observers and decision making rules. The proposed structures are compared with the known variant of diagnostic tools, which uses a bank of independent observers (Figure 1), and a decision is made as a result of fuzzy analysis of residuals. First, consider the diagnosis of structural changes. A structure of a system is very convenient to describe such faults. An example of a system structure is given in Figure 3(a). It is an attitude control system of a space launch vehicle (LV). The angular position Θ is adjusted by changing angle δ, which characterizes the inclination of the engines relative to the LV's axis. An example of structural changes is a break of the velocity feedback (Figure 3(b)).

From here on, the diagnosed dynamical system is described in the time domain (by differential or difference

equations); that is, for a linear system,

$$\dot{x}(t) = Fx(t) + Gu(t), \qquad y(t) = Hx(t), \tag{6}$$

while for a nonlinear system,

$$\dot{x}(t) = \varphi(x(t), u(t), \Theta), \qquad y(t) = Hx(t), \tag{7}$$

where x is an n-dimensional state vector, u is an m-dimensional input vector, y is a p-dimensional output vector, F is an $n \times n$ matrix of dynamic, G is an input $n \times m$ matrix, H is an output $p \times n$ matrix, φ is a function of dynamic, and Θ is a parameter vector.

The problem of synthesis of tools for fault diagnosis involves two main questions: formation of a rule for decision making and synthesis of a bank of observers. Assuming that the answer to the first question is given in the previous section, we proceed to the discussion of the second question.

Let us next study some variants of fault diagnosis that employ the banks of both independent and interacting observers. By this we mean the method used to form the system state vector estimate in each of the observers. If it is formed independently, we have independent observers and treat the obtained estimates as conditional with respect to a certain technical state. If the formation of the estimate also takes into account the estimates obtained in other observers, we have interacting observers. This chapter is referring to the independent observers.

Let us consider briefly the question of synthesis of a single observer. Observers may be synthesized by different rules, resulting from differences in the formulation of the problem. The procedure for the synthesis of a state observer for the linear system is known; however, for the sake of completeness, we will recall its main issues. As previously stated, each ith observer of the bank is adjusted to a technical state of the system, in which it is characterized by matrices F_i, G_i, H_i. The matrices F_i^*, G_i^*, H_i^* of the corresponding observer will be the same. The observer equations for diagnostics of the linear system have the form [14]

$$\begin{aligned} \dot{x}_i^*(t) &= F_i^* x_i^*(t) + G_i^* u(t) + L_i\left(y - y_i^*\right), \\ y_i^*(t) &= H_i^* x_i^*(t). \end{aligned} \tag{8}$$

As a result, an ith fault that occurs in the diagnosed system during operation leads to formation of an estimate of the system state vector in the observer. In this case, the behavior of the estimate error $e_i(t) = x_i(t) - x_i^*(t)$ is determined by the equation $\dot{e}_i = (F_i^* - L_i H_i^*)e_i$. It will suffice to determine the feedback matrix L_i to synthesize the observer. It is determined depending on the desired behavior of the estimation error. Undoubtedly, this error must tend to zero. Therefore, matrix $F_i^* - L_i H_i^*$ corresponding to each of the observers must be stable; that is, the real parts of its eigenvalues must take on negative values. For the case when the original system is linear, stationary, and observable, the selection algorithm of matrix L_i is known, and it is rather simple [14]. It uses the description of the diagnosed dynamical system in identification canonical form such that if the diagnosed system has one output, it is a single chain of integrators with feedback from the last integrator. Such system representation allows to find matrix L_i based on desired eigenvalues for the matrix $F_i^* - L_i H_i^*$. If the diagnosed system has many outputs, the procedure for determining the feedback matrix is complicated [14], although the sequence of steps is the same. In a similar way, first of all, we need to present the diagnosed system in the identification canonical form, which becomes more complicated. It contains not a single chain of integrators with feedback from the last integrator, but several—as many as there are outputs in the system.

To summarize this section, we formulate the algorithm for diagnosis of arbitrary faults in the formulation under consideration.

Algorithm 1.

(1) Formation of a list of faults.

(2) Synthesis of the independent observer for each of the faults.

(3) Assignment of membership functions for the considered fuzzy residuals based on the developer's empirical knowledge of the system operability.

(4) Decision making about faults by forming a confidence coefficient.

To illustrate the proposed algorithm, once again, we turn to the example in Figure 3.

Example 2. Let us synthesize the diagnosis tools for break of the velocity feedback. The nominal behavior of the system is described by the equation

$$\ddot{\Theta} - K_D K_{C1}\dot{\Theta} + \left(K_P + K_{C1} - K_{C2}\right)\Theta = K_P K_{C1}\Theta_c, \tag{9}$$

but in the case of fault, it is described as follows:

$$\ddot{\Theta} + \left(K_P + K_{C1} - K_{C2}\right)\Theta = K_P K_{C1}\Theta_c. \tag{10}$$

We analyzed an intermittent fault, when a device recovers after the failure and then fails again, in the Simulink environment using a sinusoidal input signal. In practice, faults of this type usually are a severe problem for diagnosis. Simulation results of a problem of diagnosis are shown in Figure 4, which presents time diagrams for the confidence coefficients formed with the use of a bank of two independent observers adjusted for nominal and faulty states, respectively. It is easy to see that the diagnosis tools show adequate results.

5. Diagnosis in Signal Space

In the case of diagnosis in the signal space, the fault is simulated as an additional term δ in the dynamics equation; that is, for an initial linear system, we have

$$\dot{x}(t) = Fx(t) + Gu(t) + \delta, \qquad y(t) = Hx(t), \tag{11}$$

and for a nonlinear system,

$$\dot{x}(t) = \varphi(x(t), u(t), \Theta) + \delta, \qquad y(t) = Hx(t), \tag{12}$$

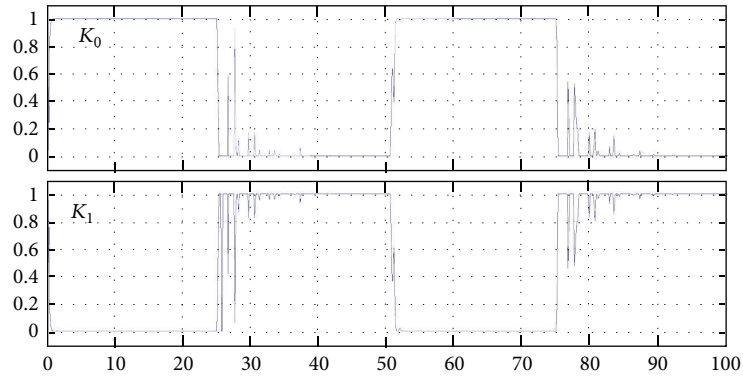

Figure 4: Time diagrams for confidence coefficients of technical states of an attitude control system of a space launch vehicle for independent observers.

where x is the n-dimensional state vector, u is the m-dimensional output vector, y is the p-dimensional output vector, F is the $n \times n$ dynamics matrix, G is the input $n \times m$ matrix, H is the output $p \times n$ matrix, φ is the dynamics function, and Θ is the parameter vector. In this case, the number of types N of single faults is equal to the dimension n of the state vector of the diagnosed system. The first type is simulated by an additional term in the first dynamics equation for the first component of vector x and the second type in the second equation for the corresponding component of vector x, and so forth. Faults within the same type are distinguished by the level of term δ.

In this case of diagnosis in the signal space, the state vector x_i^* of the observer O_i $(i = \overline{0, N})$ is formed by adding to the state vector x of the diagnosed system of the variable δ_i simulating fault; that is, $x_i^{*T} = [x^T \delta_i^T]$. Taking into account the assumption that variable δ_i is constant, the equation for this variable takes the form

$$\dot{\delta}_i = 0. \tag{13}$$

As a result, in the presence of the ith fault, the matrices of the diagnosed system take the forms

$$F_i = \begin{bmatrix} & & 0 \\ & F_0 & \cdots \\ & & 1 \\ & & \cdots \\ 0 \cdots 0 & & 0 \end{bmatrix}, \qquad G_i = \begin{bmatrix} G_0 \\ 0 \cdots 0 \end{bmatrix}, \tag{14}$$

$$H_i = \begin{bmatrix} & 0 & \\ H_0 & \cdots & \\ & 0 & \end{bmatrix},$$

where in the dynamics matrix, the unity in the last column is in the ith row. If the ith fault occurs in the diagnosed system in the course of its operation, the estimate of this compound vector is formed in the observer, as well as the estimate $\widehat{\delta}_i$ of the value of variable δ_i.

Let us discuss the proposed method for obtaining an estimate of the state vector of the system in each of the observers. Further, consider two diagnostic algorithms with the application of a bank of interacting observers. In so doing, we use the decision making rule on the fault occurrence described in the previous section. It will be shown later that in the general case, the efficiency of the considered algorithms is higher than that in the case of independent observers.

An important specific feature of the first algorithm is that on each successive step of the calculation, each of the observers is based on the estimate of state $\widehat{x}(t)$ obtained as a result of averaging of partial estimates of all the observers determined at the previous step rather than the independently formed partial estimate $\widehat{x}_i(t)$ of the state vector. Here, the current values of the confidence coefficients serve as weighting coefficients, where

$$\widehat{x}(t) = \sum_i K_i \widehat{x}_i(t). \tag{15}$$

The result of it is a nonlinear state feedback. Indeed, the residual (estimation error) formed by an adequate observer tends to zero, and the corresponding confidence coefficient increases with the decrease of confidence coefficients for other technical states. Thus, in expression (15), the relative weight of the estimate formed in an adequate observer increases.

The second algorithm, though being similar to the previous one, differs from it, first of all, in the fact that the observers are matched not with technical states but with the transitions between them. In this case, it is assumed that the observer is matched with the transition $S_i \rightarrow S_j$ if it is based on the state estimate obtained under condition S_i and was synthesized based on the model of the system in state S_j. In this case, transitions of $S_i \rightarrow S_i$ type, that is, the transitions that do not change the technical state, are also taken into account among the analyzed transitions. As a result, the confidence coefficients (denoted by K_{ij}) calculated in this algorithm according to the rule from the previous section correspond to

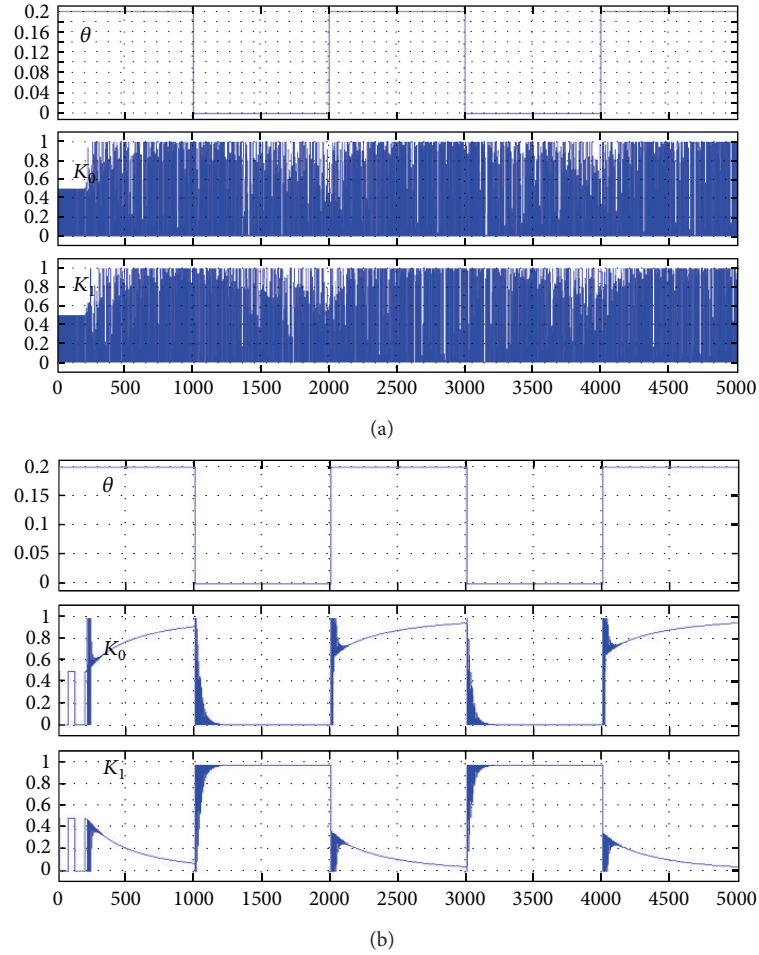

FIGURE 5: Time diagrams for alternating fault and confidence coefficients of technical states of the control system for (a) independent and (b) interacting observers.

the transitions $S_i \rightarrow S_j$ between technical states, rather than technical states themselves. This being so, at any step for each technical state S_j, we should form the conditional estimate $\widehat{x}_j(t)$ following the rule

$$\widehat{x}_j(t) = \sum_i K_{ij}\widehat{x}_{ij}(t). \tag{16}$$

In order to make a decision according to rule (2), we need to determine the confidence coefficients K_i, $(i = \overline{0, N})$ for the technical

$$K_i = \sum_{j=0}^{N} K_{ij}. \tag{17}$$

It is evident that the analysis of the behavior of the diagnosed system used in the second algorithm is more detailed, which is why we can expect this method to be more efficient. In the general case, this is proved by the simulation results given later.

Let us illustrate the described algorithms by a particular example.

Example 3. Let us consider the linear system characterized by the matrices

$$F = \begin{bmatrix} -0,0061 & 0,5122 & -0,0579 & 0,029 & 0,0377 \\ -0,5122 & -0,1868 & 0,6803 & -0,1417 & -0,2028 \\ -0,0579 & -0,6803 & -0,7645 & 0,7531 & 0,8508 \\ -0,29 & -0,1417 & -0,7531 & -0,3258 & -0,5974 \\ -0,0377 & -0,2028 & -0,8508 & -0,5974 & -1,242 \end{bmatrix},$$

$$G = \begin{bmatrix} 0,0452 \\ 0,2335 \\ 0,2779 \\ 0,09742 \\ 0,1329 \end{bmatrix},$$

$$H = \begin{bmatrix} 0,0452 & -0,2334 & 0,2779 & -0,09743 & -0,1329 \end{bmatrix}. \tag{18}$$

This system is a reduced model of an aircraft control loop at an altitude obtained by linearization of the aircraft motion equations in the neighborhood of the nominal trajectory. This description covers the controlled object, the rudder control servo drive, the altitude sensor, and the controller. For this example, the problem of diagnosis in the signal space was

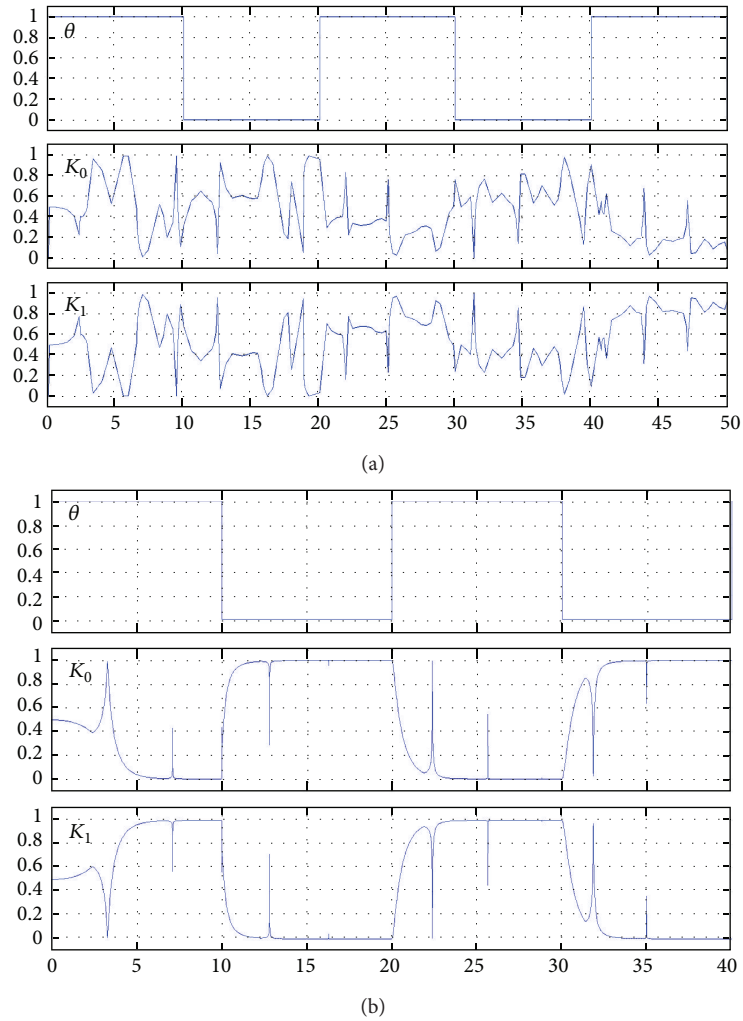

Figure 6: Time diagrams for alternating fault and confidence coefficients of technical states of a torpedo for (a) independent and (b) interacting observers.

simulated in Simulink. An intermittent fault θ in the form of a meander was simulated at the first integrator (first diagram in Figures 5(a) and 5(b)). A sinusoidal signal with amplitude of 0.5 was fed to the input of the system. Figure 5 shows the time diagrams of the obtained confidence coefficients for the cases of independent and interacting observers. It is clear that in the case of independent observers (Figure 5(a)), the diagnostic tools do not form the expected result, since before the fault occurs, coefficient K_0 should take a stable value close to unity, and coefficient K_1 a value close to zero. After the fault, the coefficient K_1 tends to the value close to unity, and K_0 to a value close to zero. When we use interacting observers (Figure 5(b)) matched with technical states, the time diagrams demonstrate an adequate operation of the diagnostic tools. Thus, on the time interval before a fault occurs, the confidence coefficient K_0 for a serviceable technical state after the transient process connected with the initial estimation takes a value equal to unity. After the fault, the corresponding confidence coefficient takes a stable value close to unity.

6. Diagnosis in Parameter Space

In the case of diagnosis in the parameter space, the fault is simulated as the deviation of the value of some system parameter from the nominal value. Thus, for example, for the linear system, it is simulated as the deviation of elements of the system matrices from the nominal, where

$$\dot{x}(t) = F(\Theta + \Delta\Theta)\, x(t) + G(\Theta + \Delta\Theta)\, u(t), \qquad y(t) = H(\Theta + \Delta\Theta)\, x(t), \tag{19}$$

and for the nonlinear system,

$$\dot{x}(t) = \varphi(x(t), u(t), \Theta + \Delta\Theta), \qquad y(t) = Hx(t). \tag{20}$$

In this case, the number of types N of single faults is equal to the number of system parameters.

Let us use the algorithms considered in the previous section in the diagnosis in the parameter space. Assume that the parameter Θ is a diagnosed parameter. Let us divide

the interval of the parameter values into l subintervals $\{\Theta_i + \Theta_{i+1} \mid i = \overline{1,l}\}$. Let us match the observer based on the system model for $\{\Theta_i \mid i = \overline{1,l}\}$ with each of the subintervals. We take into account that in this case, observers do not form the estimate of the fault value directly; however, it can be obtained according to the expression $\widehat{\Delta} = \Theta_{i^*} - \Theta_{\text{nom}}$, where $i^* = \arg\min_i \nu_i$, Θ_{nom} is the nominal value of the parameter Θ.

Let us analyze the efficiency of the diagnostic algorithms using the following example.

Example 4. Let us consider the model of a water torpedo described by the nonlinear equation

$$J\ddot{\varphi} + C_1\dot{\varphi} = -C_2C_3 \operatorname{sign}(\varphi), \qquad y = \varphi, \tag{21}$$

where J is the moment of inertia of the torpedo and φ is its angle of rotation. For this example, the problem of diagnosis of a single fault in the parameter space was simulated in Simulink using two algorithms, for independent observers and interacting observers matched with technical states. The intermittent fault in the form of the sequence of deviations of the parameter C_1 from the nominal value and returns to this value (first diagrams in Figures 6(a) and 6(b)) was simulated. The sinusoidal signal with an amplitude of 0.5 was fed to the input of the system. The second algorithm demonstrated the highest efficiency. Figure 6(b) shows the corresponding results of simulation (the confidence coefficients K_0 and K_1 for the serviceable and faulty technical states) of the diagnostic problem. It can be seen that, unlike the case of independent observers (Figure 6(a)), the diagnostic tools form the values of the confidence coefficients adequate to the real technical states. In order to quantitatively estimate the degree of adequacy of the results in both cases, the obtained realizations were used to calculate the probabilities of erroneous diagnosis. In this case, time intervals on which the system was faulty were analyzed. For these intervals, the total duration of subintervals on which erroneous signal on the serviceable state was formed (the confidence coefficient for the serviceable state reached the defined threshold value $A = 0.9$) was calculated. The resulting probability was determined as the ratio of this quantity and the total duration of the considered faulty intervals. Thus, for the method with independent observers, we obtained $P = 0.91$, and for the method with interacting observers, $P = 0.2$.

7. Conclusions

In this paper, we proposed the method of diagnosis of dynamic systems based on the application of the bank of fuzzy interacting state observers. We considered successively three different models of fault: structural changes, faults in the signal space, and faults in the parameter space. For these models of fault, we considered various structures of diagnostic tools different in the organization of the bank of the state observers and decision making rules. The proposed method was compared with the known method with independent observers by simulation in Simulink. As a result, it was demonstrated that the proposed method makes it possible to achieve higher quality of diagnosis.

Acknowledgment

This work was supported by the Russian Foundation for Basic Research, Project no. 10-08-00035a.

References

[1] R. J. Patton, P. M. Frank, and R. N. Clark, *Issues in Fault Diagnosis For Dynamic Systems*, Springer, London, UK, 2000.

[2] R. Isermann, "Model based fault detection and diagnosis-status and applications," in *Proceedings of the 16th IFAC Symposium on Automatic Control in Aerospace*, pp. 150–157, St. Petersburg, Russia, 2004.

[3] A. N. Zhirabok, "Robust observer design: logic-dynamic approach," in *Proceedings of the 7th IFAC Symposium on Fault Detection, Supervision and Safety of Technical Processes*, pp. 786–791, Barcelona, Spain, July 2009.

[4] M. Benini, M. Bonfè, P. Castaldi, W. Geri, and S. Simani, "Design and analysis of robust fault diagnosis schemes for a simulated aircraft model," *Journal of Control Science and Engineering*, vol. 2008, Article ID 274313, 18 pages, 2008.

[5] J. L. Mata-Machuca, R. Martinez-Guerra, and H. Aguilar-Sierra, "Fault estimation using a polynomial observer: a real-time application," in *Proceedings of the 8th IFAC Symposium on Fault Detection, Supervision and Safety of Technical Processes (SAFEPROCESS '12)*, pp. 552–557, Mexico City, Mexico, August 2012.

[6] O. Adrot and J. M. Flaus, "Fault detection based on uncertain switching models with bounded parameters," in *Proceedings of the 7th IFAC International Symposium on Fault Detection, Supervision and Safety of Technical Systems (SAFEPROCESS'09)*, pp. 774–779, Barcelona, Spain, July 2009.

[7] H. Rıos, C. Edwards, J. Davila, and L. Fridman, "Fault detection and isolation for nonlinear systems via HOSM multiple-observer," in *Proceedings of the 8th IFAC Symposium on Fault Detection, Supervision and Safety of Technical Processes (SAFEPROCESS '12)*, pp. 534–539, Mexico City, Mexico, August 2012.

[8] M. Muenchhof, "Multi-model based fault detection and diagnosis of a hydraulic servo axis," in *Proceedings of the 17th World Congress The International Federation of Automatic Control*, p. 13117, Seoul, Korea, July 2008.

[9] J. Davies, H. Tsunashima, R. M. Goodall, R. Dixon, and T. Steffen, "Fault detection in High Redundancy Actuation using an interacting multiple-model approach," in *Proceedings of the 7th IFAC International Symposium on Fault Detection, Supervision and Safety of Technical Systems (SAFEPROCESS'09)*, pp. 1228–1233, Barcelona, Spain, July 2009.

[10] S. P. Dmitriev, N. V. Kolesov, and A. V. Osipov, *Information Reliability, Control, and Diagnosis of Navigation Systems*, TSNII Elektropribor, Saint-Petersburg, Russia, 2003.

[11] J. M. Koscielny, "Application of fuzzy logic for fault isolation in a three tank system," in *Proceedings of the 14th World Congress International Federation of Automatic Control (IFAC '99)*, vol. 7, pp. 73–78, Beijing, China, 1999.

[12] L. F. Mendouca, J. M. Sousa, and J. M. G. Sida Cos, "Fault isolation using fuzzy model based observers," in *Proceedings of the 6th IFAC Symposium on Fault Detection*, pp. 142–150, Beijing, China, 2006.

[13] A. Akhenak, M. Chadli, J. Ragot, and D. Maquin, "Design of observers for Takagi-Sugeno fuzzy models for fault detection and isolation," in *Proceedings of the 7th IFAC International Symposium on Fault Detection, Supervision and Safety of Technical Systems (SAFEPROCESS'09)*, pp. 1109–1114, Barcelona, Spain, July 2009.

[14] Yu. N. Andreev, *Control of Finite Dimensional Linear Objects*, Nauka, Moscow, 1976.

Hindawi Publishing Corporation
Advances in Fuzzy Systems
Volume 2013, Article ID 601468, 13 pages
http://dx.doi.org/10.1155/2013/601468

Research Article

Estimation of Performance Indices for the Planning of Sustainable Transportation Systems

Alexander Paz,[1] Pankaj Maheshwari,[1] Pushkin Kachroo,[2,3] and Sajjad Ahmad[1]

[1] *Department of Civil and Environmental Engineering, University of Nevada, Las Vegas, NV 89154-4015, USA*
[2] *Transportation Research Center, Harry Reid Center for Environmental Studies, University of Nevada, Las Vegas, NV 89154-4007, USA*
[3] *Department of Electrical and Computer Engineering, University of Nevada, Las Vegas, NV 89154-4026, USA*

Correspondence should be addressed to Alexander Paz; apaz@unlv.edu

Received 15 September 2012; Revised 2 January 2013; Accepted 16 January 2013

Academic Editor: Ching-Hung Lee

In the context of sustainable transportation systems, previous studies have either focused only on the transportation system or have not used a methodology that enables the treatment of incomplete, vague, and qualitative information associated with the available data. This study proposes a system of systems (SOS) and a fuzzy logic modeling approach. The SOS includes the Transportation, Activity, and Environment systems. The fuzzy logic modeling approach enables the treatment of the vagueness associated with some of the relevant data. Performance Indices (PIs) are computed for each system using a number of performance measures. The PIs illustrate the aggregated performance of each system as well as the interactions among them. The proposed methodology also enables the estimation of a Composite Sustainability Index to summarize the aggregated performance of the overall SOS. Existing data was used to analyze sustainability in the entire United States. The results showed that the Transportation and Activity systems follow a positive trend, with similar periods of growth and contractions; in contrast, the environmental system follows a reverse pattern. The results are intuitive and are associated with a series of historic events, such as depressions in the economy as well as policy changes and regulations.

1. Introduction

1.1. Background. With the rapid increase in economic development throughout the world, there is stress on the resources used to support global economy, including petroleum, coal, silver, and water. Currently, the world is consuming energy at an unprecedented rate never seen before. Based on data from 2005, about 30.6 billion barrels of petroleum are used annually worldwide [1]. The estimates indicate that the availability of total world reserves is in the vicinity of 1.3 trillion barrels and will be depleted by 2047 [2]. The finite nature of such nonrenewable natural resources as petroleum and coal puts pressure on the environmental system and ultimately reduces the availability of resources for future generations. Hence, it is critical to develop planning and operational strategies that seek to achieve a sustainable use of existing natural resources.

The development of a sustainable system and its corresponding planning strategies requires an adequate definition of sustainability as well as mechanisms to quantify, qualify, and assess sustainability. The quantification of sustainability poses considerable challenges, ranging from data availability to adequate methods to process information. Numerous studies have established different measures to quantify sustainability [3]. According to Bell and Morse [4], sustainability primarily is measured by means of three components: (i) time scale, (ii) spatial scale, and (iii) system quality. The time and spatial scale corresponds to the analysis period and the geographical region of interest, respectively. On the other hand, system quality corresponds to the quantification of the overall system performance or state. In order to quantify system quality, Sustainability Indicators (SIs) have been developed in a diverse range of fields, including biology and the life sciences, hydrology, and transportation. Harger and Meyer [5] argued that SIs should be simple, diverse, sensitive, timely, quantifiable, and accessible. Bossel [6] proposed a system-based approach for developing 21 SIs for environmental

characteristics. The approach suggested that a system cannot exist independently, and several external factors can intrude on its boundaries. Some studies argue about the various dimensions associated with sustainability considerations [7, 8].

It is clear that a truly sustainable state for a system requires all the relevant interdependent subsystems/sectors and components, at levels so that the consumption of and the impact on the natural and economic resources do not deplete or destroy those resources. Hence, the assessment of a system state requires a holistic analysis in order to consider all the relevant sectors and impacts. However, existing approaches used to study the sustainability of a transportation system are not comprehensive enough to include key interactions with other systems such as the environment, the economy, and society in general. For example, the current planning of transportation systems is limited in terms of the number, accuracy, length, and approaches used to consider simultaneously important characteristics, including energy consumption, emissions, accidents, congestion, reliability, economic growth, and such social impacts as human health. That is, the existing practices only consider some effects, the estimations are approximate [9], and the analysis period is relatively short, in the order of 30 years [10]. In addition, these effects are synthetized only on the basis of approximated monetary considerations that are unlikely to capture the full extent of the effects, for instance, the financial cost of emissions or greenhouse gases [11, 12]. For example, Zheng et al. [3] described various system indicators by primarily considering economic aspects. Although the study provided valuable insights about the quantification of the economic domain of transportation sustainability, it is primarily focused on the transportation sector.

Among several studies that focused on different sectors, impacts, and aspects of sustainability, the following key characteristics have emerged as fundamental for a sustainable system:

(i) continuity through time [13, 14];

(ii) development of the needs of current generations without compromising the needs of future generations [15];

(iii) utilization of resources without compromising their health and productivity [16];

(iv) development that improves quality of life [17]; and

(v) assimilation of economic, ecological, social, and biophysical components of resource ecosystems [18, 19].

In terms of the methodologies available to estimate SIs, numerous studies have proposed different approaches. For example, Multi-criteria Decision Making (MCDM) and Analytical Hierarchy Process (AHP) techniques have been proposed to consider multiple criteria and estimate relevant SIs [20–26]. The MCDM approach selects or ranks different predetermined alternatives and is based on making discrete decisions [23]. Traditional MCDM techniques assume that the criteria are well-defined, certain (deterministic rather than stochastic), and independent. In reality, the criteria usually involve stochasticity and interdependence. In addition, some aspects in MCDM models are subjective in nature. The weights used in MCDM always include some uncertainty. The basic idea behind the AHP is to convert subjective assessments of relative importance to a set of overall weights or scores. The scale suggested by Saaty [27] is used to compute the weights, using linear algebra. These weights are the elements in the eigenvector associated with the maximum value of the matrix. The eigenvalue-based method has been criticized by researchers on the grounds of lack of prioritization and consistency [28]. In addition, there is an issue of rank reversal possibly arising when a new criteria is added. Due to the above reasons, the theoretical foundation of a rigid scale used in the methods is also questionable [29]. There have been attempts to address some of these limitations. The computation of the weights in MCDM and AHP requires significant amounts of data and a priori or expert knowledge of the system under study. Furthermore, different regions may require different weights to capture local conditions.

Given the complexities, interdependencies, nonlinearities, vagueness, and incomplete information associated with the various factors that are generally involved when considering the sustainability of a system, some studies have adopted concepts from fuzzy set theory for the development of SIs [30–32]. Awasthi et al. [33] applied a fuzzy Technique for Order Preference by Similarity to Ideal Situation approach, to evaluate the sustainability of transportation systems using partial or incomplete information. Opricovic and Tzeng [34] used a fuzzy multi-criteria model to evaluate post-earthquake land use planning. The modeling approach was developed to deal with qualitative or incomplete information. Mendoza and Prabhu [35] applied fuzzy logic for assessing criteria and indicators for sustainable forest management. In addition, linear aggregation techniques were used to combine multiple indicators. Liu [36] tried to integrate MCDM and fuzzy logic techniques to evaluate environmental sustainability. The environmental sustainability of 146 countries was calculated, ranked, and clustered. The study was extensive in dealing with multiple variables and indicators. However, only the environment aspects of sustainability were evaluated without considering any other SIs related to the transportation or activity system. Similarly, Prato [37] discussed a fuzzy logic approach for evaluating ecosystem sustainability. Data needs as well as the lack of technical expertise were important issues in this study. Marks et al. [38] used fuzzy logic techniques to develop a theoretical framework for the evaluation of sustainable agriculture. The study argued about the advantages of fuzzy logic over conventional MCDM techniques. An important characteristic in these studies is their limited scope in terms of the system(s) considered in the analysis.

1.2. Motivation. It is clear that sustainability analysis of transportation systems requires a broad perspective including various systems, such as the economic, and the political, social, and environmental systems. This perspective enables the consideration of such relevant aspects as biodiversity, human health, quality of life, and life expectancy. Such analysis requires significant amounts of data as well as methods to develop adequate SIs. Although not all data that one may

want to use is available, there is a vast amount of relevant information that can be obtained from such organizations as The World Bank, the United Nations, the Bureau of Transportation Statistics, and the U. S. Environmental Protection Agency.

Although fuzzy logic has been used in the context of sustainability to handle key characteristics of the relevant data, its use has not been coupled with a broad perspective considering multiple systems. To consider, explicitly, important broad effects and the characteristics of the associated data, this study proposes a system of systems (SOS) [39] and a fuzzy logic modeling approach. The SOS includes the Transportation, Activity, and Environment systems. The fuzzy logic modeling approach enables the treatment of the vagueness associated with some of the relevant data. Performance Indices (PIs) are computed for each system using a number of performance measures. The PIs illustrate the aggregated performance of each system as well as the interactions among them. The proposed methodology also enables the estimation of a Composite Sustainability Index to summarize the aggregated performance of the overall SOS.

The PIs are calculated with an emphasis on transportation systems, while explicitly considering and calculating the PIs for the other two relevant and affected systems. The PIs are calculated based on multiple performance measures with various degrees of resolution and units. These multi-resolution, multi-unit characteristics are intrinsic to the systems under consideration.

The paper is organized as follows. Section 2 describes three interdependent systems: the Transportation, Activity, and Environmental systems. Section 3 summarizes the fuzzy logic methodology used in this study. Section 4 provides information about the study region and data. Results and analysis are presented in Section 5. Some policy perspectives are illustrated in Section 6. Section 7 provides conclusions and recommendations for future work.

2. Interdependent Systems

In the context of sustainability, it is difficult to isolate systems or narrow the analysis to a particular region. Different systems such as Transportation have interdependencies with other systems including the economy and the environment. For example, energy resources, which are part of the environmental system, are required by both the transportation sector and the economy. Hence, any policy or strategy affecting the consumption or production of energy has effects at least on the transportation, the economy, and the environment. This research explicitly considers and defines three major interdependent systems, the transportation system, the activity system, and the environmental system.

2.1. The Transportation System. The transportation system includes all the infrastructure facilities, vehicles, operators, and control strategies used to provide transportation services to people and to move products. Thus, the overall transportation system includes all modes of transportation, including highways, transit, and fluvial and air modes. Existing literature uses a number of measures to describe or assess transportation system performance. Lomax et al. [40] identified several measures of congestion, such as travel time, total segment delay, corridor mobility index, delay ratio, and relative delay rate. The Roadway Congestion Index uses volume and capacity to provide a measure of congestion [41]. A Roadway Congestion Index exceeding 1.0 denotes an average congestion level that is undesirable during the peak period. Black [42] uses principal component analysis to examine the relationships among multiple performance measures, including Vehicle Miles Traveled (VMT), travel time, mobility, crashes, fuel consumption, and emissions. The results indicate that VMT is the single most important factor in the context of sustainability. High VMT values do not necessarily mean high congestion; therefore, similar to the Roadway Congestion Index, VMT needs to be used in conjunction with the corresponding capacity. Thus, VMT per lane mile is a desirable performance measure. In addition, transit passenger miles and the number of intersections per capita can be important performance measures depending on the geographic location. Thus, both the demand and supply side should be taken into account for the selection of performance measure.

The Transportation Service Index (TSI) is a performance measure that seeks to quantify the movement of passenger and freight by the for-hire transportation sector [43]. This index, which is reported every month, can be used in conjunction with economic indicators to analyze the relationships between the economy and the transportation sector. Another interesting performance measure is the amount of personal money spent on transportation; this includes motor vehicles and parts, gasoline, and such transportation services as transit. The public investment on infrastructure is another important performance measure. Depending on the available data, some or all of the above performance measures can be used to develop the Transportation System PI (TSPI). The proposed modeling framework is modular and very flexible to enable the seamlessly incorporation of additional performance measures.

2.2. The Activity System. Previous studies have described the activity system as the combination of social, economic, political, and other transactions taking place over time and space [44, 45]. These transactions create and determine the demand for transportation. For example, changes in such economic policies as gas taxes or VMT fees create changes in the demand for transportation. In this research, the activity system consists of the social, cultural, health-related, and economic/financial aspects. A commonly used indicator for the socio-economic development of any country is its Gross Domestic Product. However, the United Nations Development Program (UNDP) [46] recommends using the Human Development Index because it incorporates all the basic and necessary dimensions for economic prosperity. This index measures the average achievements in a country by considering (i) a long and healthy life, or life expectancy; (ii) access to knowledge, or the education index; and (iii) a generous standard of living, measured by gross national

income per capita. Life expectancy is the average number of years a child is expected to live, assuming that the mortality rate will remain constant [46]. The Education index includes the average number of years of education received in a lifetime and the expected number of years a child will attend school, assuming constant enrollment rates. The gross national income combines the gross domestic product of a country with its income received from other countries, less similar payments made to other countries. Some of these indices or indicators are used in this study to develop the Activity System PI (ASPI).

2.3. The Environmental System. The environmental system includes the air, water, soil, and all other natural resources as well as all living organisms that are affected and/or used by the transportation and activity systems. In the United States, data from the Federal Highway Administration and the Environmental Protection Agency suggests that emissions from the transportation system has been reduced drastically over the last 30 years, despite substantial gains in VMT, gross domestic product, population, and employment [47]. This has been attributed to the introduction of the Clean Air Act in 1973 and the emergence of fuel-efficient vehicles. However, such other sectors as industrial and chemical have generated increased carbon dioxide emissions over the years, thereby affecting climate change.

The Environmental Sustainability Index (ESI) was created by the end of the 1990s by Yale and Columbia Universities [48]. This index, which is a single indicator that provides insight into human health and the environment, was promoted by the World Economic Forum. This index currently is considered the most powerful tool available to measure environmental sustainability. The ESI uses 76 variables, including air pollution, emissions related to human health, environmental factors, water pollution, and resource minimization. In addition, it incorporates response factors relating to international agreements, such as the preservation of extinct species, limitations to the use of natural resources, limitations to the release of pollutants, and biodiversity conservation.

In 2006, the ESI became the Environmental Performance Index (EPI). Since then, the EPI has been published every two years. The primary constituents of the EPI are environmental health and ecosystem vitality. Policy weights used to calculate the EPI are approximate percentages that can be summarized as follows: environmental burden of disease, 25%; climate change, 25%; air pollution, 17%; water pollution, 17%; biodiversity and habitat, 4%; forestry, 4%; fisheries, 4%; and agriculture, 4%.

3. Methodology

This section provides a detailed framework of the modeling approach used in this study.

The concept of Fuzzy Logic was introduced by Lotfi Zadeh in 1965. It is a way of processing data by allowing partial set membership rather than crisp set membership or non-membership [49, 50]. Fuzzy logic provides a simple and efficient way to arrive at a definite conclusion based upon vague, ambiguous, imprecise, noisy, or missing input information. In the current study, multiple performance measures are combined and corresponding PIs are computed using fuzzy logic for the Transportation, Activity, and Environmental Systems. The PIs are calculated independently for each of the three systems. Their interdependencies are inherent in the data and are illustrated later in the results and discussion section. Considering a vector of performance measures X for system J as the inputs, the following three steps are used to calculate the corresponding PI: (1) an inference step (2), an aggregation step, and (3) a defuzzification step.

3.1. Inference Step. The inference step uses "*if-then*" rules and associated membership functions to develop and capture logical relationships between the different performance measures (inputs) and the PI (output).

3.1.1. If-then Rules. "*If-then*" rules are logical statements developed based on observation and expert knowledge of the system. The "*if*" part, left-hand side (LHS) or antecedent, is used with the inputs. The "*then*" part, the right-hand side (RHS) or consequent, is related to the output. An example of an "*If-then*" rule is as follows.

If [the VMT per lane mile is High and the TSI is Medium and the personal spending on transportation is Low], then [the TSPI is High].

As illustrated in this rule, in order to build the logical relationships between inputs and output, both the LHS and RHS are related to three fuzzy sets, High (H), Medium (M), and Low (L). Table 1 shows the set of "*if-then*" rules used in this study to calculate the TSPI. Here, three performance measures are used, namely. (i) the VMT per lane mile (v), (ii) the TSI, and (iii) the personal spending on transportation (ps) per year. If required, and if the relevant data is available, additional performance measures can be used; the corresponding rules are added to the table. Similar rules have been developed for each of the PIs in order to cover all possible relationships between the chosen system performance measures and the corresponding PI. Thus, the Transportation and Activity Systems each have three inputs and 27 rules while the environmental system has four inputs and 81 rules.

3.1.2. Membership Functions. The quantitative estimation of a PI requires knowledge about the interdependencies between the system performance measures and the corresponding PI. Considering the complexity of the Transportation, Activity, and Environmental Systems, this required knowledge is limited, vague, and sometimes ambiguous. Fuzzy logic provides a mathematical construct to combine all the available knowledge and develop meaningful PI estimates. The "*if-then*" rules are used in conjunction with sets of membership functions to relate the performance measures to the PIs, based on the available knowledge and data. Membership functions are used to define the grade or degree associated with every input and output. In this study, three membership functions are associated with each input and output, as illustrated in

Table 1: "*If-then*" rules for TSPI.

Rules	1	2	3	4	5	6	7	8	9	10	11	12	13	14	15	16	17	18	19	20	21	22	23	24	25	26	27		
		L	x	x	x	x	x	x	x	x	x																		
	v	M										x	x	x	x	x	x	x	x	x									
		H																			x	x	x	x	x	x	x	x	x
		L	x	x	x							x	x	x							x	x	x						
LHS	TSI	M				x	x	x							x	x	x							x	x	x			
		H							x	x	x							x	x	x							x	x	x
		L	x			x			x			x			x			x			x			x			x		
	ps	M		x			x			x			x			x			x			x			x			x	
		H			x			x			x			x			x			x			x			x			x
RHS	TSPI		L	L	L	L	L	L	M	M	M	L	L	L	M	M	M	M	H	H	M	M	M	H	H	H	H	H	H

Figure 1. Triangular membership functions are used in this study because they are easy to define; only three parameters are required: a modal point, the upper width, and the lower width. In addition, due to their conceptual and computation simplicity, triangular fuzzy numbers are commonly used in practical applications [30, 51, 52]. The domain for the membership functions corresponding to the LHS is defined based on the absolute value of the associated performance measures; the domains for the PIs corresponding to the RHS are normalized so as to use a simple $[0, 1]$ range. Figure 1 shows the membership functions for the calculation of the TSPI. Similar functions are defined for the other two PIs.

Once the "*if-then*" rules and the membership functions are defined, the Mamdani max-min composition operator and the Mamdani min implication operator are used for the fuzzy inference step [50]. For example, the three inputs for the calculation of TSPI, v, TSI, and ps are matched against the membership functions by using the "*if-then*" rules to determine the degree of activation. The degree at which each rule α is activated (δ^{α}) is obtained by using v, TSI, and ps as well as the max-min operator, as shown by (1)

$$\delta^{\alpha} = \max_{z \in Z} \min\left(\mu_{v}{}^{\alpha}(z), \mu_{\mathrm{TSI}}{}^{\alpha}(z), \mu_{\mathrm{ps}}{}^{\alpha}(z)\right), \quad (1)$$

where Z represents the universe of domains of the fuzzy sets v, TSI, and ps; and μ is a membership function. Equation (2) represents the membership functions of the fuzzy outcomes for the TSPI obtained, using the min implication operator

$$\mu_{\mathrm{TSPI}^{\alpha^*}} = \min\left(\delta^{\alpha}, \mu_{\mathrm{TSPI}^{\alpha}}\right). \quad (2)$$

3.2. Aggregation Step. The Aggregation Step represents the aggregation of all the fuzzy output sets obtained after matching all the inputs to the membership functions by using all the "*if-then*" rules. A total of R rules for the calculation of TSPI are defined. The aggregation step is given by (3):

$$\mu_{\mathrm{TSPI}^*} = \sum_{\alpha=1}^{R} \mu_{\mathrm{TSPI}^{\alpha^*}}. \quad (3)$$

3.3. Defuzzification Step. The output from the Aggregation Step combines all the available information by using all the defined rules. However, this output needs to be defuzzified to obtain a single crisp value for the corresponding PI, in this case, TSPI. The Center of Gravity method [50], illustrated in (4), is used for the Defuzzification Step:

$$\mathrm{TSPI} = \frac{\sum_{\alpha=1}^{R} \overline{\theta}^{\alpha} \cdot S\left(\mu_{\mathrm{TSPI}^{\alpha^*}}\right)}{\sum_{\alpha=1}^{R} S\left(\mu_{\mathrm{TSPI}^{\alpha^*}}\right)}, \quad (4)$$

where $\overline{\theta}^{\alpha}$ is the centroid of the fuzzy set for the TSPI, given by the RHS of rule α; and $S(\cdot)$ calculates the area of the membership function for a fuzzy set.

4. Study Region and Data

Sustainability considerations make it difficult to isolate systems and narrow the analysis to a particular transportation system or region. It is clear that impacts on the Environmental System, the Activity System, and even the Transportation System extend across regions and boundaries. In addition, the level of resolution of the available data may limit localized analyses. Hence, to illustrate the proposed method, without loss of generality, the United States is used as the study area. Similar analyses can be conducted for other regions and, ideally, the entire globe. In this case, the analysis was conducted for a period of 20 years between 1990 and 2010.

The three performance measures used in the examples in Section 3 for the estimation of the TSPI in this study were obtained from the Bureau of Transportation Statistics [43]. The ASPI includes the following performance measures provided by the United Nations [46]:

(i) Gross national income (*gni*);

(ii) The Education Index (*ei*);

(iii) Life expectancy (*le*).

The Environmental System Performance Index (ESPI) is based on the following performance measures:

(i) Carbon dioxide emissions (*ce*) [53];

(ii) Air pollutants (*ap*) [54];

(iii) Water pollutants (*wp*) [55];

(iv) Energy consumption (*ec*) [56].

5. Results and Discussion

Figure 2 shows the normalized performance measures and performance index for the Transportation System. The historic trend for the VMT per lane mile (in thousands) covers a period from 1990 to 2008. It is clear that the trend is increasing except between 1990 and 1991. This could be attributed to the recession during each of those time periods [57, 58]. During 2005-2006, the VMT started decreasing probably as a consequence of the rising oil prices [59]. The trend for the TSI covers from 1990 to 2010. The base year for TSI = 100 is taken as the year 2000. The figure shows the decrease in TSI between the years 2000 and 2002, when the terrorist attack on September 11 occurred. In 2001, there was less freight and passenger travel. Between years 2008 and 2010, the financial crisis resulted in a severe recession with consequences on TSI, as illustrated in Figure 2. Personal spending on transportation is included during 1995–2010. It is evident that spending increases from 1995–2005 as a result of economic development. However, in 2006, spending started decreasing as a result of a rise in gas prices, which hit $4 a gallon. Later, the financial crisis during 2007–2010 resulted in decreased spending for transportation-related activities.

Figure 2 also shows the historic trend of the Transportation System performance index from 1990 to 2009. The crisp value in the y-axis is obtained by using the fuzzy approach discussed in earlier sections. Here, the closer the TSPI to 1, the better the performance of the Transportation System; if its value is close to 0, then performance is poor. The crisp values can only be used as a relative measure to compare between alternatives and scenarios. It cannot be used to assess

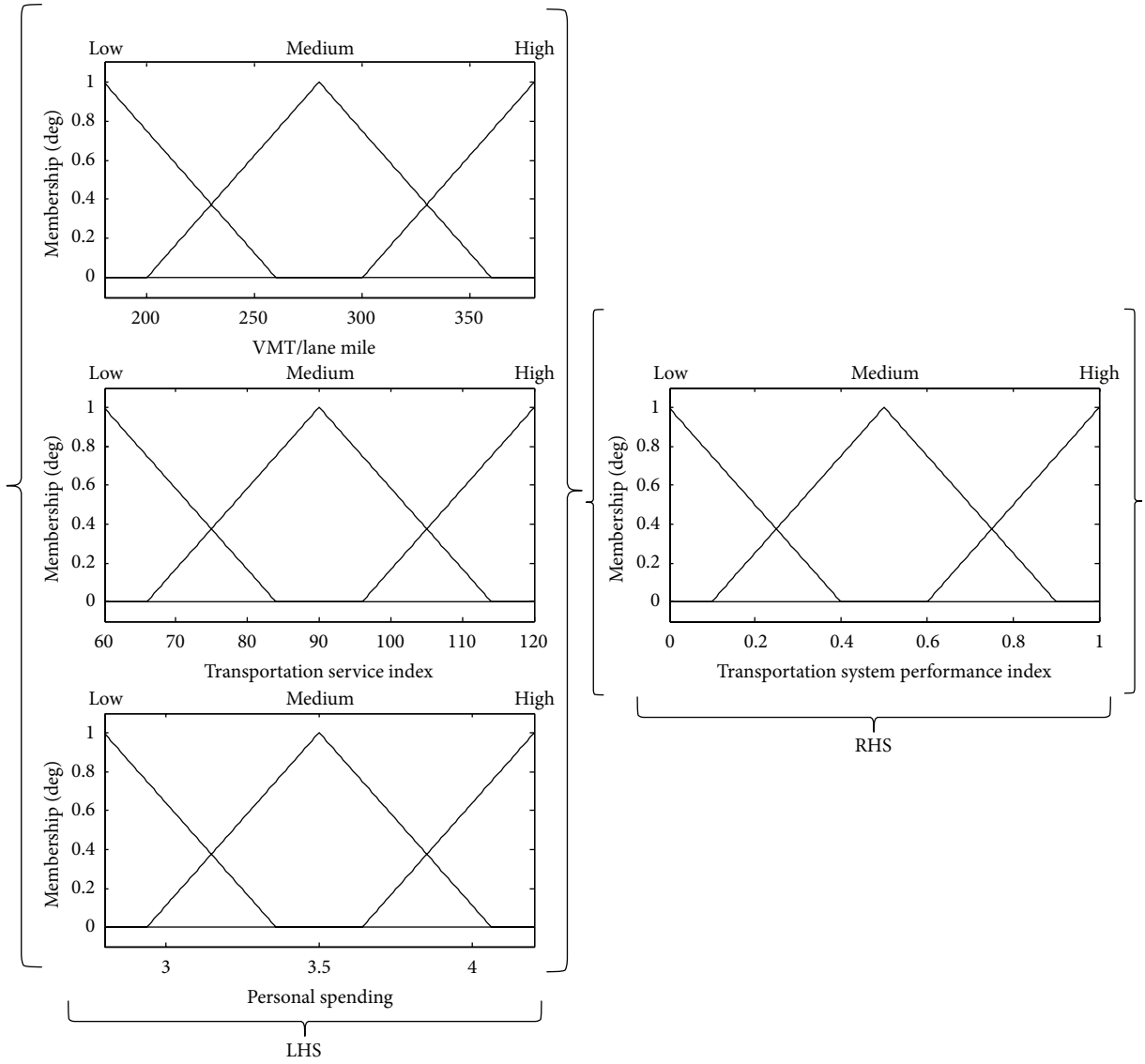

Figure 1: Membership functions for the calculation of the Transportation System Performance Index.

the absolute value of the sustainability of the system. It is evident that TSPI has the best value between years 2005 and 2006, when the economy was booming, and the least value between years 1990 and 1991. The curve for the TSPI follows a pattern consistent with VMT/lane mile and TSI. That is, the TSPI increases with the increase in VMT/lane mile and TSI. According to Genier [59], rising oil prices during 2005-2006 has led to reduced VMT and promoted alternate modes of transportation, such as transit and car-pooling, as well as the use of more efficient vehicles.

Figure 3 shows the normalized performance measures and performance index for the Activity System. The trend of the average annual income in Gross National Income per capita is provided from 1990 to 2010. The trend increased, with a high growth rate until 1999. The rate started decreasing in 2000 following the technology bust, also known as the Dot-Com Bubble, and later in 2006, following the housing crisis. It is noted that the rate of growth in income is less in the past decade as compared to earlier decades.

The trend of the average annual education index is provided from 1990 to 2010. This index started increasing from 1990 to 2000, the primary reason being the invention of new technologies and innovations that kept the United States in the forefront of education. In addition, a new wave of technological revolution was seen in the form of startups. Also, science, engineering, and medical disciplines saw a new era of growth and development. The reason for a slight decline in the education index between 2000 and 2004 is not clear yet. The trend of the average annual life expectancy is provided from 1990 to 2010. The average life expectancy has increased from 74 years in 1990 to 80 years in 2010. This increase can be attributed to the technological advancement in medical facilities and billions of dollars spent on research and the development of new and effective drugs.

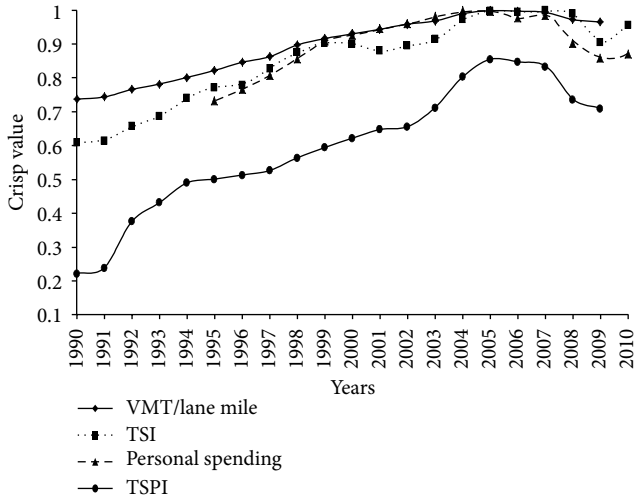

Figure 2: Historical Trend of Transportation System Performance Index and its Performance Measures.

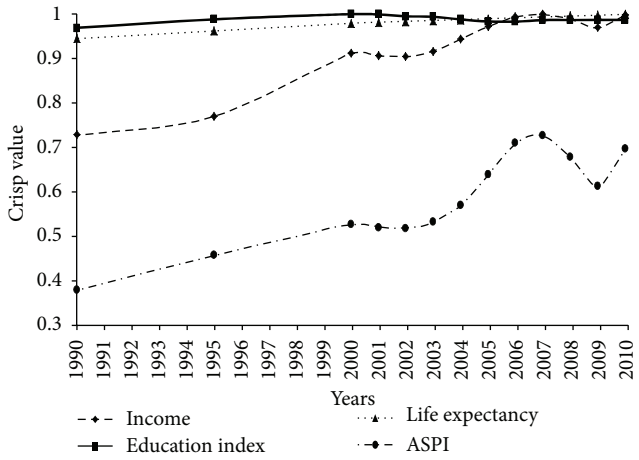

Figure 3: Historical Trend of Activity System Performance Index and its Performance Measures.

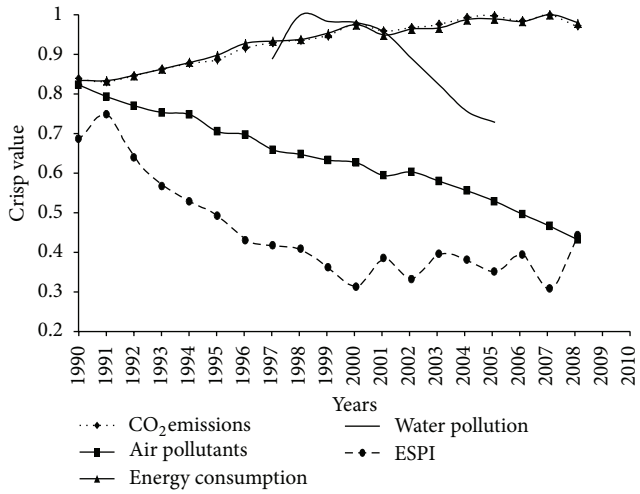

Figure 4: Historical Trend of Environmental System Performance Index and its Performance Measures.

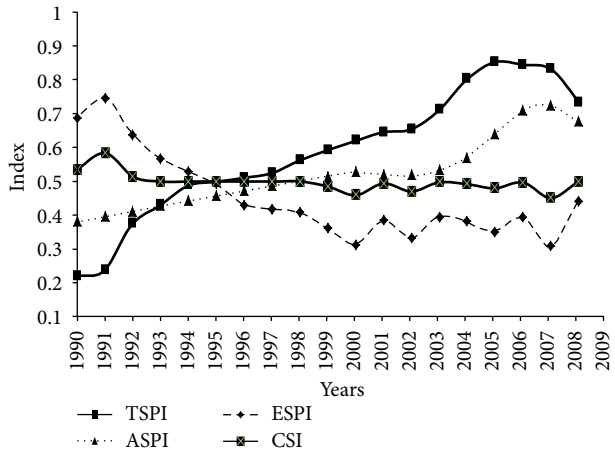

Figure 5: Historical Trend of Performance Indices and the Composite Sustainability Index for the Transportation, Activity, and Environmental systems.

Figure 3 also shows the trend for the Activity System's performance index from 1990 to 2010. This index started increasing from year 1990 until the year 2000 as a result of economic development. Starting with the technology bust in 2000 and terrorist attacks in 2001, the economic activity started to decrease and did not recover until the end of the year in 2003. Since 2003, the Activity System started an upward trend before hitting a peak in 2007. The financial crisis from 2007 to 2009 resulted in a dramatic decrease in economic activity, often compared as equivalent to the Great Depression of 1930s. The year 2009 marks the period of "official recovery" from the recession.

Figure 4 shows the normalized performance measures and performance index for the Environmental System. The trend of carbon dioxide emissions is provided from years 1990 to 2008. This is an increasing trend except during 1990-1991, a time of global political unrest and high inflation; 2000–2002, due to the technology bust and September 11 attacks; 2005-2006, due to high gas prices; and 2007-2008, with the financial crisis. The trend of air pollutants is provided from 1990 to 2008. With the introduction of the Clean Air Act in 1973, there has been a dramatic reduction in air pollution. In addition, the introduction of innovative technologies, such as hybrid and battery powered vehicles, have led to reduced air pollution over the years.

The trend for water pollutants is provided from 1997 to 2005. This trend decreases with time as a result of innovative and efficient waste management techniques. The trend for the average annual energy consumption in quadrillion British Thermal Units is provided from 1990 to 2008. This trend indicates that energy consumption decreased during the financial crisis of 1990-1991. After 1991, energy consumption started an upward trend and finally peaked in 2007. However, there were short periods of decline in energy consumption

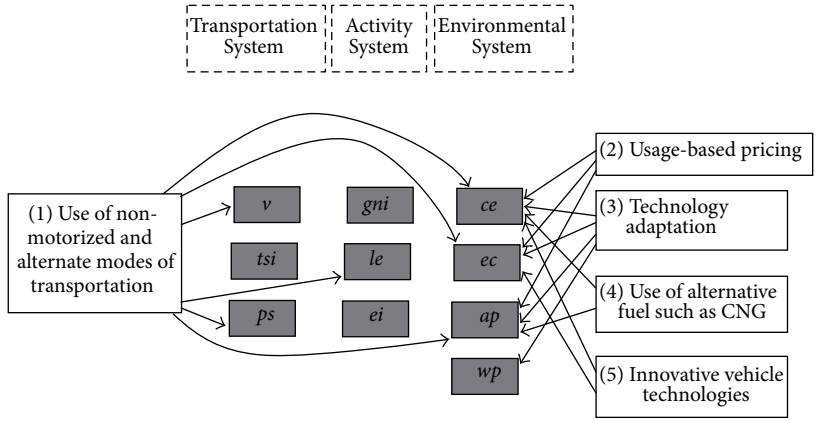

Figure 6: Direct effects of policy options on Performance Measures.

both in 2001, attributed to the September 11 terrorist attacks, and 2006, due to high oil prices. The terrorist attack resulted in decreased travel and less economic activity, while the exorbitant high oil prices promoted the use of new battery-powered and hybrid vehicle technologies.

Figure 4 also shows the trend of the Environmental System's performance index from 1990 to 2008. If the value for ESPI is close to 1, then the environmental system is excellent; if its value is close to 0, then the system quality is very poor. The best value for ESPI occurred during 1990–1995, when economic development was slow as a result of global political unrest and the first gulf war. Since 2000, the quality started to improve, probably as a consequence of multiple periods of economic contractions. Again, the year 2007 marked the beginning of a slight uptrend in the index as a result of a global financial crisis. In general, the environment improves during periods when economic activity is down and/or oil prices are high. In addition, the curve for the ESPI follows a pattern consistent with carbon-dioxide emissions and energy consumption. That is, the ESPI decreases with the increase in carbon-dioxide emissions and energy consumption.

Figure 5 shows the three performance indices from 1990 to 2009. In this figure the Transportation and Activity Systems follow an increasing trend over the years, with similar periods of growth and contractions; on the other hand, the Environmental System follows a reverse pattern. These trends seem intuitive, as growth in the economy and the transportation sectors are expected to happen simultaneously; this growth requires resources from the environment, thereby increasing emissions and energy consumption.

Figure 5 also illustrates a Composite Sustainability Index (CSI), an index used to access the overall sustainability of the SOS used this research. It is calculated using the proposed fuzzy logic approach and the performance index for the Transportation, Activity, and Environmental Systems. The CSI shows an overall increasing trend from year 1990 to 1995. However, considering the overall negative slope and corresponding decrease on the ESPI, the CSI does not continue increasing after 1995 presenting some negative periods and increases only when there is a significant improvement on the ESPI. Based on these observations and the chosen performance measures, negative impacts to the environment seem to be associated with negative consequences on the overall sustainability of the SOS. In general, under the proposed framework, a system is sustainable if the slope of the corresponding PI curve presents a nonnegative slope. Similarly, the overall SOS is sustainable if the slope of the CSI is nonnegative. The axioms presented in this paper are an attempt to summarize our observations based on chosen performance measures. There is a vast literature with similar observations. For example, Young et al. [60] as well as Lahiri and Yao [61] have observed that the transportation and activity system follows a lead-lag phase pattern and environment system is inversely related to the other two. The following axioms can be postulated to assess the sustainability or the unsustainability of our SOS.

(1) The SOS is sustainable when the overall slopes for the TSPI, ASPI, and ESPI have a positive trend. This is an ideal scenario with positive growth in all systems, and implies that there is no need of nonrenewable natural resources to sustain growth in the transportation and the economy.

(2) The SOS is unsustainable when the slopes of TSPI and ASPI have a positive trend but the slope of ESPI has a negative trend. This is the scenario that we have been observing in the USA. In general, the SOS is unsustainable when the overall trend of at least one of the three slopes is negative.

(3) The SOS is sustainable when the overall slopes for the TSPI, ASPI, and ESPI have a nonnegative trend. This scenario is sustainable because all the transportation and other social activities can continue in perpetuity without degradation of the environmental system. Although this is a scenario preferred over an unsustainable situation, it may represent an unstable equilibrium that can easily become unsustainable.

6. Policy Perspectives

This section discusses some policy options for the sustainability of the SOS studied in this research. Some of these options have been implemented in the past revealing some of their effects. Other options are currently under consideration by multiple stakeholders. Figure 6 illustrates five policy options that can be used to improve performance and support the sustainability of the SOS considered here. The dashed boxes correspond to the three major systems, the grey boxes represent the performance measures within each system, and the suggested policies are depicted by rectangular boxes. These policies have direct and indirect effects on some performance measures and systems. Only the direct effects of the proposed policies are shown through the arrows in Figure 6. Conclusion regarding indirect effects will be immature at this point; hence are not discussed here. Each policy is described as follows.

Use of Nonmotorized and Alternate Modes of Transportation. This policy consists of the promotion of non-motorized modes of transportation, such as bicycles, and the use of alternatives for driving alone, such as transit and carpooling. The success of this policy depends on multiple factors, including land use. It may require the establishment of commuter-friendly and transit-friendly development near the central business district. In addition, changes in travel and demand patterns depend on the users' preferences and attitudes as well as convenience. Expected consequences of implementing this policy, among others, include reductions on (i) VMT [62, 63], (ii) air pollution, (iii) carbon dioxide emissions, (iv) energy consumption, (v) health issues, and (vi) out-of-pocket cost. The money and resources saved can be used to improve such sectors as education and research with further impacts on the gross domestic product.

Usage Based Pricing. Currently, the implementation of a VMT fee is being considered as a viable alternative to replace the current fuel tax for collecting the required resources for highway maintenance [64]. This policy also can promote the reduction of VMT, along with all the other associated consequences. However, this policy faces a number of deployment as well as acceptance issues.

Technology Adaptation. The rapid industrialization and technological revolution has resulted in reduced emissions over the years. For example, the use of efficient boilers in coal-fired plants will help reduce carbon dioxide emissions, pollution, and energy consumption [65, 66]. Health related issues will be reduced as a consequence of less pollution.

Use of Alternative Fuels Such As Compressed Natural Gas (CNG). The use of alternative fuels in the form of CNG will reduce carbon-dioxide emissions and pollution [67, 68]. This will lead to a green and cleaner environment [69] with all the associated benefits to health, the economy, and the quality of life. In the United States, the reserves of natural gas are larger than those of petroleum [70]. Hence, this policy seems plausible from an environmental and economic perspective. The only drawbacks are the time and cost associated with retrofitting vehicles and the supply chain.

Innovative Vehicle Technologies. Replacement of conventionally powered vehicles with hybrid and electric vehicles will reduce carbon-dioxide emissions and nonrenewable fuel consumption [71]. Automakers are particularly interested in this policy [72]. In addition, the federal government provides tax incentives to develop and manufacture lithium ion batteries in the United States.

Ideally, each of these policies is evaluated before deployment and adoption. Some of them are currently under analysis by multiple agencies and sectors. The proposed framework in this study is descriptive rather than normative. Hence, it can only be used to appreciate the effectiveness and benefits of past policies. Currently, the proposed framework is been extended to enable a normative analysis in order to evaluate potential policy alternatives such as those described earlier.

7. Conclusions

Previous studies about sustainable transportation have either focused only on the transportation system, or have not used a methodology that enables the treatment of incomplete, vague, and qualitative information present in the problem context. This study adopted a holistic approach to compute Performance Indices for a SOS including the Transportation, Activity, and Environmental systems. The Performance Indices are synthetized to calculate a Composite Sustainability Index to evaluate the sustainability of the overall SOS. Considering the complexity, vagueness, nonlinearity, qualitative, and incomplete information characterizing the quantification of the Performance and Composite Sustainability Indices, a fuzzy logic approach was used to calculate these indices. Historic events and policy changes indicated that fuzzy logic provided an adequate approach to estimate both the Performance Indices and the Composite Sustainability Index.

Results of the analysis for the US showed that the Transportation and Activity Systems both follow a positive trend over the years, with similar periods of growth and contractions. In contrast, the environmental system follows a reverse pattern. This seems intuitive, as periods of economic and transportation growth is expected to have a negative effect on the environment, leading to increased emissions and energy consumption. In general, the performance of the environmental system has decreased significantly over time. Policies adopted to protect the system have shown positive effects. However, the current performance of the Environmental System is questionable, and long-term policies need to be developed.

The conclusions provided here are based on the results obtained using a limited number of performance measures. Adding or removing performance measures are expected to change the results and conclusions. In general, following a holistic approach, it is expected that the more relevant performance measures are used, the more comprehensive

and accurate the analysis is. Planning and operational policies for the sustainability of the Transportation, Activity, and Environmental systems can be developed using the proposed approach. Considering the current practice of making planning decisions at the regional and jurisdictional level, the framework used in this study is currently been extended to enable the analysis of regional systems including large metropolitan areas. A simulation-based approach has been developed to estimate multiple performance measures required to calculate adequate performance indices.

References

[1] EIA (Energy Information Administration), *International Energy Outlook*, EIA, Washington, DC, USA, 2006.

[2] J. J. MacKenzie, "Alternative fuels to reduce petroleum consumption, global warming gases, and urban air pollution," in *Symposium on Challenges and Opportunities for Global Transportation in the 21st Century*, John A. Volpe Transportation Systems Center, Cambridge, Mass, USA, 1995.

[3] J. Zheng, C. Atkinson-Palombo, C. McCahill, R. O'Hara, and N. W. Garrick, "Quantifying the economic domain of transportation sustainability," in *Proceedings of the Annual Meeting of the Transportation Research Board—CDROM*, Washington, DC, USA, 2011.

[4] S. Bell and S. Morse, *Sustainability Indicators: Measuring the Immeasurable*, Earthscan, London, UK, 2nd edition, 2008.

[5] J. R. E. Harger and F. M. Meyer, "Definition of indicators for environmentally sustainable development," *Chemosphere*, vol. 33, no. 9, pp. 1749–1775, 1996.

[6] H. Bossel, "Assessing viability and sustainability: a systems-based approach for deriving comprehensive indicator sets," *Conservation Ecology*, vol. 5, no. 2, article 12, 2001.

[7] C. M. Jeon, A. A. Amekudzi, and R. L. Guensler, "Evaluating plan alternatives for transportation system sustainability: Atlanta metropolitan region," *International Journal of Sustainable Transportation*, vol. 4, no. 4, pp. 227–247, 2010.

[8] T. Litman, "Developing indicators for comprehensive and sustainable transport planning," *Transportation Research Record*, no. 2017, pp. 10–15, 2007.

[9] J. A. Paravantis and D. A. Georgakellos, "Trends in energy consumption and carbon dioxide emissions of passenger cars and buses," *Technological Forecasting and Social Change*, vol. 74, no. 5, pp. 682–707, 2007.

[10] S. Huzayyin and H. Salem, "Analysis of thirty years evolution of urban growth, transport demand and supply, energy consumption, greenhouse and pollutants emissions in Greater Cairo," *Research in Transportation Economics*, vol. 40, no. 1, pp. 104–115, 2013.

[11] T. Litman, *Climate Change Emission Valuation for Transportation Economic Analysis*, Victoria Transport Policy Institute, 2012.

[12] E. J. Zolnik, "Estimates of statewide and nationwide carbon dioxide emission reductions and their costs from cash for clunkers," *Journal of Transport Geography*, vol. 24, pp. 271–281, 2012.

[13] G. R. Conway, "Sustainability in agricultural development: trade-offs with productivity, stability and equitability," *Journal of Farming Systems Research and Extension*, vol. 4, no. 2, pp. 1–14, 1994.

[14] R. Gray, "Economic measures of sustainability," *Canadian Journal of Agricultural Economics*, vol. 39, no. 4, pp. 627–635, 1991.

[15] WCED (World Commission on Environment and Development), *Our Common Future*, Oxford University Press, Oxford, UK, 1987.

[16] R. Costanza, B. Norton, and B. D. Haskell, *Ecosystem Health: New Goals for Environmental Management*, Island Press, Washington, DC, USA, 1992.

[17] IUCN (World Conservation Union), UNEP (United Nations Environment Programme), and WWF (World Wide Fund for Nature), *Caring for the Earth: A Strategy for Sustainable Living*, IUCN, Gland, Switzerland, 1991.

[18] K. Rennings and H. Wiggering, "Steps towards indicators of sustainable development: linking economic and ecological concepts," *Ecological Economics*, vol. 20, no. 1, pp. 25–36, 1997.

[19] G. Munda, *Fuzzy Information on Multi-Criteria Environmental Models*, Physika, Heidelberg, Germany, 1995.

[20] J. Zietsman, L. R. Rilett, and S. J. Kim, "Transportation corridor decision-making with multi-attribute utility theory," *International Journal of Management and Decision Making*, vol. 7, no. 2-3, pp. 254–266, 2006.

[21] R. Islam and T. L. Saaty, "The analytic hierarchy process in the transportation sector," in *Multiple Criteria Decision Making for Sustainable Energy and Transportation Systems*, vol. 634 of *Lecture Notes in Economics and Mathematical Systems*, Springer, Physica, Berlin, Heidelberg, 2010.

[22] G. A. Mendoza and R. Prabhu, "Multiple criteria decision making approaches to assessing forest sustainability using criteria and indicators: a case study," *Forest Ecology and Management*, vol. 131, no. 1-3, pp. 107–126, 2000.

[23] H. J. Zimmermann, *Fuzzy Set Theory and Its Applications*, Kluwer Academic, Boston, Mass, USA, 4th edition, 2001.

[24] S. Yedla and R. M. Shrestha, "Multi-criteria approach for the selection of alternative options for environmentally sustainable transport system in Delhi," *Transportation Research A*, vol. 37, no. 8, pp. 717–729, 2003.

[25] D. Tsamboulas and G. Mikroudis, "EFECT—evaluation framework of environmental impacts and costs of transport initiatives," *Transportation Research D*, vol. 5, no. 4, pp. 283–303, 2000.

[26] A. Awasthi and H. Omrani, "A hybrid approach based on AHP and belief theory for evaluating sustainable transportation solutions," *International Journal of Global Environmental Issues*, vol. 9, no. 3, pp. 212–226, 2009.

[27] T. L. Saaty, *The Analytic Hierarchy Process*, McGraw-Hill, New York, NY, USA, 1980.

[28] G. Crawford and C. Williams, "A note on the analysis of subjective judgment matrices," *Journal of Mathematical Psychology*, vol. 29, no. 4, pp. 387–405, 1985.

[29] J. Barzilai, "Consistency measures for pairwise comparison matrices," *Journal of Multi-Criteria Decision Analysis*, vol. 7, no. 3, pp. 123–132, 1998.

[30] G. J. Klir and B. Yuan, *Fuzzy Sets and Logic: Theory and Application*, Prentice Hall, Upper Saddle River, NJ, USA, 1995.

[31] R. R. Yager, "Aggregation operators and fuzzy systems modeling," *Fuzzy Sets and Systems*, vol. 67, no. 2, pp. 129–145, 1994.

[32] W. Silvert, "Ecological impact classification with fuzzy sets," *Ecological Modelling*, vol. 96, no. 1–3, pp. 1–10, 1997.

[33] A. Awasthi, S. S. Chauhan, and H. Omrani, "Application of fuzzy TOPSIS in evaluating sustainable transportation systems,"

Expert Systems with Applications, vol. 38, no. 10, pp. 12270–12280, 2011.

[34] S. Opricovic and G. H. Tzeng, "Fuzzy multicriteria model for postearthquake land-use planning," *Natural Hazards Review*, vol. 4, no. 2, pp. 59–64, 2003.

[35] G. A. Mendoza and R. Prabhu, "Fuzzy methods for assessing criteria and indicators of sustainable forest management," *Ecological Indicators*, vol. 3, no. 4, pp. 227–236, 2004.

[36] K. F. R. Liu, "Evaluating environmental sustainability: an integration of multiple-criteria decision-making and fuzzy logic," *Environmental Management*, vol. 39, no. 5, pp. 721–736, 2007.

[37] T. Prato, "A fuzzy logic approach for evaluating ecosystem sustainability," *Ecological Modelling*, vol. 187, no. 2-3, pp. 361–368, 2005.

[38] L. A. Marks, E. G. Dunn, J. M. Keller, and L. D. Godsey, "Multiple criteria decision making (MCDM) using fuzzy logic: an innovative approach to sustainable agriculture," in *Proceedings of the 3rd International Symposium on Uncertainty Modeling and Analysis and Annual Conference of the North American Fuzzy Information Processing Society (ISUMA-NAFIPS'95)*, pp. 503–508, IEEE Computer Society, Washington, DC, USA, September 1995.

[39] R. L. Ackoff, "Towards a system of systems concepts," *Management Science*, vol. 17, no. 11, pp. 661–671, 1971.

[40] T. Lomax, S. Turner, and G. Shunk, *Quantifying Congestion*, vol. 1, National Cooperative Highway Research Program, Transportation Research Board, National Academy Press, Washington, DC, USA, 1997.

[41] D. L. Schrank and T. J. Thomas, *Urban Mobility Report*, Texas Transportation Institute, College Station, Tex, USA, 2009.

[42] W. R. Black, "Sustainable transport and potential mobility," *European Journal of Transport and Infrastructure Research*, vol. 2, no. 3-4, pp. 179–196, 2002.

[43] BTS (Bureau of Transportation Statistics), "Key Transportation Indicators," 2011, http://www.bts.gov/publications/key_transportation_indicators.

[44] M. L. Manheim, *Fundamentals of Transportation Systems Analysis, Volume 1: Basic Concepts*, MIT Press, Boston, Mass, USA, 1979.

[45] E. Cascetta, *Transportation Systems Analysis: Models and Applications*, Springer, New York, NY, USA, 2009.

[46] UNDP (United Nations Development Programme), "Human Development Report," 2010, http://www.hdr.undp.org/en/statistics/.

[47] ARTBA (American Road and Transportation Builders Association), 2011, http://www.artba.org/mediafiles/regulatorylegalartbacafecommentsjanuary2011.pdf.

[48] ESI (Environmental Sustainability Index), Benchmarking National Environmental Stewardship, Yale Center for Environmental Law and Policy, Yale University, 2005, http://www.yale.edu/esi/ESI2005_Main_Report.pdf.

[49] R. R. Yager, S. Ovchinnikov, R. M. Tong, and H. T. Nguyen, *Fuzzy Sets and Applications: Selected Papers By L.A. Zadeh*, John Wiley & Sons, New York, NY, USA, 1987.

[50] L. H. Tsoukalas and R. E. Uhrig, *Fuzzy and Neural Approaches in Engineering*, John Wiley & Sons, New York, NY, USA, 1997.

[51] W. Pedrycz, "Why triangular membership functions?" *Fuzzy Sets and Systems*, vol. 64, no. 1, pp. 21–30, 1994.

[52] C. H. Yeh and H. Deng, "A practical approach to fuzzy utilities comparison in fuzzy multicriteria analysis," *International Journal of Approximate Reasoning*, vol. 35, no. 2, pp. 179–194, 2004.

[53] EIA (Energy Information Administration), *Emissions of Greenhouse Gases in the United States*, Washington, DC, USA, 2009, http://www.eia.gov/environment/emissions/ghg_report/pdf/tbl6.pdf.

[54] EPA (Environmental Protection Agency), Clearinghouse for Inventories and Emissions Factors (CHIEF), Current Emission Trends Summaries, 2009, http://www.epa.gov/ttn/chief/trends/index.html.

[55] World Databank, World Development Indicators and Global Development Finance, 2010, http://www.databank.worldbank.org/ddp/home.do?Step=2&id=4&hActiveDimensionId=WDI_Series.

[56] EIA (Environmental Information Administration), Monthly Energy Review, 2011, http://www.eia.doe.gov/emeu/mer/contents.html.

[57] M. Mussa, "U.S. Macroeconomic policy and third world debt," *Cato Journal*, vol. 4, no. 1, 1984, http://www.cato.org/sites/cato.org/files/serials/files/cato-journal/1984/5/cj4n1-5.pdf.

[58] R. H. Kamery, "A brief review of the recession of 1990-1991," *Allied Academies International Conference, Proceedings of the Academy of Legal, Ethical and Regulatory Issues*, vol. 8, no. 2, 2004.

[59] B. Genier, "Peak Demand—U.S. Gasoline Demand Likely Peaked in 2007," Cambridge Energy Research Associates (CERA), 2008, http://www2.cera.com/news/details/1,2318,9568,00.html.

[60] P. Young, K. Notis, G. Feuerberg, and L. Nguyen, "BTS Technical Report: transportation services index and the economy," 2007.

[61] K. Lahiri and W. Yao, "A dynamic factor model of the coincident indicators for the US transportation sector," *Applied Economics Letters*, vol. 11, no. 10, pp. 595–600, 2004.

[62] T. Litman and R. Steele, *Land Use Impacts on Transport: How Land Use Factors Affect Travel Behavior*, Victoria Transport Policy Institute, 2011.

[63] Nelson/Nygaard, *Crediting Low-Traffic Developments: Adjusting Site-Level Vehicle Trip Generation Using URBEMIS, Urban Emissions Model*, California Air Districts, 2005.

[64] D. S. Kim, D. Porter, and R. Wurl, *Technology Evaluation for Implementation of VMT Based Revenue Collection Systems*, Oregon Department of Transportation, Road User Fee Task Force, Salem, Ore, USA, 2002.

[65] K. Jordal, M. Anheden, J. Yan, and L. Strömberg, "Oxy-fuel Combustion for coal-fired power generation with CO_2 capture—opportunities and challenges," in *Proceedings of the 7th International Conference on Greenhouse Gas Control Technologies (GHGT-7)*, Vancouver, Canada, 2004.

[66] M. B. Toftegaard, J. Brix, P. A. Jensen, P. Glarborg, and A. D. Jensen, "Oxy-fuel combustion of solid fuels," *Progress in Energy and Combustion Science*, vol. 36, no. 5, pp. 581–625, 2010.

[67] M. P. Hekkert, F. H. J. F. Hendriks, A. P. C. Faaij, and M. L. Neelis, "Natural gas as an alternative to crude oil in automotive fuel chains well-to-wheel analysis and transition strategy development," *Energy Policy*, vol. 33, no. 5, pp. 579–594, 2005.

[68] P. Goyal and Sidhartha, "Present scenario of air quality in Delhi: a case study of CNG implementation," *Atmospheric Environment*, vol. 37, no. 38, pp. 5423–5431, 2003.

[69] S. Yeh, "An empirical analysis on the adoption of alternative fuel vehicles: the case of natural gas vehicles," *Energy Policy*, vol. 35, no. 11, pp. 5865–5875, 2007.

[70] M. Q. Wang and H. S. Huang, "A full fuel-cycle analysis of energy and emissions impacts of transportation fuels produced from natural gas," Report No. ANL/ESD-40, Center for Transportation Research, Energy Systems Division, Argonne National Laboratory, IL, US Department of Energy, 2000.

[71] M. S. Dresselhaus and I. L. Thomas, "Alternative energy technologies," *Nature*, vol. 414, no. 6861, pp. 332–337, 2001.

[72] S. G. Wirasingha, N. Schofield, and A. Emadi, "Plug-in hybrid electric vehicle developments in the US: trends, barriers, and economic feasibility," in *Proceedings of the IEEE Vehicle Power and Propulsion Conference (VPPC'08)*, Harbin, China, September 2008.

Hindawi Publishing Corporation
Advances in Fuzzy Systems
Volume 2013, Article ID 342805, 7 pages
http://dx.doi.org/10.1155/2013/342805

Research Article

Fuzzy Retractions of Fuzzy Open Flat Robertson-Walker Space

A. E. El-Ahmady[1,2] and A. S. Al-Luhaybi[1]

[1] *Mathematics Department, Faculty of Science, Taibah University, Madinah, Saudi Arabia*
[2] *Mathematics Department, Faculty of Science, Tanta University, Tanta 31527, Egypt*

Correspondence should be addressed to A. E. El-Ahmady; a_elahmady@hotmail.com

Received 24 April 2012; Accepted 28 August 2012

Academic Editor: Ching-Hung Lee

Our aim in the present paper is to introduce and study new types of fuzzy retractions of fuzzy open flat Robertson-Walker $\widetilde{W}^4$ model. New types of the fuzzy deformation retracts of $\widetilde{W}^4$ model are obtained. The relations between the fuzzy foldings and the fuzzy deformation retracts of $\widetilde{W}^4$ model are deduced. Types of fuzzy minimal retractions are also presented. New types of homotopy maps are deduced. New types of conditional fuzzy folding are presented. Some commutative diagrams are obtained.

1. Introduction and Background

Robertson-Walker space represents one of the most intriguing and emblematic discoveries in the history of geometry. Although if it were introduced for a purely geometrical purpose, they came into prominence in many branches of mathematics and physics. This association with applied science and geometry generated synergistic effect: applied science gave relevance to Robertson-Walker space and Robertson-Walker space allowed formalizing practical problems [1–6]. As is well known, the theory of retractions is always one of interesting topics in Euclidian and Non-Euclidian spaces and it has been investigated from the various viewpoints by many branches of topology and differential geometry [7–11]. There are many diverse applications of certain phenomena for which it is impossible to get relevant data. It may not be possible to measure essential parameters of a process such as the temperature inside molten glass or the homogeneity of a mixture inside some tanks. The required measurement scale may not exist at all, such as in the case of evaluation of offensive smells, evaluating the taste of foods or medical diagnoses by touching [7, 8, 12–18]. The aim of the present paper is to describe the above phenomena geometrically, specifically concerned with the study of the new types of fuzzy retractions, fuzzy deformation retracts, and fuzzy folding of fuzzy open flat Robertson-Walker $\widetilde{W}^4$ model. A fuzzy manifold is manifold which has a physical character. This character is represented by the density function μ, where $\mu \in [0,1]$ [7, 8, 12].

A fuzzy subset $(\underset{\sim}{A},\mu)$ of a fuzzy manifold $(\underset{\sim}{M},\mu)$ is called a fuzzy retraction of $(\underset{\sim}{M},\mu)$ if there exist a continuous map $\tilde{r}:(\underset{\sim}{M},\mu)\to(\underset{\sim}{A},\mu)$ such that $\tilde{r}(a,\mu(a))=(a,\mu(a))$, for all $a\in\underset{\sim}{A}$, $\mu\in[0,1]$ [7, 8, 12].

A fuzzy subset $(\overline{\underset{\sim}{M}},\tilde{\mu})$ of a fuzzy manifold $(\underset{\sim}{M},\mu)$ is called a fuzzy deformation retract if there exists a fuzzy retraction $\tilde{r}:(\underset{\sim}{M},\mu)\to(\overline{\underset{\sim}{M}},\tilde{\mu})$ and a fuzzy homotopy $\tilde{F}:(\underset{\sim}{M},\mu)\times I\to(\underset{\sim}{M},\mu)$ [7, 13, 14] such that

$$\begin{aligned}\tilde{F}((x,\mu),0)&=(x,\mu),\\ \tilde{F}((x,\mu),1)&=\tilde{r}(x,\mu),\end{aligned}\quad x\in\underset{\sim}{M}, \tag{1}$$

$\tilde{F}((a,\mu),t)=(a,\mu)$, for all $(a,\mu)\in\overline{\underset{\sim}{M}}$, $t\in I$, $\mu\in[0,1]$, where $\tilde{r}(x,\mu)$ is the retraction mentioned above.

Topological folding of fuzzy open flat Robertson-Walker space $\widetilde{W}^4$ model [7, 8]. A map $\widetilde{\mathfrak{F}}:\widetilde{W}^4\to\widetilde{W}^4$ is said to be an isometric folding of $\widetilde{W}^4$ model into itself if and only if for any piecewise fuzzy geodesic path $\gamma:J\to\widetilde{W}^4$ the induced path $\tilde{F}\circ\gamma:J\to\widetilde{W}^4$ is a piecewise fuzzy geodesic and of the same length as γ, where $J=[0,1]$. If $\widetilde{\mathfrak{F}}$ does not preserve lengths, then $\widetilde{\mathfrak{F}}$ is a topological folding of fuzzy Robertson-Walker space $\widetilde{W}^4$ model [12–14].

The fuzzy folding of $\bigcup\widetilde{M}_i\subseteq\widetilde{W}^4$ model is a folding $\tilde{f}:\bigcup\widetilde{M}_i\to\bigcup\widetilde{M}_i$ such that $\tilde{f}(\widetilde{M})=\widetilde{M}$ and any $\widetilde{M}_i$ belong to

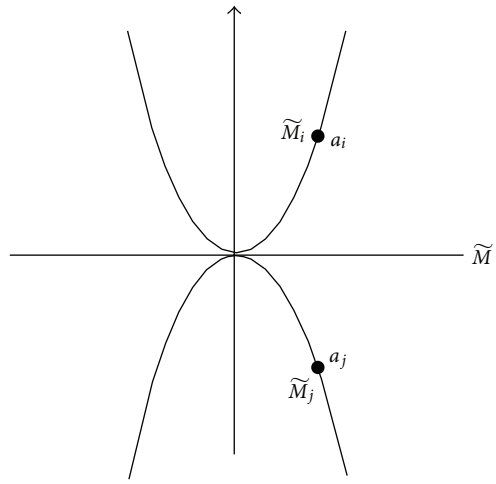

Figure 1

the upper hypermanifolds $\exists\, \widetilde{M}_j$ down $\widetilde{M}$ such that $\mu_i = \mu_j$ for every corresponding points, that is, $\mu(a_i) = \mu(a_j)$ [15]. See Figure 1.

2. Main Results

Theorem 1. *The fuzzy retractions of $\widetilde{W}^4$ model are the fuzzy unit hyperboloid, fuzzy hyperbolic, fuzzy hypersphere, fuzzy circle, and fuzzy minimal manifolds.*

Proof. Consider the $\widetilde{W}^4$ model with metric

$$ds^2(\mu) = d\chi^2(\mu) + \sinh^2\chi(\mu) \times \left(d\theta^2(\mu) + \sin^2\theta(\mu)\, d\emptyset^2(\mu)\right), \quad \mu \in [0,1]. \tag{2}$$

The coordinate of $\widetilde{W}^4$ model is

$$\begin{aligned} \widetilde{x}_1 &= \sinh\chi(\mu)\sin\theta(\mu)\cos\emptyset(\mu), \\ \widetilde{x}_2 &= \sinh\chi(\mu)\sin\theta(\mu)\sin\emptyset(\mu), \\ \widetilde{x}_3 &= \sinh\chi(\mu)\cos\theta(\mu), \\ \widetilde{x}_4 &= \cosh\chi(\mu), \end{aligned} \tag{3}$$

where the ranges are $0 \le \chi(\mu) < \infty, 0 \le \theta(\mu) < \pi$, and $0 \le \emptyset(\mu) < 2\pi$.

Now, we use Lagrangian equations:

$$\frac{d}{ds}\left(\frac{\partial T}{\partial \psi'(\mu)_i}\right) - \frac{\partial T}{\partial \psi(\mu)_i} = 0, \quad i = 1,2,3,4. \tag{4}$$

To find a fuzzy geodesic which is a fuzzy subset of $\widetilde{W}^4$ model, since

$$T = \frac{1}{2}\left\{\dot{\chi}^2(\mu) + \sinh^2\chi(\mu)\left(\dot{\theta}^2(\mu) + \sin^2\theta(\mu)\,\dot{\emptyset}^2(\mu)\right)\right\}, \tag{5}$$

then the Lagrangian equations for $\widetilde{W}^4$ model are

$$\frac{d}{ds}(\dot{\chi}(\mu)) - (\sinh\chi(\mu)\cosh\chi(\mu) \times \left(\dot{\theta}^2(\mu) + \sin^2\theta(\mu)\,\dot{\emptyset}^2(\mu)\right)) = 0, \tag{6}$$

$$\frac{d}{ds}\left(\sinh^2\chi(\mu)\,\dot{\theta}(\mu)\right) - \left(\sinh^2\chi(\mu)\sin\theta(\mu)\cos\theta(\mu)\,\dot{\emptyset}^2(\mu)\right) = 0,$$

$$\frac{d}{ds}\left(\sin^2\chi(\mu)\sin^2\theta(\mu)\,\dot{\emptyset}(\mu)\right) = 0, \tag{7}$$

$$-(\dot{\chi}(\mu)) + \left(\sinh\chi(\mu)\cosh\chi(\mu)\,\dot{\theta}^2(\mu) + \sinh^2\chi(\mu)\,\dot{\theta}(\mu)\right) + \left(\sinh\chi(\mu)\cosh\chi(\mu)\sin^2\theta(\mu)\,\dot{\emptyset}^2(\mu)\right. + \sinh^2\chi(\mu)\sin\theta(\mu)\cos\theta(\mu)\,\dot{\emptyset}^2(\mu) + \left.\sinh^2\chi(\mu)\sin^2\theta(\mu)\,\emptyset(\dot{\mu})\right) = 0. \tag{8}$$

From (7) we obtain $\sinh^2\chi(\mu)\sin^2\theta(\mu)\dot{\emptyset}(\mu) =$ constant, say β_1, if $\beta_1 = 0$, we obtain the following cases.

If initially θ equal $\pi/6$ or $\pi/4$ and $\pi/3$ hence we obtain the following fuzzy geodesics of fuzzy unit hyperboloid $\widetilde{H}_1^3$, $\widetilde{H}_2^3$, and $\widetilde{H}_3^3$, respectively. Also, if $\theta = \pi/2$, hence we obtain the following coordinates of $\widetilde{W}^4$ model given by

$$\begin{aligned} \widetilde{x}_1 &= \sinh\chi(\mu)\cos\emptyset(\mu), \\ \widetilde{x}_2 &= \sinh\chi(\mu)\sin\emptyset(\mu), \\ \widetilde{x}_3 &= 0, \\ \widetilde{x}_4 &= \cosh\chi(\mu), \end{aligned} \tag{9}$$

which is a fuzzy hyperbolic $\widetilde{H}_1^2$, $-\widetilde{x}_4^2 + \widetilde{x}_1^2 + \widetilde{x}_2^2 + \widetilde{x}_3^2 = -1$, which is a fuzzy geodesic retraction. Now, If $\emptyset = \pi/6$ or $\pi/4$ and $\pi/3$ hence we get the fuzzy unit hyperboloid retractions $\widetilde{H}_4^3$, $\widetilde{H}_5^3$ and, $\widetilde{H}_6^3$ in $\widetilde{W}^4$ model, respectively. Also, in a special case if $\emptyset = \pi/2$ or π and $3\pi/2$ hence we get the fuzzy hyperbolic geodesics $\widetilde{H}_2^2$, $\widetilde{H}_3^2$, and $\widetilde{H}_4^2$ in $\widetilde{W}^4$ model, respectively. In a special case if $\chi = \pi/2$, hence we get the coordinates of $\widetilde{W}^4$ model represented by

$$\begin{aligned} \widetilde{x}_1 &= \sin\theta(\mu)\cos\emptyset(\mu), \\ \widetilde{x}_2 &= \sin\theta(\mu)\sin\emptyset(\mu), \\ \widetilde{x}_3 &= \cos\theta(\mu) \\ \widetilde{x}_4 &= 0, \end{aligned} \tag{10}$$

which is a fuzzy sphere $\widetilde{S}_1^2$, $-\widetilde{x}_4^2 + \widetilde{x}_1^2 + \widetilde{x}_2^2 + \widetilde{x}_3^2 = -1$, which

is a fuzzy geodesic retraction. Also, If $\emptyset = 90$, and $\chi = 90$ we obtain the fuzzy retraction, $\widetilde{S}^1 = (0, \sin\theta(\mu), \cos\theta(\mu), 0)$, which is a fuzzy circle $\widetilde{S}^1$. Again, If $\chi = \pi$, we get the following minimal fuzzy geodesic $\widetilde{W}^0$ $(0, 0, 0, 1)$ in $\widetilde{W}^4$ model.

In what follows, we present some cases of fuzzy deformation retracts of $\widetilde{W}^4$ model. The fuzzy deformation retract of $\widetilde{W}^4$ model is $\eta : \widetilde{W}^4 \times I \to \widetilde{W}^4$, where I is the closed interval $[0, 1]$, present as

$$\begin{aligned}\widetilde{\eta}(x,h) : \{&\sinh\chi(\mu)\sin\theta(\mu)\cos\emptyset(\mu),\\ &\sinh\chi(\mu)\sin\theta(\mu)\sin\emptyset(\mu),\\ &\sinh\chi(\mu)\cos\theta(\mu), \cosh\chi(\mu)\} \times I\\ \longrightarrow \{&\sinh\chi(\mu)\sin\theta(\mu)\cos\emptyset(\mu),\\ &\sinh\chi(\mu)\sin\theta(\mu)\sin\emptyset(\mu),\\ &\sinh\chi(\mu)\cos\theta(\mu), \cosh\chi(\mu)\}.\end{aligned} \tag{11}$$

The fuzzy deformation retract of $\widetilde{W}^4$ model into the fuzzy minimal geodesic $\widetilde{W}^0$ is

$$\begin{aligned}\widetilde{\eta}(m,h) = (1+h)\{&\sinh\chi(\mu)\sin\theta(\mu)\cos\emptyset(\mu),\\ &\sinh\chi(\mu)\sin\theta(\mu)\sin\emptyset(\mu),\\ &\sinh\chi(\mu)\cos\theta(\mu), \cosh\chi(\mu)\}\\ &+ \tan\frac{\pi h}{4}\{0,0,0,1\},\end{aligned} \tag{12}$$

where

$$\begin{aligned}\widetilde{\eta}(m,0) = \{&\sinh\chi(\mu)\sin\theta(\mu)\cos\emptyset(\mu),\\ &\sinh\chi(\mu)\sin\theta(\mu)\sin\emptyset(\mu), \sinh\chi(\mu)\cos\theta(\mu),\\ &\cosh\chi(\mu)\},\\ \widetilde{\eta}(m,1) = \{&0,0,0,1\}.\end{aligned} \tag{13}$$

The fuzzy deformation retract of $\widetilde{W}^4$ model into the fuzzy hyperboloid $\widetilde{H}_1^2$ is

$$\begin{aligned}\widetilde{\eta}(m,h) = \cos\frac{\pi h}{2}\{&\sinh\chi(\mu)\sin\theta(\mu)\cos\emptyset(\mu),\\ &\sinh\chi(\mu)\sin\theta(\mu)\sin\emptyset(\mu),\\ &\sinh\chi(\mu)\cos\theta(\mu), \cosh\chi(\mu)\}\\ &+ \sin\frac{\pi h}{2}\{\sinh\chi(\mu)\cos\emptyset(\mu), \sinh\chi(\mu)\\ &\times\sin\emptyset(\mu), 0, \cosh\chi(\mu)\}.\end{aligned} \tag{14}$$

Now, we are going to discuss the fuzzy folding $\widetilde{\mathfrak{F}}$ of $\widetilde{W}^4$ model. Let $\widetilde{\mathfrak{F}} : \widetilde{W}^4 \to \widetilde{W}^4$, where

$$\widetilde{\mathfrak{F}}(\widetilde{x}_1, \widetilde{x}_2, \widetilde{x}_3, \widetilde{x}_4) = (\widetilde{x}_1, \widetilde{x}_2, |\widetilde{x}_3|, \widetilde{x}_4). \tag{15}$$

An isometric fuzzy folding of $\widetilde{W}^4$ model into itself may be defined by

$$\begin{aligned}\widetilde{\mathfrak{F}} : \{&\sinh\chi(\mu)\sin\theta(\mu)\cos\emptyset(\mu), \sinh\chi(\mu)\sin\theta(\mu)\\ &\times\sin\emptyset(\mu), \sinh\chi(\mu)\cos\theta(\mu), \cosh\chi(\mu)\}\\ \longrightarrow \{&\sinh\chi(\mu)\sin\theta(\mu)\cos\emptyset(\mu), \sinh\chi(\mu)\sin\theta(\mu)\\ &\times\sin\emptyset(\mu), |\sinh\chi(\mu)\cos\theta(\mu)|, \cosh\chi(\mu)\}.\end{aligned} \tag{16}$$

The fuzzy deformation retract of the fuzzy folded $\widetilde{\mathfrak{F}}(\widetilde{W}^4)$ model into the fuzzy folded geodesic $\widetilde{\mathfrak{F}}(\widetilde{W}^0)$ is

$$\begin{aligned}\widetilde{\eta}_{\widetilde{\mathfrak{F}}} : \{&\sinh\chi(\mu)\sin\theta(\mu)\cos\emptyset(\mu), \sinh\chi(\mu)\sin\theta(\mu)\\ &\sin\emptyset(\mu), |\sinh\chi(\mu)\cos\theta(\mu)|, \cosh\chi(\mu)\} \times I\\ \longrightarrow \{&\sinh\chi(\mu)\sin\theta(\mu)\cos\emptyset(\mu), \sinh\chi(\mu)\\ &\times\sin\theta(\mu)\sin\emptyset(\mu), |\sinh\chi(\mu)\cos\theta(\mu)|,\\ &\cosh\chi(\mu)\}.\end{aligned} \tag{17}$$

with

$$\begin{aligned}\widetilde{\eta}_{\widetilde{\mathfrak{F}}}(m,h) = (1+h)\{&\sinh\chi(\mu)\sin\theta(\mu)\cos\emptyset(\mu),\\ &\sinh\chi(\mu)\sin\theta(\mu)\sin\emptyset(\mu),\\ &|\sinh\chi(\mu)\ \cos\theta(\mu)|, \cosh\chi(\mu)\}\\ &+ \tan\frac{\pi h}{4}\{0,0,0,1\}.\end{aligned} \tag{18}$$

The fuzzy deformation retract of the fuzzy folded $\widetilde{\mathfrak{F}}(\widetilde{W}^4)$ model into the fuzzy folded geodesic $\widetilde{\mathfrak{F}}(\widetilde{H}_1^2)$ is

$$\begin{aligned}\widetilde{\eta}_{\widetilde{\mathfrak{F}}}(m,h) = \cos\frac{\pi h}{2}\{&\sinh\chi(\mu)\sin\theta(\mu)\cos\emptyset(\mu),\\ &\sinh\chi(\mu)\sin\theta(\mu)\sin\emptyset(\mu),\\ &|\sinh\chi(\mu)\cos\theta(\mu)|, \cosh\chi(\mu)\}\\ &+ \sin\frac{\pi h}{2}\{\sinh\chi(\mu)\ \cos\emptyset(\mu),\\ &\sinh\chi(\mu)\sin\emptyset(\mu), 0, \cosh\chi(\mu)\}.\end{aligned} \tag{19}$$

Then, the following theorem has been proved. □

Theorem 2. *Under the defined fuzzy folding and any fuzzy folding homeomorphic to this type of fuzzy folding, the fuzzy deformation retract of the fuzzy folded $\widetilde{\mathfrak{F}}(\widetilde{W}^4)$ model into the fuzzy folded geodesics is the same as the fuzzy deformation retract of $\widetilde{W}^4$ model into the fuzzy geodesics.*

Proof. Now, let the fuzzy folding be defined by $\widetilde{\mathfrak{F}}^* : \widetilde{W}^4 \to \widetilde{W}^4$, where

$$\widetilde{\mathfrak{F}}^* (\tilde{x}_1, \tilde{x}_2, \tilde{x}_3, \tilde{x}_4) = (|\tilde{x}_1|, \tilde{x}_2, \tilde{x}_3, \tilde{x}_4). \tag{20}$$

The isometric fuzzy folded $\widetilde{\mathfrak{F}}^*(\widetilde{W}^4)$ model is

$$\begin{aligned}\overline{\widetilde{R}} = \{&|\sinh \chi(\mu) \sin\theta(\mu) \cos\emptyset(\mu)|,\\ &\sinh \chi(\mu) \sin\theta(\mu) \sin\emptyset(\mu),\\ &\sinh \chi(\mu) \cos\theta(\mu), \cosh \chi(\mu)\}.\end{aligned} \tag{21}$$

The fuzzy deformation retract of the fuzzy folded $\widetilde{\mathfrak{F}}^*(\widetilde{W}^4)$ model into the fuzzy folded geodesic $\widetilde{\mathfrak{F}}^*(\widetilde{S}_1^2)$ is

$$\begin{aligned}\widetilde{\eta_{\mathfrak{F}^*}}(m,h) = (1-h)&\\ \times \{&|\sinh \chi(\mu) \sin\theta(\mu) \cos\emptyset(\mu)|,\\ &\sinh \chi(\mu) \sin\theta(\mu) \sin\emptyset(\mu),\\ &\sinh \chi(\mu) \cos\theta(\mu), \cosh \chi(\mu)\}\\ + \tan\frac{\pi h}{4} \{&|\sin\theta(\mu) \cos\emptyset(\mu)|,\\ &\sin\theta(\mu) \sin\emptyset(\mu), \cos\theta(\mu), 0\}.\end{aligned} \tag{22}$$

The fuzzy deformation retract of the fuzzy folded $\widetilde{\mathfrak{F}}^*(\widetilde{W}^4)$ model into the fuzzy folded geodesic $\widetilde{\mathfrak{F}}^*(\widetilde{H}_3^2)$ is

$$\begin{aligned}\widetilde{\eta_{\mathfrak{F}^*}}(m,h) = \cos\frac{\pi h}{2} \{&|\sinh \chi(\mu) \sin\theta(\mu) \cos\emptyset(\mu)|,\\ &\sinh \chi(\mu) \sin\theta(\mu) \sin\emptyset(\mu),\\ &\sinh \chi(\mu) \cos\theta(\mu), \cosh \chi(\mu)\}\\ + \sin\frac{\pi h}{2} \{&|\sinh \chi(\mu) \sin\theta(\mu)|, 0,\\ &\sinh \chi(\mu) \cos\theta(\mu), \cosh \chi(\mu)\}.\end{aligned} \tag{23}$$

Then, the following theorem has been proved. □

Theorem 3. *Under the defined fuzzy folding and any fuzzy folding homeomorphic to this type of fuzzy folding, the fuzzy deformation retract of the fuzzy folded $\widetilde{\mathfrak{F}}^*(\widetilde{W}^4)$ model into the fuzzy folded geodesics is different from the fuzzy deformation retract of $\widetilde{W}^4$ model into the fuzzy geodesics.*

Theorem 4. *Let $\widetilde{H}^3 \subset \widetilde{W}^4$ be a fuzzy hyperboloid in $\widetilde{W}^4$ model which is homeomorphic to $\{\widetilde{D}^2 - \widetilde{\beta}\} \subset \widetilde{R}^3$, and $\tilde{r}_1 : \widetilde{H}^3 \to \widetilde{H}^2$ a fuzzy retraction. Then, there is an induced fuzzy retraction $\tilde{r}_2 : \{\widetilde{D}^2 - \widetilde{\beta}\} \to \widetilde{D}^1$ such that the following diagram is commutative:*

$$\begin{array}{ccc} \tilde{H}^3 \subset \widetilde{W}^4 & \xrightarrow{\quad \tilde{P}_1 \quad} & \{\tilde{D}^2 - \tilde{\beta}\} \subset \tilde{R}^3 \\ \Big\downarrow \tilde{r}_1 & & \Big\downarrow \tilde{r}_2 \\ \tilde{H}^2 \subset \widetilde{W}^4 & \xrightarrow{\quad \tilde{P}_2 \quad} & \tilde{D}^1 \subset \tilde{R}^3 \end{array} \tag{24}$$

Proof. Under the condition $\theta = \pi/2$, then $\tilde{r}_1 : \widetilde{H}^3 \to \widetilde{H}^2$ is defined as $\tilde{r}_1\{\sinh\chi(\mu)\ \sin\theta(\mu)\ \cos\emptyset(\mu),\ \sinh\chi(\mu)\ \sin\theta(\mu)\ \sin\emptyset(\mu), \sinh\chi(\mu)\ \cos\theta(\mu),\ \cosh\chi(\mu)\} = \{\sinh\chi(\mu)\cos\emptyset(\mu), \sinh\chi(\mu)\sin\emptyset(\mu), 0, \cosh\chi(\mu)\}$ also under the condition $\theta = \pi/2$, then $\tilde{r}_2 : \{\widetilde{D}^2 - \widetilde{\beta}\} \to \widetilde{D}^1$ is defined as $\tilde{r}_2\{\{\sin\theta(\mu)\cos\emptyset(\mu),\ \sin\theta(\mu)\sin\emptyset(\mu),\ \cos\theta(\mu), 0\} - \widetilde{\beta}\} = \{\cos\emptyset(\mu), \sin\emptyset(\mu), 0, 0\}$. Under the homeomorphism map $\tilde{P}_1 : \widetilde{H}^3 \subset \widetilde{W}^4 \to \{\widetilde{D}^2 - \widetilde{\beta}\} \subset \widetilde{R}^3$ and $\tilde{P}_2 : \widetilde{H}^2 \subset \widetilde{W}^4 \to \widetilde{D}^1 \subset \widetilde{R}^3$. This proves that the diagram is commutative.

Also, the corresponding relations are described as that is,

$$\overline{\tilde{r}_2} \circ \overline{\tilde{p}_1} = \overline{\tilde{p}_2} \circ \overline{\tilde{r}_1}, \qquad \underline{\tilde{r}_2} \circ \underline{\tilde{p}_1} = \underline{\tilde{p}_2} \circ \underline{\tilde{r}_1}. \tag{25}$$

□

Theorem 5. *Let $\widetilde{H}^3 \subset \widetilde{W}^4$ be a fuzzy hyperboloid which is homeomorphic to $\{\widetilde{D}^2 - \widetilde{\beta}\} \subset \widetilde{R}^3$, and $\lim_{n\to\infty} \tilde{r}_n : \widetilde{H}^3 \to \widetilde{H}^2$ a limit fuzzy retraction. Then, there is an induced limit fuzzy retraction $\lim_{n\to\infty} \tilde{r}_{n+1} : \{\widetilde{D}^2 - \widetilde{\beta}\} \to \widetilde{D}^1$ such that the following diagram is commutative:*

$$\begin{array}{ccc} \tilde{H}^3 \subset \widetilde{W}^4 & \xrightarrow{\quad \tilde{P}_1 \quad} & (\tilde{D}^2 - \tilde{\beta}) \subset \tilde{R}^3 \\ \Big\downarrow \lim_{n\to\infty} \tilde{r}_n & & \Big\downarrow \lim_{n+1\to\infty} \tilde{r}_{n+1} \\ \tilde{H}^2 \subset \widetilde{W}^4 & \xrightarrow{\quad \tilde{P}_2 \quad} & \tilde{D}^1 \subset \tilde{R}^3 \end{array} \tag{26}$$

Proof. Since $\lim_{n\to\infty} \tilde{r}_n : \widetilde{H}^3 \to \widetilde{H}^2$ and $\lim_{n+1\to\infty} \tilde{r}_{n+1} : \{\widetilde{D}^2 - \widetilde{\beta}\} \to \widetilde{D}^1$, under the homeomorphism map $\tilde{P}_1 : \widetilde{H}^3 \subset \widetilde{W}^4 \to \{\widetilde{D}^2 - \widetilde{\beta}\} \subset \widetilde{R}^3$ and $\tilde{P}_2 : \widetilde{H}^2 \subset \widetilde{W}^4 \to \widetilde{D}^1 \subset \widetilde{R}^3$. This proves that the diagram is commutative. Also, the corresponding relations are presented as

$$\begin{aligned}\overline{\widetilde{\lim_{n+1\to\infty}} \tilde{r}_{n+1}} \circ \overline{\tilde{p}_1} &= \overline{\tilde{p}_2} \circ \overline{\widetilde{\lim_{n\to\infty}} \tilde{r}_n},\\ \underline{\widetilde{\lim_{n+1\to\infty}} \tilde{r}_{n+1}} \circ \underline{\tilde{p}_1} &= \underline{\tilde{p}_2} \circ \underline{\widetilde{\lim_{n\to\infty}} \tilde{r}_n}.\end{aligned} \tag{27}$$

□

Theorem 6. *If the fuzzy deformation retract of the fuzzy hyperboloid $\widetilde{H}^3 \subset \widetilde{W}^4$ is $\widetilde{D} : \widetilde{H}^3 \times I \to \widetilde{H}^3$, the fuzzy retraction of $\widetilde{H}^3 \subset \widetilde{W}^4$ is $\widetilde{r} : \widetilde{H}^3 \to \widetilde{H}^2$, and the limit of the fuzzy folding of $\widetilde{H}^3$ is $\lim_{m\to\infty}\widetilde{f}_m : \widetilde{H}^3 \to \widetilde{H}^2$. Then there are induced fuzzy deformation retract, fuzzy retraction, and the limit of the fuzzy foldings such that the following diagram is commutative.*

Proof. Let the fuzzy deformation retract of $\widetilde{H}^3 \subset \widetilde{W}^4$ be $\widetilde{D}_1 : \widetilde{H}^3 \times I \to \widetilde{H}^3$; the fuzzy retraction of $\widetilde{H}^3 \times I$ is defined by $\widetilde{r}_1 : (\widetilde{H}^3 \times I) \to \widetilde{H}^2 \times I$, $\lim_{m\to\infty}\widetilde{f}_m : \widetilde{D}_1(\widetilde{H}^3 \times I) \to \widetilde{H}^2$, the fuzzy deformation retract of $\widetilde{r}_1(\widetilde{H}^3 \times I)$ is $\widetilde{D}_2 : \widetilde{r}_1(\widetilde{H}^3 \times I) \to \widetilde{H}^2$, the fuzzy retraction of $\lim_{m\to\infty}\widetilde{f}_m \cdot (\widetilde{D}_1(\widetilde{H}^3 \times I))$ is given by $\widetilde{r}_2 : \lim_{m\to\infty}\widetilde{f}_m(\widetilde{D}_1(\widetilde{H}^3 \times I)) \to \widetilde{H}^1$, and $\lim_{m+1\to\infty}\widetilde{f}_{m+1} : \widetilde{D}_2(\widetilde{r}_1(\widetilde{H}^3 \times I)) \to \widetilde{H}^1$, $\widetilde{H}^1$ is a 1-dimensional space. Hence, the following diagram is commutative,

$$\begin{array}{ccccc}
(\widetilde{H}^3 \times I) & \longrightarrow & \widetilde{H}^2 \times I & \longrightarrow & \widetilde{H}^2 \\
\downarrow{\scriptstyle \widetilde{D}_1} & & & & \downarrow{\scriptstyle \lim_{m+1\to\infty}\widetilde{f}_{m+1}} \\
\widetilde{H}^3 & \xrightarrow[\lim_{m\to\infty}\widetilde{f}_m]{} & \widetilde{H}^2 & \xrightarrow[\widetilde{r}_2]{} & \widetilde{H}^1
\end{array} \tag{28}$$

that is, $\lim_{m+1\to\infty}\widetilde{f}_{m+1} \circ \widetilde{D}_2 \circ \widetilde{r}_1(\widetilde{H}^3 \times I) = \widetilde{r}_2 \circ \lim_{m\to\infty}\widetilde{f}_m \circ \widetilde{D}_1$. □

Theorem 7. *Let $\widetilde{H}^3 \subset \widetilde{W}^4$ be the fuzzy hyperboloid, then the relation between the fuzzy folding $\widetilde{f} : \widetilde{H}^3 \to \widetilde{H}^3$ and the limit of the fuzzy retractions $\lim_{m\to\infty}\widetilde{r}_m : \widetilde{H}^3 \to \widetilde{H}^2$ is discussed from the following commutative diagram.*

Proof. Let the fuzzy folding is $\widetilde{f}_1 : \widetilde{H}^3 \to \widetilde{H}^3$, the limit of the fuzzy retractions of $\widetilde{H}^3$ and $\widetilde{f}_1(\widetilde{H}^3)$ are $\lim_{m\to\infty}\widetilde{r}_m : \widetilde{H}^3 \to \widetilde{H}^2$ and $\lim_{m+1\to\infty}\widetilde{r}_{m+1} : \widetilde{f}_1(\widetilde{H}^3) \to \widetilde{H}^2$, and $\widetilde{f}_2 : (\lim_{m\to\infty}\widetilde{r}_m(\widetilde{H}^3)) \to \widetilde{H}^2$. Then, the following diagram is commutative:

$$\begin{array}{ccc}
\widetilde{H}^3 & \xrightarrow{\widetilde{f}_1} & \widetilde{H}^3 \\
\downarrow{\scriptstyle \lim_{m\to\infty}\widetilde{r}_m} & & \downarrow{\scriptstyle \lim_{m+1\to\infty}\widetilde{r}_{m+1}} \\
\widetilde{H}^2 & \xrightarrow[\widetilde{f}_2]{} & \widetilde{H}^2
\end{array} \tag{29}$$

that is, $\lim_{m+1\to\infty}\widetilde{r}_{m+1} \circ \widetilde{f}_1(\widetilde{H}^3) = \widetilde{f}_2 \circ \lim_{m\to\infty}\widetilde{r}_m(\widetilde{H}^3)$, and the corresponding relations between the two chains of fuzzy folding and the limit of fuzzy retraction are given by

$$\begin{aligned}
\overline{\lim_{m+1\to\infty}\widetilde{r}_{m+1}} \circ \overline{\widetilde{f}_1} &= \overline{\widetilde{f}_2} \circ \overline{\lim_{m\to\infty}\widetilde{r}_m}, \\
\underline{\lim_{m+1\to\infty}\widetilde{r}_{m+1}} \circ \widetilde{f}_1 &= \widetilde{f}_2 \circ \underline{\lim_{m\to\infty}\widetilde{r}_m}.
\end{aligned} \tag{30}$$

□

Theorem 8. *Let the fuzzy retraction of $\widetilde{H}^3$ is $\widetilde{r} : \widetilde{H}^3 \to \widetilde{H}^2$, $\widetilde{H}^2 \subset \widetilde{H}^3$, and the fuzzy folding of $\widetilde{H}^3$ is $\widetilde{f} : \widetilde{H}^3 \to \widetilde{H}^3$, then*

(i) $\widetilde{f}_2 \circ \widetilde{r}_1(\widetilde{H}^3) = \widetilde{r}_2 \circ \widetilde{f}_1(\widetilde{H}^3)$

(ii) $\widetilde{\sigma}_{n+1} \circ (\lim_{i\to\infty}(\widetilde{f}_{2i} \circ \widetilde{r}_{2i-1})(\cdots(\widetilde{f}_4 \circ \widetilde{r}_3(\widetilde{f}_2 \circ \widetilde{r}_1(\widetilde{H}^3)))\cdots)) = (\lim_{i\to\infty}(\widetilde{r}_{2i} \circ \widetilde{f}_{2i-1})(\cdots(\widetilde{r}_4 \circ \widetilde{f}_3(\widetilde{r}_2 \circ \widetilde{f}_1(\widetilde{H}^3)))\cdots)) \circ \widetilde{\sigma}_1$.

Proof. (i) Let the fuzzy retraction of the fuzzy hyperboloid in $\widetilde{H}^3 \subset \widetilde{W}^4$ model be $\widetilde{r}_1 : \widetilde{H}^3 \to \widetilde{H}^2$; $\widetilde{f}_1 : \widetilde{H}^3 \to \widetilde{H}^3$, the fuzzy retraction of $\widetilde{f}_1(\widetilde{H}^3)$ is folding of $\widetilde{r}_1(\widetilde{H}^3)$ is $\widetilde{f}_2 : \widetilde{r}_1(\widetilde{H}^3) \to \widetilde{r}_2 : \widetilde{f}_1(\widetilde{H}^3) \to \widetilde{H}^2$, and the fuzzy $\widetilde{H}^2$. Then $\widetilde{f}_2 \circ \widetilde{r}_1(\widetilde{H}^3) = \widetilde{r}_2 \circ \widetilde{f}_1(\widetilde{H}^3)$.

(ii) Let $\widetilde{f}_{2i} \circ \widetilde{r}_{2i-1}$ and $\widetilde{r}_{2i} \circ \widetilde{f}_{2i-1}$ are the compositions between the fuzzy retractions and the fuzzy foldings of $\widetilde{H}^3$ into itself. Also, $\widetilde{\sigma}_l$ are the homeomorphisms. Then

$$\begin{array}{ccccccccc}
\widetilde{H}^3 & \xrightarrow{\widetilde{f}_2 \circ \widetilde{r}_1} & H_1^3 & \xrightarrow{\widetilde{f}_4 \circ \widetilde{r}_3} & \widetilde{H}_2^3 & \cdots & \widetilde{H}_{n-1}^3 & \xrightarrow[i\to\infty]{\lim(\widetilde{f}_{2i} \circ \widetilde{r}_{2i-1})} & \widetilde{H}^2 \\
\downarrow{\scriptstyle \widetilde{\sigma}_1} & & \downarrow{\scriptstyle \widetilde{\sigma}_2} & & \downarrow{\scriptstyle \widetilde{\sigma}_3} & & \downarrow{\scriptstyle \widetilde{\sigma}_n} & & \downarrow{\scriptstyle \widetilde{\sigma}_{n+1}} \\
\widetilde{H}^3 & \xrightarrow[\widetilde{r}_2 \circ \widetilde{f}_1]{} & \widetilde{H}_1^3 & \xrightarrow[\widetilde{r}_4 \circ \widetilde{f}_3]{} & \widetilde{H}_2^3 & \cdots & \widetilde{H}_{n-1}^3 & \xrightarrow[i\to\infty]{\lim(\widetilde{r}_{2i} \circ \widetilde{f}_{2i-1})} & \widetilde{H}^2
\end{array} \tag{31}$$

□

Theorem 9. *Given the fuzzy deformation retract of $\widetilde{H}^3 \subset \widetilde{W}^4$ model is $\widetilde{D} : \widetilde{H}^3 \times I \to \widetilde{H}^3$; the limit of the fuzzy folding of $\widetilde{H}^3 \times I$ is $\lim_{m\to\infty}\widetilde{f}_m : \widetilde{H}^3 \times I \to \widetilde{H}^2 \times I$. Then, the following diagram is commutative.*

Proof. Let the limit of the fuzzy folding of $(\widetilde{H}^3 \times I)$ is $\lim_{m\to\infty}\widetilde{f}_m : \widetilde{H}^3 \times I \to \widetilde{H}^2 \times I$, the fuzzy deformation retract of $\widetilde{H}^3 \subset \widetilde{W}^4$ onto $\widetilde{H}^2$ is $\widetilde{D}_1(\widetilde{H}^3 \times I) = \widetilde{H}^2$, the limit of the fuzzy folding of $\widetilde{D}_1(\widetilde{H}^3 \times I)$ is $\lim_{m+1\to\infty}\widetilde{f}_{m+1} : \widetilde{D}_1(\widetilde{H}^3 \times I) \to \widetilde{H}^1$, and the fuzzy deformation retract of $\lim_{m\to\infty}\widetilde{f}_m(\widetilde{H}^3 \times I)$ onto $\widetilde{H}^1$ is $\widetilde{D}_2(\lim_{m\to\infty}\widetilde{f}_m(\widetilde{H}^3 \times I)) = \widetilde{H}^1$. Hence

$$\begin{array}{ccc}
\widetilde{H}^3 \times I & \xrightarrow{\lim_{m\to\infty}\widetilde{f}_m} & \widetilde{H}^2 \times I \\
\downarrow{\scriptstyle \widetilde{D}_1} & & \downarrow{\scriptstyle \widetilde{D}_2} \\
\widetilde{H}^2 & \xrightarrow[\lim_{m+1\to\infty}\widetilde{f}_{m+1}]{} & \widetilde{H}^1
\end{array} \tag{32}$$

that is, $\widetilde{D}_2 \circ \lim_{m\to\infty}\widetilde{f}_m(\widetilde{H}^3 \times I) = \lim_{m+1\to\infty}\widetilde{f}_{m+1} \circ \widetilde{D}_1(\widetilde{H}^3 \times I)$ □

Theorem 10. *The composition of fuzzy deformation retracts of fuzzy hyperboloid $\widetilde{H}^3 \subset \widetilde{W}^4$ model is a minimal retraction.*

Proof. Now consider the following fuzzy continuous map $\widetilde{\eta}: \widetilde{H}^3 \times [0,1] \to \widetilde{H}^3$, such that $\widetilde{\eta}(\widetilde{x},\widetilde{s}) = \widetilde{\beta}(\widetilde{x},(\widetilde{s}/(1-\widetilde{s})))$, then it is easy to see that

$$\begin{aligned}\widetilde{\eta}(\widetilde{x},0) &= \widetilde{\beta}(\widetilde{x},0) = 0,\\ \widetilde{\eta}(\widetilde{x},1) &= \lim_{s\to 1}\widetilde{\beta}\left(\widetilde{x},\frac{\widetilde{s}}{1-\widetilde{s}}\right) = \widetilde{S}_1^2 \subset \widetilde{H}^3,\\ \widetilde{\eta}(\widetilde{y},s) &= \widetilde{\beta}\left(\widetilde{y},\frac{\widetilde{s}}{1-\widetilde{s}}\right) = \widetilde{S}^1 \subset \widetilde{S}_1^2.\end{aligned} \tag{33}$$

The fuzzy deformation retract of the fuzzy circle $\widetilde{S}^1 \subset \widetilde{S}_1^2$ onto minimal fuzzy retraction $((0,1),\mu)$ is given in polar coordinates by

$$\widetilde{\mu}\left(r(\mu)e^{i\theta(\mu)}\right) = \begin{cases}\widetilde{r}e^{i(1-r(\mu))\theta(\mu)}, & |\theta(\mu)| \le \dfrac{\pi}{2},\\ \widetilde{r}e^{i\{\theta(\mu)-(\pi-\theta(\mu))r(\mu)\}}, & \dfrac{\pi}{2} \le \theta(\mu) \le \pi,\\ \widetilde{r}e^{i\{\theta(\mu)+(\pi+\theta(\mu))r(\mu)\}}, & -\pi \le \theta(\mu) \le -\dfrac{\pi}{2},\end{cases} \tag{34}$$

that is, $\widetilde{\mu}\circ\widetilde{\eta}$ is a fuzzy minimal retraction. □

Theorem 11. *Let $\widetilde{H}^3 \subset \widetilde{W}^4$ be a fuzzy hyperboloid in $\widetilde{W}^4$ model which is homeomorphic to $\{\widetilde{D}^2 - \widetilde{\beta}\} \subset \widetilde{R}^3$, $\widetilde{P}_1: \widetilde{H}^3 \to \{\widetilde{D}^2 - \widetilde{\beta}\}$, the fuzzy retraction $\widetilde{r}_1 : \widetilde{H}^3 \to \widetilde{H}^2$, and the limit fuzzy folding of $\widetilde{D}^2$ is $\lim_{n\to\infty} \widetilde{f}_n : \{\widetilde{D}^2 - \widetilde{\beta}\} \to \widetilde{D}^1$. Then there are induced fuzzy retraction, limit fuzzy folding, and homeomorphism map such that the following diagram is commutative:*

$$\begin{array}{ccccc}\widetilde{H}^3 \subset \widetilde{W}^4 & \xrightarrow{\widetilde{r}_1} & \widetilde{H}^2 \subset \widetilde{W}^4 & \xrightarrow{\widetilde{r}_2} & \widetilde{H}^1 \subset \widetilde{W}^4\\ \downarrow \widetilde{P}_1 & & & & \downarrow \widetilde{P}_2\\ \{\widetilde{D}^2 - \widetilde{\beta}\} & \xrightarrow{\lim_{n\to\infty}\widetilde{f}_n} & \widetilde{D}^1 \subset \widetilde{R}^3 & \xrightarrow{\lim_{n+1\to\infty}\widetilde{f}_{n+1}} & \widetilde{D}^0\end{array} \tag{35}$$

Proof. Let the homeomorphism map, $\widetilde{P}_1 : \widetilde{H}^3 \to \{\widetilde{D}^2 - \widetilde{\beta}\}$ and $\widetilde{r}_1 : \widetilde{H}^3 \to \widetilde{H}^2$, also, $\lim_{n\to\infty} \widetilde{f}_n : \{\widetilde{D}^2 - \widetilde{\beta}\} \to \widetilde{D}^1$, the fuzzy retraction of $\widetilde{r}_1(\widetilde{H}^3)$ be $\widetilde{r}_2 : \widetilde{H}^2 \to \widetilde{H}^1$; the limit fuzzy folding of $\lim_{n\to\infty} \widetilde{f}_n(\{\widetilde{D}^2 - \widetilde{\beta}\})$ is given by $\lim_{n+1\to\infty} \widetilde{f}_{n+1} : \widetilde{D}^1 \to \widetilde{D}^0$, and $\widetilde{P}_2 : \widetilde{r}_2(\widetilde{r}_1(\widetilde{H}^3)) \to \widetilde{D}^0$. This proves that the diagram is commutative. □

Theorem 12. *If the limit fuzzy folding of the fuzzy hyperboloid $\widetilde{H}^3 \subset \widetilde{W}^4$ is $\lim_{n\to\infty}\widetilde{f}_n : \widetilde{H}^3 \to \widetilde{H}^2$, the fuzzy retraction of $\widetilde{H}^3 \subset \widetilde{W}^4$ is $\widetilde{r}_1 : \widetilde{H}^3 \to \widetilde{H}^2$ and the homeomorphism map of $\widetilde{H}^2 \subset \widetilde{W}^4$ is $\widetilde{P}_1 : \widetilde{H}^2 \to \widetilde{D}^1$. Then there are induced limit fuzzy retractions, limit fuzzy folding, and homeomorphism map such that the following diagram is commutative:*

$$\begin{array}{ccccc}\widetilde{H}^3 \subset \widetilde{W}^4 & \xrightarrow{\widetilde{r}_1} & \widetilde{H}^2 \subset \widetilde{W}^4 & \xrightarrow{\lim_{m\to\infty}\widetilde{r}_m} & \widetilde{H}^1 \subset \widetilde{W}^4\\ \downarrow \lim_{n\to\infty}\widetilde{f}_n & & & & \downarrow \widetilde{P}_2\\ \widetilde{H}^2 & \xrightarrow{\widetilde{P}_1} & \widetilde{D}^1 & \xrightarrow{\lim_{n+1\to\infty}\widetilde{f}_{n+1}} & \widetilde{D}^0\end{array} \tag{36}$$

Proof. Consider the limit fuzzy folding of the fuzzy hyperboloid $\widetilde{H}^3 \subset \widetilde{W}^4$ is $\lim_{n\to\infty}\widetilde{f}_n : \widetilde{H}^3 \to \widetilde{H}^2$, the fuzzy retraction of $\widetilde{H}^3 \subset \widetilde{W}^4$ is $\widetilde{r}_1 : \widetilde{H}^3 \to \widetilde{H}^2$, and the homeomorphism map of $\widetilde{H}^2 \subset \widetilde{W}^4$ is $\widetilde{P}_1 : \widetilde{H}^2 \to \widetilde{D}^1$, the limit fuzzy retraction of $\widetilde{r}_1(\widetilde{H}^3)$ is $\lim_{m\to\infty}\widetilde{r}_m : \widetilde{H}^2 \to \widetilde{H}^1$, the limit fuzzy folding of $\widetilde{P}_1(\widetilde{H}^2)$ is $\lim_{n+1\to\infty} \widetilde{f}_{n+1} : \widetilde{D}^1 \to \widetilde{D}^0$, and $\widetilde{P}_2 : \lim_{m\to\infty}\widetilde{r}_m(\widetilde{r}_1(\widetilde{H}^3)) \to \widetilde{D}^0$. This proves that the diagram is commutative. □

Theorem 13. *Let $\widetilde{D\cdot R} : \widetilde{H}^3 \times I \to \widetilde{H}^3$ and $\widetilde{r}_1 : \widetilde{H}^3 \times I \to \widetilde{H}^2$ be a fuzzy retraction, and also $\widetilde{f} : \widetilde{H}^3 \times I \to \widetilde{H}^3 \times I$ a fuzzy folding. Then, there is induced limit fuzzy folding $\lim_{n\to\infty}\widetilde{f}_n : \widetilde{H}^3 \to \widetilde{H}^2$ such that the following diagram is commutative:*

$$\begin{array}{ccc}\widetilde{H}^3 \times I & \xrightarrow{\widetilde{D}\cdot\widetilde{R}} & \widetilde{H}^3\\ \downarrow \widetilde{f} & & \downarrow \lim_{n\to\infty}\widetilde{f}_n\\ \widetilde{H}^3 \times I & \xrightarrow{\widetilde{r}_1} & \widetilde{H}^2\end{array} \tag{37}$$

Proof. Let $\widetilde{D\cdot R} : \widetilde{H}^3 \times I \to \widetilde{H}^3$, and the fuzzy folding $\widetilde{f} : \widetilde{H}^3 \times I \to \widetilde{H}^3 \times I$, also $\widetilde{r}_1 : \widetilde{H}^3 \times I \to \widetilde{H}^2$, and the limit fuzzy folding $\lim_{n\to\infty}\widetilde{f}_n : \widetilde{H}^3 \to \widetilde{H}^2$. This proves that the diagram is commutative. □

Theorem 14. *If the fuzzy retraction of the fuzzy hyperboloid $\widetilde{H}^3 \subset \widetilde{W}^4$ is $\widetilde{r} : \widetilde{H}^3 \times I \to \widetilde{H}^2 \times I$, the fuzzy deformation retract of $\widetilde{H}^3 \times I \subset \widetilde{W}^4$ is $\widetilde{D}_1 : \widetilde{H}^3 \times I \to \widetilde{H}^3$, and the fuzzy deformation retract of $\widetilde{H}^2$ is $\widetilde{D}_2 : \widetilde{H}^2 \times I \to \widetilde{H}^2$. Then there are induced end limit fuzzy retractions and fuzzy folding such that the following diagram is commutative.*

Proof. Let $\widetilde{r}_1 : \widetilde{H}^3 \times I \to \widetilde{H}^2 \times I$ and $\widetilde{D}_1 : \widetilde{H}^3 \times I \to \widetilde{H}^3$ also, $\widetilde{D}_2 : \widetilde{r}_1(\widetilde{H}^3 \times I) \to \widetilde{H}^2$; the end limits fuzzy retractions of $\widetilde{D}_1(\widetilde{H}^3 \times I)$ are end $\lim \widetilde{r}_1 : \widetilde{D}_1(\widetilde{H}^3 \times I) \to 0$; the end limits fuzzy retractions of $\widetilde{D}_2(\widetilde{H}^2 \times I)$ are end $\lim r_2$:

$\widetilde{D}_2(\widetilde{H}^2 \times I)) \to 0$, and $\widetilde{f}$: end lim $\widetilde{r}_1(\widetilde{D}_1(\widetilde{H}^3 \times I) \to 0$, then the following diagram is commutative,

$$\begin{array}{ccccc} (\widetilde{H}^3 \times I) & \xrightarrow{\widetilde{D_1}} & \widetilde{H}^3 & \xrightarrow{\text{end lim}\,\widetilde{r_1}} & 0 \\ \downarrow{\scriptstyle \widetilde{r}_1} & & & & \downarrow{\scriptstyle \widetilde{f}} \\ \widetilde{H}^2 \times I & \xrightarrow{\widetilde{D_2}} & \widetilde{H}^2 & \xrightarrow{\text{end lim}\,\widetilde{r_2}} & 0 \end{array} \tag{38}$$

that is, $\widetilde{f} \circ (\text{end lim } \widetilde{r}_1 \circ \widetilde{D}_1(\widetilde{H}^3 \times I)) = \text{end lim } \widetilde{r}_2 \circ (\widetilde{D}_2 \circ \widetilde{r}_1)$.

Also, the corresponding relation is described by the two induced chains, that is,

$$\begin{aligned} \overline{\widetilde{f}} \circ \overline{\left(\text{ end lim } \widetilde{r}_1 \circ \widetilde{D}_1 \left(\widetilde{H}^3 \times I\right)\right)} &= \overline{\text{end lim}\,\widetilde{r}_2} \circ \overline{\left(\widetilde{D}_2 \circ \widetilde{r}_1\right)}, \\ \underline{\widetilde{f}} \circ \underline{\left(\text{end lim } \widetilde{r}_1 \circ \widetilde{D}_1 \left(\widetilde{H}^3 \times I\right)\right)} &= \underline{\text{end lim}\,\widetilde{r}_2} \circ \underline{\left(\widetilde{D}_2 \circ \widetilde{r}_1\right)}. \end{aligned} \tag{39}$$

□

Theorem 15. *Let $\widetilde{H}^3 \subset \widetilde{W}^4$ be the fuzzy hyperboloid, then the relations between the fuzzy deformation retract and the limit fuzzy folding is discussed from the following commutative diagram.*

Proof. Let the fuzzy deformation retract $\widetilde{D}_1 : \widetilde{H}^3 \times I \to \widetilde{H}^3$; the limit fuzzy folding of $\widetilde{H}^3$ and $\widetilde{D}_1(\widetilde{H}^3 \times I)$ is $\lim_{m\to\infty}\widetilde{f}_m : \widetilde{H}^3 \times I \to \widetilde{H}^2 \times I$ and $\lim_{m+1\to\infty}\widetilde{f}_{m+1} : \widetilde{D}_1(\widetilde{H}^3 \times I) \to \widetilde{H}^2$, and $\widetilde{D}_2 : (\lim_{m\to\infty}\widetilde{f}_m(\widetilde{H}^3 \times I)) \to \widetilde{H}^2$. Then, we have the following diagram,

$$\begin{array}{ccc} \widetilde{H}^3 \times I & \xrightarrow{\widetilde{D}_1} & \widetilde{H}^3 \\ \downarrow{\scriptstyle \lim_{m\to\infty}\widetilde{f}_m} & & \downarrow{\scriptstyle \lim_{m+1\to\infty}\widetilde{f}_{m+1}} \\ \widetilde{H}^2 \times I & \xrightarrow[\widetilde{D}_2]{} & \widetilde{H}^2 \end{array} \tag{40}$$

that is, $\lim_{m+1\to\infty}\widetilde{f}_{m+1} \circ \widetilde{D}_1(\widetilde{H}^3 \times I) = \widetilde{D}_2 \circ \lim_{m\to\infty}\widetilde{f}_m(\widetilde{H}^3 \times I)$.

Also, the corresponding relations are described by the two induced chains, that is,

$$\begin{aligned} \overline{\widetilde{\lim_{m+1\to\infty}} f_{m+1}} \circ \overline{\widetilde{D}_1} &= \overline{\widetilde{D}_2} \circ \overline{\widetilde{\lim_{m\to\infty}} f_m}, \\ \underline{\widetilde{\lim_{m+1\to\infty}} f_{m+1}} \circ \underline{\widetilde{D}_1} &= \underline{\widetilde{D}_2} \circ \underline{\widetilde{\lim_{m\to\infty}} f_m}. \end{aligned} \tag{41}$$

□

3. Conclusion

In the present paper, we obtain and study new types of fuzzy retractions of $\widetilde{W}^4$ model. Also, we deduced new types of fuzzy deformation retract of $\widetilde{W}^4$ model. The relations between the fuzzy folding and the fuzzy deformation retracts of $\widetilde{W}^4$ model is obtained. New types of minimal fuzzy retraction of $\widetilde{W}^4$ model is also presented. New types of homotopy maps are described. The isometric and topological fuzzy folding in each case and the relation between the fuzzy deformation retract after and before fuzzy folding have been obtained. Types of conditional fuzzy folding of $\widetilde{W}^4$ model are described.

References

[1] B. Schmeikal, *Primordial Space—The Metric Case*, Nova Science, New York, NY, USA, 2010.

[2] F. Catoni, D. Boccaletti, R. Cannata, V. Catoni, and P. Zampetti, *Geometry of Minkowski Space-Time*, Birkhauser, Boston, Mass, USA, 2011.

[3] F. Catoni, D. Boccaletti, R. Cannata, V. Catoni, E. Nichelatti, and P. Zampetti, *The Mathematics of Minkowski Space-Time*, Birkhauser, Boston, Mass, USA, 2008.

[4] J. B. Hartle, *Gravity, An Introduction to Einstein's General Relativity*, Addison-Wesley, New York, NY, USA, 2003.

[5] J. B. Griffiths and J. Podolsky, *Exact Space-Times in Einstein's General Relativity*, Cambridge University Press, Cambridge, UK, 2009.

[6] N. Straumann, *General Relativity with Application to Astrophysics*, Springer, New York, NY, USA, 2004.

[7] A. E. El-Ahmady, "Folding of fuzzy hypertori and their retractions," *Proceedings of the Mathematical and Physical Society of Egypt*, vol. 85, no. 1, pp. 1–10, 2007.

[8] A. E. El-Ahmady, "Limits of fuzzy retractions of fuzzy hyperspheres and their foldings," *Tamkang Journal of Mathematics*, vol. 37, no. 1, pp. 47–55, 2006.

[9] G. L. Naber, *Topology, Geometry and Gauge Fields: Foundations*, Texts in Applied Mathematics 25, Springer, New York, NY, USA, 2nd edition, 2011.

[10] G. L. Naber, *Topology, Geometry and Gauge Fields: Interactions, Applied Mathematics Sciences*, Springer, New York, NY, USA, 2nd edition, 2011.

[11] M. Reid and B. Szendroi, *Topology and Geometry*, Cambridge University Press, Cambridge, UK, 2005.

[12] A. E. El-Ahmady, "The variation of the density functions on chaotic spheres in chaotic space-like Minkowski space time," *Chaos, Solitons and Fractals*, vol. 31, no. 5, pp. 1272–1278, 2007.

[13] A. E. El-Ahmady and A. El-Araby, "On fuzzy spheres in fuzzy Minkowski space," *Nuovo Cimento della Societa Italiana di Fisica B*, vol. 125, no. 10, pp. 1153–1160, 2010.

[14] A. E. El-Ahmady, "Fuzzy Lobachevskian space and its folding," *The Journal of Fuzzy Mathematics*, vol. 12, no. 2, pp. 609–614, 2004.

[15] A. E. El-Ahmady, "Fuzzy folding of fuzzy horocycle," *Circolo Matematico Di Palermo Serie II*, vol. 53, no. 3, pp. 443–450, 2004.

[16] A. P. Balachandran, S. Kurkcuoglu, and S. Vaidya, *Lectures on Fuzzy and Fuzzy Susy Physics*, World Scientific Publishing, New York, NY, USA, 2007.

[17] L. A. Zadeh, *Fuzzy Sets and Their Application to Congnitive and Decision*, Academic Press, New York, NY, USA, 1975.

[18] N. Palaniappan, *Fuzzy Topology*, Alpha Science International, London, UK, 2005.

Hindawi Publishing Corporation
Advances in Fuzzy Systems
Volume 2013, Article ID 294971, 9 pages
http://dx.doi.org/10.1155/2013/294971

Research Article

Stabilizing Fuzzy Output Control for a Class of Nonlinear Systems

Dušan Krokavec and Anna Filasová

Department of Cybernetics and Artificial Intelligence, Faculty of Electrical Engineering and Informatics, Technical University of Košice, Letná 9, 042 00 Košice, Slovakia

Correspondence should be addressed to Dušan Krokavec; dusan.krokavec@tuke.sk

Received 27 September 2012; Revised 15 December 2012; Accepted 17 December 2012

Academic Editor: Sendren Sheng-Dong Xu

The paper presents new conditions suitable in design of a stabilizing output controller for a class of continuous-time nonlinear systems, represented by Takagi-Sugeno models. Taking into account the affine properties of the TS model structure and applying the fuzzy control scheme relating to the parallel distributed output compensators, the sufficient design conditions are outlined in terms of linear matrix inequalities. The proposed procedure decouples the Lyapunov matrix and the system parameter matrices in the LMIs and guarantees global stability of the system. Simulation result illustrates the design procedure and demonstrates the performances of the proposed design method.

1. Introduction

Contrarily to the linear framework, nonlinear systems are too complex to be represented by unified mathematical resources, and so a generic method has not been developed yet to design a controller valid for all types of nonlinear systems. An alternative to nonlinear system models is Takagi-Sugeno (TS) fuzzy approach [1], which benefits from the advantages of suitable linear approximation. Using the TS fuzzy model, each rule utilizes the local system dynamics by a linear model and the nonlinear system is represented by a collection of fuzzy rules. Recently, TS model based fuzzy control approaches are being fast and successfully used in nonlinear control frameworks. As a result, a range of stability analysis conditions [2–5], as well as control design methods [6–11], have been developed for TS fuzzy systems, relying mostly on the feasibility of an associated set of linear matrix inequalities (LMI) [12]. An important fact is that the design problem is a standard feasibility problem with several LMIs, potentially reformulated such that the feedback gains can be solved numerically. In consequence, the state feedback control based on fuzzy TS systems model is mostly realized in such structures which can be designed using a technique based on LMIs.

The TS fuzzy model-based state control is based on an implicit assumption that all states are available for measurement. If it is impossible, TS fuzzy observers are used to estimate the unmeasurable states variables, and the state controller exploits the system state variable estimate values [13–15]. The nonlinear output feedback design is so formulated as the two LMI set problems, and treated by the two-stage procedure, that is, dealing with a set of LMIs for the observer parameters at first and then solving another set of LMIs for the controller parameters [16]. Since the fuzzy control design problem is preferred to be formulated as a one LMI set problem, such formulation for the output feedback control design is proposed in [17, 18].

The main contribution of the paper is the presentation of the original design condition of the fuzzy output feedback control for the continuous-time nonlinear MIMO systems approximated by a TS model. The central idea of the TS fuzzy model-based control design, that is, to derive control rules so as to compensate each rule of a fuzzy system and construct the control strategy based on the parallel distributed compensators, is reflected in the approach of output control, taking into account the fact that the desired output variables are measurable. Motivated by the above-mentioned observations, the proposed design method combines the principles given in [15, 17], respecting the results presented in [19], and is constructed on an enhanced form of quadratic Lyapunov function [20]. Comparing with the approaches based on a quadratic Lyapunov matrix [15, 17, 21], which are particularly in the case of a large number of rules very conservative as a common symmetric positive definite matrix

is used to verify all Lyapunov inequalities, presented principle naturally extends the affine TS model properties using slack matrix variables to decouple Lyapunov matrix and the system matrices in LMIs, does not use iterative algorithms based on LMIs or matrix norm bounds, and gives substantial reducing of conservativeness. Potentially, extra constraints can be imposed to the slack matrices, but such additive constraints can potentially increase the conservativeness of the proposed design conditions.

The remainder of this paper is organized as follows. In Section 2 the structure of TS model for considered class of nonlinear systems is briefly described, and some of its properties are outlined. The output feedback control design problem for systems with measurable premise variables is given in Section 3, where the design conditions that guarantee global quadratic stability are formulated and proven. The method is reformulated in Section 4 in a newly defined enhanced criterion for fuzzy output feedback control design. Section 5 gives the numerical example to illustrate the effectiveness of the proposed approach and to confirm the validity of the control scheme. The last section draws conclusions and some future directions.

Throughout the paper, the following notations are used: $\mathbf{x}^T$, $\mathbf{X}^T$ denote the transpose of the vector $\mathbf{x}$ and matrix $\mathbf{X}$, respectively, diag[·] denotes a block diagonal matrix, for a square matrix $\mathbf{X} = \mathbf{X}^T > 0$ (resp., $\mathbf{X} = \mathbf{X}^T < 0$) means that $\mathbf{X}$ is a symmetric positive definite matrix (resp., negative definite matrix), the symbol $\mathbf{I}_n$ represents the nth order unit matrix, $\mathbb{R}$ denotes the set of real numbers, and $\mathbb{R}^{n\times r}$ denotes the set of all $n \times r$ real matrices.

2. Takagi-Sugeno Fuzzy Models

The systems under consideration are from one class of multiinput and multioutput nonlinear (MIMO) dynamic systems, represented in state-space form as

$$\dot{\mathbf{q}}(t) = \mathbf{a}(\mathbf{q}(t)) + \mathbf{b}(\mathbf{q}(t))\,\mathbf{u}(t), \tag{1}$$

$$\mathbf{y}(t) = \mathbf{C}\mathbf{q}(t), \tag{2}$$

where $\mathbf{q}(t) \in \mathbb{R}^n$, $\mathbf{u}(t) \in \mathbb{R}^r$, and $\mathbf{y}(t) \in \mathbb{R}^m$ are vectors of the state, input, and output variables, $\mathbf{C} \in \mathbb{R}^{m\times n}$ is a real finite values matrix, and $m \le n$, $r \le n$, respectively.

Considering that the number of the nonlinear terms in $\mathbf{a}(\mathbf{q}(t))$ is p, there exists a set of nonlinear sector functions as follows:

$$\begin{aligned} &m_{lj}\left(\theta_j(t)\right), \quad j = 1, 2, \dots, k,\ l = 1, 2, \dots, p, \\ &m_{l1}\left(\theta_j(t)\right) = 1 - \sum_{j=2}^{k} m_{lj}\left(\theta_j(t)\right), \end{aligned} \tag{3}$$

where k is the number of sectors, and

$$\boldsymbol{\theta}(t) = \left[\theta_1(t)\ \ \theta_2(t)\ \ \cdots\ \ \theta_q(t)\right] \tag{4}$$

is the vector of premise variables. It is assumed that the premise variable is a system state variable, or a measurable external variable, and none of the premise variables does not depend on the inputs $\mathbf{u}(t)$.

Using a TS model, the conclusion part of a single rule consists no longer of a fuzzy set [3], but determines a function with state variables as arguments, and the corresponding function is a local function for the fuzzy region that is described by the premise part of the rule. Thus, using linear functions, a system state is described locally (in fuzzy regions) by linear models, and at the boundaries between regions an interpolation is used between the corresponding local models.

Thus, constructing the set of membership functions $\{w_i(\boldsymbol{\theta}(t)) = \prod_{j=1}^{s} m_{lj}(\theta_j(t)),\ i = 1, 2, \dots s,\ s = 2^k\}$ from all combinations of sector functions, the final states of the systems are inferred as follows:

$$\dot{\mathbf{q}}(t) = \sum_{i=1}^{s} h_i(\boldsymbol{\theta}(t))\left(\mathbf{A}_i\mathbf{q}(t) + \mathbf{B}_i\mathbf{u}(t)\right) \tag{5}$$

with the output given by the relation

$$\mathbf{y}(t) = \mathbf{C}\mathbf{q}(t), \tag{6}$$

where

$$h_i(\boldsymbol{\theta}(t)) = \frac{w_i(\boldsymbol{\theta}(t))}{\sum_{i=1}^{s} w_i(\boldsymbol{\theta}(t))} \tag{7}$$

is the average weight for the ith rule, representing the normalized grade of membership (membership function). By definition, the membership functions satisfy the following convex sum properties:

$$0 \le h_i(\boldsymbol{\theta}(t)) \le 1, \quad \sum_{i=1}^{s} h_i(\boldsymbol{\theta}(t)) = 1 \quad \forall i \in \langle 1, \dots, s\rangle. \tag{8}$$

Assuming that $\mathbf{a}(\mathbf{q}(t))$ and $\mathbf{b}(\mathbf{q}(t))$ are bounded in sectors, that is, in the fuzzy regions within the system will operate, and $\mathbf{a}(\mathbf{q}(t))$ takes the value $\mathbf{a}(\mathbf{0}) = \mathbf{0}$, the fuzzy approximation of (1) leads to (6). Thus, $\mathbf{A}_i \in \mathbb{R}^{n\times n}$ is the matrix of $\mathbf{a}(\mathbf{p}(t))$, $\mathbf{B}_i \in \mathbb{R}^{n\times r}$ is the matrix of $\mathbf{b}(\mathbf{p}(t))$, respectively, both for $\mathbf{p}(t) = \mathbf{p}_i$, where $\mathbf{p}_i$ is the ith combination of the bounds of the sector functions with respect to the center of the ith fuzzy region, dedicated by (3). It is evident that a general fuzzy model is achieved by fuzzy amalgamation of the linear systems models.

Note, the model (5) and (6) is mostly considered for analysis, control, and state estimation of nonlinear systems.

Assumption 1. Each triplet $(\mathbf{A}_i, \mathbf{B}_i, \mathbf{C})$ is locally controllable and observable, the matrix $\mathbf{C}$ is the same for all local models, and the number of input variables is equal to the number of output variables.

It is supposed in the following considerations that the aforementioned model does not include parameter uncertainties or external disturbances, and the premise variables are measured.

3. Fuzzy Output Control Design

In the next, the fuzzy output controller is designed using the concept of parallel distributed compensation, in which the fuzzy controller shares the same sets of normalized membership functions like the TS fuzzy system model.

Definition 1. Considering (5) and (6), and using the same set of normalized membership function (8), the fuzzy static output controller is defined as

$$\mathbf{u}(t) = -\sum_{j=1}^{s} h_j(\boldsymbol{\theta}(t))\,\mathbf{K}_j\mathbf{y}(t) = -\sum_{j=1}^{s} h_j(\boldsymbol{\theta}(t))\,\mathbf{K}_j\mathbf{C}\mathbf{q}(t). \quad (9)$$

Note that the fuzzy controller (9) is in general nonlinear.

Theorem 2. *The equilibrium of the fuzzy system* (5) *and* (6)*, controlled by the fuzzy controller* (9)*, is global asymptotically stable if there exist a positive definite symmetric matrix* $\mathbf{W} \in \mathbb{R}^{n\times n}$ *and matrices* $\mathbf{N}_j, \mathbf{Y}_{ij} \in \mathbb{R}^{r\times n}$ *such that*

$$\mathbf{W} = \mathbf{W}^T > 0, \quad \begin{bmatrix} \mathbf{Y}_{11} & \mathbf{Y}_{12} & \cdots & \mathbf{Y}_{1s} \\ \mathbf{Y}_{12} & \mathbf{Y}_{22} & \cdots & \mathbf{Y}_{2s} \\ \vdots & \vdots & \ddots & \vdots \\ \mathbf{Y}_{1s} & \mathbf{Y}_{2s} & \cdots & \mathbf{Y}_{ss} \end{bmatrix} > 0, \quad (10)$$

$$\mathbf{A}_i\mathbf{W} + \mathbf{W}\mathbf{A}_i^T - \mathbf{B}_i\mathbf{N}_j\mathbf{C} - \mathbf{C}^T\mathbf{N}_j^T\mathbf{B}_i^T + \mathbf{Y}_{ij} < 0 \quad (11)$$

for $h_i(\theta(t))h_j(\theta(t)) \neq 0$, $i, j = 1, 2, \ldots, s$.

If the above conditions hold, the set of control law gain matrices is given as

$$\mathbf{K}_j = \mathbf{N}_j\mathbf{M}^{-1}, \quad j = 1, 2, \ldots, s, \quad (12)$$

where

$$\mathbf{M} = \mathbf{C}\mathbf{W}\mathbf{C}^{\ominus 1}, \quad \mathbf{C}^{\ominus 1} = \mathbf{C}^T\left(\mathbf{C}\mathbf{C}^T\right)^{-1}. \quad (13)$$

$\mathbf{C}^{\ominus 1}$ *is Moore-Penrose pseudo-inverse of* $\mathbf{C}$.

Proof. Considering the model (6) and (2) and the control law (9), then it yields

$$\dot{\mathbf{q}}(t) = \sum_{i=1}^{s}\sum_{j=1}^{s} h_i(\boldsymbol{\theta}(t))\,h_j(\boldsymbol{\theta}(t))\left(\mathbf{A}_i - \mathbf{B}_i\mathbf{K}_j\mathbf{C}\right)\mathbf{q}(t). \quad (14)$$

In order to analyze the convergence of the system state, the quadratic positive Lyapunov function is considered as follows:

$$v(\mathbf{q}(t)) = \mathbf{q}^T(t)\,\mathbf{P}\mathbf{q}(t) > 0, \quad (15)$$

where $\mathbf{P} \in \mathbb{R}^{n\times n}$ is a positive definite symmetric matrix. Then, the time derivative of $v(\mathbf{q}(t))$ along the system trajectory is

$$\dot{v}(\mathbf{q}(t)) = \dot{\mathbf{q}}^T(t)\,\mathbf{P}\mathbf{q}(t) + \mathbf{q}^T(t)\,\mathbf{P}\dot{\mathbf{q}}(t) < 0. \quad (16)$$

Substituting (14) in (16), and introducing the term as follows:

$$v_v(\boldsymbol{\theta}(t)) = \mathbf{q}^T(t)\,\mathbf{Z}(\boldsymbol{\theta}(t))\,\mathbf{q}(t), \quad (17)$$

where

$$\mathbf{Z}(\boldsymbol{\theta}(t)) = \sum_{i=1}^{s}\sum_{j=1}^{s} h_i(\boldsymbol{\theta}(t))\,h_j(\boldsymbol{\theta}(t))\,\mathbf{X}_{ij} > 0 \quad (18)$$

and $\{\mathbf{X}_{ij} = \mathbf{X}_{ji}^T \in \mathbb{R}^{n\times n},\ i, j = 1, 2, \ldots, s\}$ is the set of matrices. In the sense of Krasovskii theorem (see, e.g., [22]) it can be set up as follows:

$$\begin{aligned} &\dot{v}(\mathbf{q}(t)) \\ &= \mathbf{q}^T(t)\sum_{i=1}^{s}\sum_{j=1}^{s} h_i(\boldsymbol{\theta}(t))\,h_j(\boldsymbol{\theta}(t))\,\mathbf{P}\left(\mathbf{A}_i - \mathbf{B}_i\mathbf{K}_j\mathbf{C}\right)\mathbf{q}(t) \\ &\quad + \mathbf{q}^T(t)\sum_{i=1}^{s}\sum_{j=1}^{s} h_i(\boldsymbol{\theta}(t))\,h_j(\boldsymbol{\theta}(t)) \\ &\quad \times \left(\mathbf{A}_i - \mathbf{B}_i\mathbf{K}_j\mathbf{C}\right)^T\mathbf{P}\mathbf{q}(t) \\ &< -\mathbf{q}^T(t)\sum_{i=1}^{s}\sum_{j=1}^{s} h_i(\boldsymbol{\theta}(t))\,h_j(\boldsymbol{\theta}(t))\,\mathbf{X}_{ij}\mathbf{q}(t) \\ &= -\mathbf{q}^T(t)\,\mathbf{Z}(\boldsymbol{\theta}(t))\,\mathbf{q}(t) < 0, \end{aligned} \quad (19)$$

$$\dot{v}(\mathbf{q}(t)) = \sum_{i=1}^{s}\sum_{j=1}^{s} h_i(\boldsymbol{\theta}(t))\,h_j(\boldsymbol{\theta}(t))\,\mathbf{q}^T(t)\,\mathbf{P}_{ij}\mathbf{q}(t) < 0, \quad (20)$$

respectively, which implies

$$\mathbf{P}_{ij} = \mathbf{P}\left(\mathbf{A}_i - \mathbf{B}_i\mathbf{K}_j\mathbf{C}\right) + \left(\mathbf{A}_i - \mathbf{B}_i\mathbf{K}_j\mathbf{C}\right)^T\mathbf{P} + \mathbf{X}_{ij} < 0. \quad (21)$$

It is evident that $\mathbf{P}_{ij}$ has to be negative definite.

Since $r = m$, it is possible to set

$$\mathbf{B}_i\mathbf{K}_j\mathbf{C} = \mathbf{B}_i\mathbf{K}_j\mathbf{M}\mathbf{M}^{-1}\mathbf{C} = \mathbf{B}_i\mathbf{N}_j\mathbf{C}\mathbf{P}, \quad (22)$$

where

$$\mathbf{K}_j\mathbf{M} = \mathbf{N}_j, \qquad \mathbf{M}^{-1}\mathbf{C} = \mathbf{C}\mathbf{P} \quad (23)$$

and $\mathbf{M} \in \mathbb{R}^{m\times m}$ is a regular square matrix. Substituting (22) into (21) results in

$$\mathbf{P}\left(\mathbf{A}_i - \mathbf{B}_i\mathbf{N}_j\mathbf{C}\mathbf{P}\right) + \left(\mathbf{A}_i - \mathbf{B}_i\mathbf{N}_j\mathbf{C}\mathbf{P}\right)^T\mathbf{P} + \mathbf{X}_{ij} < 0. \quad (24)$$

Premultiplying the left side and the right side of (24) by $\mathbf{P}^{-1}$ leads to

$$\mathbf{A}_i\mathbf{P}^{-1} - \mathbf{B}_i\mathbf{N}_j\mathbf{C} + \mathbf{P}^{-1}\mathbf{A}_i^T - \mathbf{C}^T\mathbf{N}_j^T\mathbf{B}_i^T + \mathbf{P}^{-1}\mathbf{X}_{ij}\mathbf{P}^{-1} < 0 \quad (25)$$

and using the notations

$$\mathbf{W} = \mathbf{P}^{-1}, \qquad \mathbf{Y}_{ij} = \mathbf{W}\mathbf{X}_{ij}\mathbf{W} \quad (26)$$

then (25) implies (11). Since (25) also implies

$$\tilde{\mathbf{P}}_{ij} = \mathbf{A}_i\mathbf{W} + \mathbf{W}\mathbf{A}_i^T - \mathbf{B}_i\mathbf{N}_j\mathbf{C} - \mathbf{C}^T\mathbf{N}_j^T\mathbf{B}_i^T + \mathbf{Y}_{ij} < 0. \quad (27)$$

Using the membership functions property (8) and defining $\mathbf{q}^{\diamond}(t) = \mathbf{W}^{-1}\mathbf{q}(t)$, it can be written as follows:

$$\begin{aligned}
&\dot{v}_v(\mathbf{q}(t)) \\
&= \sum_{i=1}^{s}\sum_{j=1}^{s} h_i(\boldsymbol{\theta}(t))\, h_j(\boldsymbol{\theta}(t))\, \mathbf{q}^T(t)\, \mathbf{W}^{-1}\mathbf{W}\mathbf{X}_{ij}\mathbf{W}\mathbf{W}^{-1}\mathbf{q}(t) \\
&= \sum_{i=1}^{s}\sum_{j=1}^{s} h_i(\boldsymbol{\theta}(t))\, h_j(\boldsymbol{\theta}(t))\, \mathbf{q}^{\diamond T}(t)\, \mathbf{Y}_{ij}\mathbf{q}^{\diamond}(t) \\
&= \mathbf{q}^{\diamond T}(t)\, \mathbf{W}\mathbf{Z}(\boldsymbol{\theta}(t))\, \mathbf{W}\mathbf{q}^{\diamond}(t) > 0.
\end{aligned} \tag{28}$$

Writing $\mathbf{Z}(\boldsymbol{\theta}(t))$ as follows:

$$\begin{aligned}
\mathbf{Z}(\boldsymbol{\theta}(t)) = &\begin{bmatrix} h_1(\boldsymbol{\theta}(t))\mathbf{q}^{\diamond}(t) \\ h_2(\boldsymbol{\theta}(t))\mathbf{q}^{\diamond}(t) \\ \vdots \\ h_s(\boldsymbol{\theta}(t))\mathbf{q}^{\diamond}(t) \end{bmatrix}^T \begin{bmatrix} \mathbf{Y}_{11} & \mathbf{Y}_{12} & \cdots & \mathbf{Y}_{1s} \\ \mathbf{Y}_{21} & \mathbf{Y}_{22} & \cdots & \mathbf{Y}_{2s} \\ \vdots & \vdots & \ddots & \vdots \\ \mathbf{Y}_{s1} & \mathbf{Y}_{s2} & \cdots & \mathbf{Y}_{ss} \end{bmatrix} \\
&\times \begin{bmatrix} h_1(\boldsymbol{\theta}(t))\mathbf{q}^{\diamond}(t) \\ h_2(\boldsymbol{\theta}(t))\mathbf{q}^{\diamond}(t) \\ \vdots \\ h_s(\boldsymbol{\theta}(t))\mathbf{q}^{\diamond}(t) \end{bmatrix} > 0
\end{aligned} \tag{29}$$

then (29) implies (10). In addition, (23) gives

$$\mathbf{M}\mathbf{C} = \mathbf{C}\mathbf{P}^{-1} = \mathbf{C}\mathbf{W}. \tag{30}$$

Premultiplying the right side of (30) by $\mathbf{C}^T$ gives

$$\mathbf{C}\mathbf{W}\mathbf{C}^T = \mathbf{M}\mathbf{C}\mathbf{C}^T \tag{31}$$

and so it is

$$\mathbf{M} = \mathbf{C}\mathbf{W}\mathbf{C}^T\left(\mathbf{C}\mathbf{C}^T\right)^{-1} = \mathbf{C}\mathbf{W}\mathbf{C}^{\ominus 1}. \tag{32}$$

Thus, (23) and (32) imply (12)–(13), respectively. This concludes the proof. □

Note, the derived results are linked to some existing finding when the design problem involves additive performance requirements and the relaxed quadratic stability conditions of fuzzy control systems (see, e.g., [13, 23]) are equivalently steered.

Trying to minimize the number of LMIs owing to the limitation of solvers, Theorem 2 can be presented in the equivalent structure in which the number of stabilization conditions, used in fuzzy controller design, is equal to $N = (s^2+s)/2+1$. Evidently, the number of stabilization conditions is substantially reduced if s is large.

Theorem 3. *The equilibrium of the fuzzy system* (5) *and* (6)*, controlled by the fuzzy controller* (9)*, is global asymptotically stable if there exist a positive definite symmetric matrix* $\mathbf{W} \in \mathbb{R}^{n\times n}$ *and matrices* $\mathbf{N}_j, \mathbf{Y}_{ij} \in \mathbb{R}^{r\times n}$ *such that*

$$\mathbf{W} = \mathbf{W}^T > 0, \qquad \begin{bmatrix} \mathbf{Y}_{11} & \mathbf{Y}_{12} & \cdots & \mathbf{Y}_{1s} \\ \mathbf{Y}_{21} & \mathbf{Y}_{22} & \cdots & \mathbf{Y}_{2s} \\ \vdots & \vdots & \ddots & \vdots \\ \mathbf{Y}_{s1} & \mathbf{Y}_{s2} & \cdots & \mathbf{Y}_{ss} \end{bmatrix} > 0 \tag{33}$$

$$\begin{aligned}
&\mathbf{H}_{ii} + \mathbf{H}_{ii}^T + \mathbf{Y}_{ii} < 0, \\
&\frac{\mathbf{H}_{ij} + \mathbf{H}_{ji}}{2} + \frac{\mathbf{H}_{ij}^T + \mathbf{H}_{ji}^T}{2} + \frac{\mathbf{Y}_{ij} + \mathbf{Y}_{ji}}{2} < 0
\end{aligned} \tag{34}$$

for all $i \in \langle 1, 2, \ldots, s\rangle$, $i < j \le s$, $i, j \in \langle 1, 2, \ldots, s\rangle$, *respectively, and* $h_i(\boldsymbol{\theta}(t))h_j(\boldsymbol{\theta}(t)) \neq 0$. *Here it is*

$$\mathbf{H}_{ij} = \mathbf{A}_i\mathbf{W} - \mathbf{B}_i\mathbf{N}_j\mathbf{C} \tag{35}$$

and if the above conditions hold, the set of control law gain matrices is given as in (12) *and* (13).

Proof. Now (28) can be written as

$$\begin{aligned}
\dot{v}(\mathbf{q}(t)) = &\sum_{i=1}^{s}\sum_{j=1}^{s} h_i(\boldsymbol{\theta}(t))\, h_j(\boldsymbol{\theta}(t))\, \mathbf{q}^T(t) \\
&\times \left(\mathbf{H}_{ij} + \mathbf{H}_{ij}^T + \mathbf{Y}_{ij}\right)\mathbf{q}(t),
\end{aligned} \tag{36}$$

where $\mathbf{H}_{ij}$ is given in (35). Permuting the subscripts i and j in (36) gives

$$\begin{aligned}
\dot{v}(\mathbf{q}(t)) = &\sum_{i=1}^{s}\sum_{j=1}^{s} h_i(\boldsymbol{\theta}(t))\, h_j(\boldsymbol{\theta}(t))\, \mathbf{q}^T(t) \\
&\times \left(\mathbf{H}_{ji} + \mathbf{H}_{ji}^T + \mathbf{Y}_{ji}\right)\mathbf{q}(t)
\end{aligned} \tag{37}$$

and adding (36) and (37) results in

$$\begin{aligned}
&2\dot{v}(\mathbf{q}(t)) \\
&= \sum_{i=1}^{s}\sum_{j=1}^{s} h_i(\boldsymbol{\theta}(t))\, h_j(\boldsymbol{\theta}(t))\, \mathbf{q}^T(t) \\
&\times \left(\mathbf{H}_{ij} + \mathbf{H}_{ji} + \left(\mathbf{H}_{ij} + \mathbf{H}_{ji}\right)^T + \left(\mathbf{Y}_{ij} + \mathbf{Y}_{ji}\right)\right)\mathbf{q}(t).
\end{aligned} \tag{38}$$

Rearranging the computation, (38) takes the following form:

$$\begin{aligned}
\dot{v}(\mathbf{q}(t)) = &\sum_{i=1}^{s} h_i^2(\boldsymbol{\theta}(t))\, \mathbf{q}^T(t)\left(\mathbf{H}_{ii} + \mathbf{H}_{ii}^T - \mathbf{Y}_{ii}\right)\mathbf{q}(t) \\
&+ 2\sum_{i=1}^{s-1}\sum_{j=i+1}^{s} h_i(\boldsymbol{\theta}(t))\, h_j(\boldsymbol{\theta}(t))\, \mathbf{q}^T(t) \\
&\times \left(\frac{\mathbf{H}_{ij} + \mathbf{H}_{ji}}{2} + \frac{\mathbf{H}_{ij}^T + \mathbf{H}_{ji}^T}{2} + \frac{\mathbf{Y}_{ij} + \mathbf{Y}_{ji}}{2}\right)\mathbf{q}(t)
\end{aligned} \tag{39}$$

and, evidently, (39) implies (34). This concludes the proof. □

4. Enhanced Criterion for Output Control Design

Theorem 4. *The equilibrium of the fuzzy system* (5) *and* (6)*, controlled by the fuzzy controller* (9) *is global asymptotically stable if there exist positive definite symmetric matrices* $\mathbf{U}, \mathbf{V} \in \mathbb{R}^{n\times n}$*, a matrix* $\mathbf{T} \in \mathbb{R}^{n\times n}$*, and matrices* $\mathbf{N}_j, \mathbf{Y}_{ij} \in \mathbb{R}^{r\times n}$ *such that*

$$\mathbf{U} = \mathbf{U}^T > 0, \qquad \mathbf{V} = \mathbf{V}^T > 0,$$
$$\begin{bmatrix} \mathbf{Y}_{11} & \mathbf{Y}_{12} & \cdots & \mathbf{Y}_{1s} \\ \mathbf{Y}_{12} & \mathbf{Y}_{22} & \cdots & \mathbf{Y}_{2s} \\ \vdots & \vdots & \ddots & \vdots \\ \mathbf{Y}_{1s} & \mathbf{Y}_{2s} & \cdots & \mathbf{Y}_{ss} \end{bmatrix} > 0, \tag{40}$$

$$\mathbf{P}_{ij}^{\bullet} = \begin{bmatrix} \mathbf{A}_i\mathbf{V} + \mathbf{V}\mathbf{A}_i^T - \mathbf{B}_i\mathbf{N}_j\mathbf{C} - \mathbf{C}^T\mathbf{N}_j^T\mathbf{B}_i^T + \mathbf{Y}_{ij} & * \\ \mathbf{T} - \mathbf{U} + \mathbf{A}_i\mathbf{V} - \mathbf{B}_i\mathbf{N}_j\mathbf{C} & -2\mathbf{U} \end{bmatrix} < 0 \tag{41}$$

for $h_i(\boldsymbol{\theta}(t))h_j(\boldsymbol{\theta}(t)) \neq 0$, $i, j = 1, 2, \ldots, s$.

If the above conditions hold, the set of control law gain matrices is given as

$$\mathbf{K}_j = \mathbf{N}_j\mathbf{M}^{-1}, \quad j = 1, 2, \ldots, s, \tag{42}$$

where

$$\mathbf{M} = \mathbf{C}\mathbf{V}\mathbf{C}^{\ominus 1}, \quad \mathbf{C}^{\ominus 1} = \mathbf{C}^T\left(\mathbf{C}\mathbf{C}^T\right)^{-1}, \tag{43}$$

$\mathbf{C}^{\ominus 1}$ *is Moore-Penrose pseudo-inverse of* $\mathbf{C}$.

Here, and hereafter, $*$ *denotes the symmetric item in a symmetric matrix.*

Proof. Writing (14) in the following form:

$$\dot{\mathbf{q}}(t) - \sum_{i=1}^{s}\sum_{j=1}^{s} h_i(\boldsymbol{\theta}(t))\, h_j(\boldsymbol{\theta}(t)) \left(\mathbf{A}_i - \mathbf{B}_i\mathbf{K}_j\mathbf{C}\right)\mathbf{q}(t) = 0 \tag{44}$$

then with arbitrary symmetric regular matrices $\mathbf{S}_1, \mathbf{S}_2 \in \mathbb{R}^{n\times n}$ it yields

$$-\left(\mathbf{q}^T(t)\,\mathbf{S}_1 + \dot{\mathbf{q}}^T(t)\,\mathbf{S}_2\right) \times\left(\dot{\mathbf{q}}(t) - \sum_{i=1}^{s}\sum_{j=1}^{s} h_i(\boldsymbol{\theta}(t))\, h_j(\boldsymbol{\theta}(t)) \left(\mathbf{A}_i - \mathbf{B}_i\mathbf{K}_j\mathbf{C}\right)\mathbf{q}(t)\right) = 0. \tag{45}$$

Thus, adding (45) as well as the transposition of (45) to (19), it yields

$$\begin{aligned} \dot{v}(\mathbf{q}(t)) = {} & \dot{\mathbf{q}}^T(t)\,\mathbf{P}\mathbf{q}(t) + \mathbf{q}^T(t)\,\mathbf{P}\dot{\mathbf{q}}(t) \\ & - \left(\mathbf{q}^T(t)\,\mathbf{S}_1 + \dot{\mathbf{q}}^T(t)\,\mathbf{S}_2\right) \\ & \times\left(\dot{\mathbf{q}}(t) - \sum_{i=1}^{s}\sum_{j=1}^{s} h_i(\boldsymbol{\theta}(t))\, h_j(\boldsymbol{\theta}(t)) \right. \\ & \left. \times\left(\mathbf{A}_i - \mathbf{B}_i\mathbf{K}_j\mathbf{C}\right)\mathbf{q}(t)\right) \\ & - \left(\dot{\mathbf{q}}^T(t) - \mathbf{q}^T(t)\sum_{i=1}^{s}\sum_{j=1}^{s} h_i(\boldsymbol{\theta}(t))\, h_j(\boldsymbol{\theta}(t)) \right. \\ & \left. \times\left(\mathbf{A}_i - \mathbf{B}_i\mathbf{K}_j\mathbf{C}\right)^T\right)\left(\mathbf{S}_1\mathbf{q}(t) + \mathbf{S}_2\dot{\mathbf{q}}(t)\right) \\ < {} & -\mathbf{q}^T(t)\sum_{i=1}^{s}\sum_{j=1}^{s} h_i(\boldsymbol{\theta}(t))\, h_j(\boldsymbol{\theta}(t))\,\mathbf{X}_{ij}\mathbf{q}(t) \\ = {} & -\mathbf{q}^T(t)\,\mathbf{Z}(\boldsymbol{\theta}(t))\,\mathbf{q}(t) < 0. \end{aligned} \tag{46}$$

Using the notation

$$\mathbf{q}^{\circ T}(t) = \left[\mathbf{q}^T(t) \;\; \dot{\mathbf{q}}^T(t)\right] \tag{47}$$

the inequality (46) can be set and written as

$$\dot{v}(\mathbf{q}(t)) = \sum_{i=1}^{s}\sum_{j=1}^{s} h_i(\boldsymbol{\theta}(t))\, h_j(\boldsymbol{\theta}(t))\,\mathbf{q}^{\circ T}(t)\,\mathbf{P}_{ij}^{\circ}\mathbf{q}^{\circ}(t) < 0, \tag{48}$$

where

$$\mathbf{P}_{ij}^{\circ} = \begin{bmatrix} \mathbf{S}_1\left(\mathbf{A}_i - \mathbf{B}_i\mathbf{K}_j\mathbf{C}\right) + \left(\mathbf{A}_i - \mathbf{B}_i\mathbf{K}_j\mathbf{C}\right)^T\mathbf{S}_1 + \mathbf{X}_{ij} & * \\ \mathbf{P} - \mathbf{S}_1 + \mathbf{S}_2\left(\mathbf{A}_i - \mathbf{B}_i\mathbf{K}_j\mathbf{C}\right) & -2\mathbf{S}_2 \end{bmatrix} < 0 \tag{49}$$

$$\mathbf{Z}^{\circ}(\boldsymbol{\theta}(t)) = \operatorname{diag}\left[\mathbf{Z}(\boldsymbol{\theta}(t)) \;\; \mathbf{0}\right] \geq 0. \tag{50}$$

Since $r = m$, it is now possible to set

$$\mathbf{B}_i\mathbf{K}_j\mathbf{C} = \mathbf{B}_i\mathbf{K}_j\mathbf{M}\mathbf{M}^{-1}\mathbf{C} = \mathbf{B}_i\mathbf{N}_j\mathbf{C}\mathbf{S}_1, \tag{51}$$

where

$$\mathbf{K}_j\mathbf{M} = \mathbf{N}_j, \qquad \mathbf{M}^{-1}\mathbf{C} = \mathbf{C}\mathbf{S}_1, \tag{52}$$

and $\mathbf{M} \in \mathbb{R}^{m\times m}$ is a regular square matrix. Substituting (51) into (49) results in

$$\mathbf{P}_{ij}^{\circ} = \begin{bmatrix} \boldsymbol{\Phi}_{ij} & * \\ \mathbf{P} - \mathbf{S}_1 + \mathbf{S}_2\left(\mathbf{A}_i - \mathbf{B}_i\mathbf{N}_j\mathbf{C}\mathbf{S}_1\right) & -2\mathbf{S}_2 \end{bmatrix}, \tag{53}$$

where

$$\mathbf{\Phi}_{ij} = \mathbf{X}_{ij} + \mathbf{S}_1\left(\mathbf{A}_i - \mathbf{B}_i\mathbf{N}_j\mathbf{C}\mathbf{S}_1\right) + \left(\mathbf{A}_i - \mathbf{B}_i\mathbf{N}_j\mathbf{C}\mathbf{S}_1\right)^T\mathbf{S}_1. \tag{54}$$

Defining the congruence transform matrix $\mathbf{T}_c$ as follows:

$$\mathbf{T}_c = \begin{bmatrix}\mathbf{S}_1^{-1} & \mathbf{S}_2^{-1}\end{bmatrix}. \tag{55}$$

Premultiplying the left and the right side of (53) and (50) by $\mathbf{T}_c$ gives

$$\begin{bmatrix}\mathbf{\Pi}_{ij} & * \\ \mathbf{S}_2^{-1}\mathbf{P}\mathbf{S}_1^{-1} - \mathbf{S}_2^{-1} + \left(\mathbf{A}_i\mathbf{S}_1^{-1} - \mathbf{B}_i\mathbf{N}_j\mathbf{C}\right) & -2\mathbf{S}_2^{-1}\end{bmatrix} < 0 \tag{56}$$

$$\operatorname{diag}\begin{bmatrix}\mathbf{S}_1^{-1}\mathbf{Z}\left(\boldsymbol{\theta}\left(t\right)\right)\mathbf{S}_1^{-1} & \mathbf{0}\end{bmatrix} \geq 0, \tag{57}$$

where

$$\begin{aligned}\mathbf{\Pi}_{ij} &= \mathbf{S}_1^{-1}\mathbf{\Phi}_{ij}\mathbf{S}_1^{-1} = \mathbf{S}_1^{-1}\mathbf{X}_{ij}\mathbf{S}_1^{-1} \\ &\quad + \left(\mathbf{A}_i\mathbf{S}_1^{-1} - \mathbf{B}_i\mathbf{N}_j\mathbf{C}\right) + \left(\mathbf{A}_i\mathbf{S}_1^{-1} - \mathbf{B}_i\mathbf{N}_j\mathbf{C}\right)^T.\end{aligned} \tag{58}$$

Thus, using the notations

$$\mathbf{V} = \mathbf{S}_1^{-1}, \qquad \mathbf{U} = \mathbf{S}_2^{-1}, \qquad \mathbf{T} = \mathbf{U}\mathbf{P}\mathbf{V}, \qquad \mathbf{Y}_{ij} = \mathbf{V}\mathbf{X}_{ij}\mathbf{V} \tag{59}$$

then (56), (58) implies (41).

Since now, $\mathbf{V}\mathbf{Z}(\boldsymbol{\theta}(t))\mathbf{V}$ in (57) and $\mathbf{W}\mathbf{Z}(\boldsymbol{\theta}(t))\mathbf{W}$ in (28), both have the same structure if $\mathbf{V} = \mathbf{W}$, (57) implies (40).

In addition, (52) gives

$$\mathbf{M}\mathbf{C} = \mathbf{C}\mathbf{S}_1^{-1} = \mathbf{C}\mathbf{V} \tag{60}$$

and since (60) and (30) both have the same structure if $\mathbf{V} = \mathbf{W}$, then (60) implies (42). This concludes the proof. □

This principle naturally exploits the affine TS model properties. Introducing the slack matrix variables $\mathbf{U}$, $\mathbf{V}$ into the LMIs, the system matrices are decoupled from the equivalent Lyapunov matrix $\mathbf{T}$. Note, the above-presented inequalities are linear matrix inequalities, but the equivalent Lyapunov matrix $\mathbf{T}$ is not a symmetric matrix. Introducing a scalar design parameter $\delta > 0$, $\delta \in \mathbb{R}$, Theorem 4 can be modified in the next form.

Corollary 5. *If, instead of the notations* (56)*, there are used in* (59) *the next substitutions*

$$\mathbf{U} = \delta\mathbf{V}, \qquad \mathbf{T} = \delta\mathbf{V}\mathbf{P}\mathbf{V}, \quad \delta > 0,\ \delta \in \mathbb{R}. \tag{61}$$

It is evident that (53) *and* (54) *with* (61) *imply*

$$\mathbf{T} = \mathbf{T}^T > 0, \qquad \mathbf{V} = \mathbf{V}^T > 0,$$

$$\begin{bmatrix}\mathbf{Y}_{11} & \mathbf{Y}_{12} & \cdots & \mathbf{Y}_{1s} \\ \mathbf{Y}_{12} & \mathbf{Y}_{22} & \cdots & \mathbf{Y}_{2s} \\ \vdots & \vdots & \ddots & \vdots \\ \mathbf{Y}_{1s} & \mathbf{Y}_{2s} & \cdots & \mathbf{Y}_{ss}\end{bmatrix} > 0, \tag{62}$$

$$\begin{bmatrix}\mathbf{A}_i\mathbf{V} + \mathbf{V}\mathbf{A}_i^T - \mathbf{B}_i\mathbf{N}_j\mathbf{C} - \mathbf{C}^T\mathbf{N}_j^T\mathbf{B}_i^T + \mathbf{Y}_{ij} & * \\ \mathbf{T} - \delta\mathbf{V} + \mathbf{A}_i\mathbf{V} - \mathbf{B}_i\mathbf{N}_j\mathbf{C} & -2\delta\mathbf{V}\end{bmatrix} < 0, \tag{63}$$

for $h_i(\boldsymbol{\theta}(t))h_j(\boldsymbol{\theta}(t)) \neq 0$, $i, j = 1, 2, \ldots, s$.

Thus, the equilibrium of the fuzzy system (5) *and* (6)*, controlled by the fuzzy controller* (9)*, is global asymptotically stable if for given positive scalar* $\delta > 0$, $\delta \in \mathbb{R}$ *there exist positive definite symmetric matrices* $\mathbf{T}, \mathbf{V} \in \mathbb{R}^{n\times n}$*, and matrices* $\mathbf{N}_j, \mathbf{Y}_{ij} \in \mathbb{R}^{r\times n}$ *such that* (62)–(63) *hold. Subsequently, the set of control law gain matrices is given by* (42)–(43).

Note, (63) represents the set of LMIs only if δ is a prescribed constant (δ can be considered as a tuning parameter). Considering δ as a LMI variable, (63) represents the set of bilinear matrix inequalities (BMI).

Theorem 6. *The equilibrium of the fuzzy system* (5) *and* (6)*, controlled by the fuzzy controller* (9) *is global asymptotically stable if there exist positive definite symmetric matrices* $\mathbf{U}, \mathbf{V} \in \mathbb{R}^{n\times n}$*, a matrix* $\mathbf{T} \in \mathbb{R}^{n\times n}$*, and matrices* $\mathbf{N}_j, \mathbf{Y}_{ij} \in \mathbb{R}^{r\times n}$ *such that*

$$\mathbf{U} = \mathbf{U}^T > 0, \qquad \mathbf{V} = \mathbf{V}^T > 0,$$

$$\begin{bmatrix}\mathbf{Y}_{11} & \mathbf{Y}_{12} & \cdots & \mathbf{Y}_{1s} \\ \mathbf{Y}_{12} & \mathbf{Y}_{22} & \cdots & \mathbf{Y}_{2s} \\ \vdots & \vdots & \ddots & \vdots \\ \mathbf{Y}_{1s} & \mathbf{Y}_{2s} & \cdots & \mathbf{Y}_{ss}\end{bmatrix} > 0, \tag{64}$$

$$\begin{bmatrix}\mathbf{H}_{ii} + \mathbf{H}_{ii}^T + \mathbf{Y}_{ii} & * \\ \mathbf{T} - \mathbf{U} + \mathbf{H}_{ii} & -2\mathbf{U}\end{bmatrix} < 0, \tag{65}$$

$$\begin{bmatrix}\dfrac{\mathbf{H}_{ij} + \mathbf{H}_{ji}}{2} + \dfrac{\left(\mathbf{H}_{ij} + \mathbf{H}_{ji}\right)^T}{2} + \dfrac{\mathbf{Y}_{ij} + \mathbf{Y}_{ji}}{2} & * \\ \mathbf{T} - \mathbf{U} + \dfrac{\mathbf{H}_{ij} + \mathbf{H}_{ji}}{2} & -2\mathbf{U}\end{bmatrix} < 0 \tag{66}$$

for all $i \in \langle 1, 2, \ldots s\rangle$, $i < j \leq s$, $i, j \in \langle 1, 2, \ldots s\rangle$, *respectively, and* $h_i(\boldsymbol{\theta}(t))h_j(\boldsymbol{\theta}(t)) \neq 0$. *Here it is*

$$\mathbf{H}_{ij} = \mathbf{A}_i\mathbf{V} - \mathbf{B}_i\mathbf{N}_j\mathbf{C} \tag{67}$$

and if the above conditions hold, the set of control law gain matrices is given as in (42)–(43).

Proof. Considering (41) and (67), (48) can be written as

$$\begin{aligned}\dot{v}\left(\mathbf{q}\left(t\right)\right) &= \sum_{i=1}^{s}\sum_{j=1}^{s} h_i\left(\boldsymbol{\theta}\left(t\right)\right)h_j\left(\boldsymbol{\theta}\left(t\right)\right) \\ &\quad \times \mathbf{q}^{\circ T}\left(t\right)\mathbf{T}_c^{-1}\mathbf{T}_c\mathbf{P}_{ij}^{\circ}\mathbf{T}_c\mathbf{T}_c^{-1}\mathbf{q}^{\circ}\left(t\right) \\ &= \sum_{i=1}^{s}\sum_{j=1}^{s} h_i\left(\boldsymbol{\theta}\left(t\right)\right)h_j\left(\boldsymbol{\theta}\left(t\right)\right)\mathbf{q}^{\bullet T}\left(t\right)\mathbf{P}_{ij}^{\bullet}\mathbf{q}^{\bullet}\left(t\right) < 0,\end{aligned} \tag{68}$$

where with $\mathbf{T}_c$ defined in (55), it is

$$\begin{aligned}\mathbf{q}^{\bullet}\left(t\right) &= \mathbf{T}_c^{-1}\mathbf{q}^{\circ}\left(t\right), \\ \mathbf{P}_{ij}^{\bullet} &= \mathbf{T}_c\mathbf{P}_{ij}^{\circ}\mathbf{T}_c = \begin{bmatrix}\mathbf{H}_{ij} + \mathbf{H}_{ij}^T + \mathbf{Y}_{ij} & * \\ \mathbf{T} - \mathbf{U} + \mathbf{H}_{ij} & -2\mathbf{U}\end{bmatrix} < 0.\end{aligned} \tag{69}$$

Permuting the subscripts i and j in (68) gives

$$\dot{v}(\mathbf{q}(t)) = \sum_{i=1}^{s}\sum_{j=1}^{s} h_i(\boldsymbol{\theta}(t))\, h_j(\boldsymbol{\theta}(t))\, \mathbf{q}^{\bullet T}(t)\, \mathbf{P}_{ji}^{\bullet}\mathbf{q}^{\bullet}(t) \quad (70)$$

and adding (68) and (70) results in

$$2\dot{v}(\mathbf{q}(t)) = \sum_{i=1}^{s}\sum_{j=1}^{s} h_i(\boldsymbol{\theta}(t))\, h_j(\boldsymbol{\theta}(t))\, \mathbf{q}^{\bullet T}(t)\, \widetilde{\mathbf{P}}_{ij}^{\bullet}\mathbf{q}^{\bullet}(t), \quad (71)$$

where

$$\widetilde{\mathbf{P}}_{ij}^{\bullet} = \begin{bmatrix} \mathbf{H}_{ij} + \mathbf{H}_{ji} + \mathbf{H}_{ij}^{T} + \mathbf{H}_{ji}^{T} + \mathbf{Y}_{ij} + \mathbf{Y}_{ji} & * \\ 2\mathbf{T} - 2\mathbf{U} + \mathbf{H}_{ij} + \mathbf{H}_{ji} & -4\mathbf{U} \end{bmatrix} < 0. \quad (72)$$

Rearranging the computation, (71) takes the form

$$\dot{v}(\mathbf{q}(t)) = \sum_{i=1}^{s} h_i^2(\boldsymbol{\theta}(t))\, \mathbf{q}^{T}(t)\, \frac{1}{2}\widetilde{\mathbf{P}}_{ii}^{\bullet}\mathbf{q}^{\bullet}(t) + 2\sum_{i=1}^{s-1}\sum_{j=i+1}^{s} h_i(\boldsymbol{\theta}(t))\, h_j(\boldsymbol{\theta}(t))\, \mathbf{q}^{\bullet T}(t)\, \frac{1}{2}\widetilde{\mathbf{P}}_{ij}^{\bullet}\mathbf{q}^{\bullet}(t), \quad (73)$$

where

$$\frac{1}{2}\widetilde{\mathbf{P}}_{ii}^{\bullet} = \begin{bmatrix} \mathbf{H}_{ii} + \mathbf{H}_{ii}^{T} + \mathbf{Y}_{ii} & * \\ \mathbf{T} - \mathbf{U} + \mathbf{H}_{ii} & -2\mathbf{U} \end{bmatrix} < 0 \quad (74)$$

$$\frac{1}{2}\widetilde{\mathbf{P}}_{ij}^{\bullet} = \begin{bmatrix} \dfrac{\mathbf{H}_{ij} + \mathbf{H}_{ji}}{2} + \dfrac{\left(\mathbf{H}_{ij} + \mathbf{H}_{ji}\right)^{T}}{2} + \dfrac{\mathbf{Y}_{ij} + \mathbf{Y}_{ji}}{2} & * \\ \mathbf{T} - \mathbf{U} + \dfrac{\mathbf{H}_{ij} + \mathbf{H}_{ji}}{2} & -2\mathbf{U} \end{bmatrix} < 0 \quad (75)$$

and, evidently, (74), (75) imply (65),(66) respectively. This concludes the proof. □

5. Illustrative Example

The nonlinear dynamics of the hydrostatic transmission was taken from [24] and this model was used in control design and simulation.

The hydrostatic transmission dynamics is represented by a nonlinear fourth-order state-space model as follows.

$$\begin{aligned} \dot{q}_1(t) &= -a_{11}q_1(t) + b_{11}u_1(t), \\ \dot{q}_2(t) &= -a_{22}q_2(t) + b_{22}u_2(t), \\ \dot{q}_3(t) &= a_{31}q_1(t)\, p(t) - a_{33}q_3(t) - a_{34}q_2(t)\, q_4(t), \\ \dot{q}_4(t) &= a_{43}q_2(t)\, q_3(t) - a_{44}q_4(t), \end{aligned} \quad (76)$$

where $q_1(t)$ is the normalized hydraulic pump angle, $q_2(t)$ is the normalized hydraulic motor angle, $q_3(t)$ is the pressure difference (bar), $q_4(t)$ is the hydraulic motor speed (rad/s), $p(t)$ is the speed of hydraulic pump (rad/s), $u_1(t)$ is the normalized control signal of the hydraulic pump, and $u_2(t)$ is the normalized control signal of the hydraulic motor. It is supposed that the external variable $p(t)$, as well as the second state variable $q_2(t)$ are measurable. In given working point the parameters are

$$\begin{aligned} &a_{11} = 7.6923 \quad a_{22} = 4.5455 \quad a_{33} = 7.6054.10^{-4}, \\ &a_{31} = 0.7877 \quad a_{34} = 0.9235 \quad b_{11} = 1.8590.10^{3}, \text{and} \\ &a_{43} = 12.1967 \quad a_{44} = 0.4143 \quad b_{22} = 1.2879.10^{3}. \end{aligned} \quad (77)$$

Since the variables $p(t) \in \langle 105, 300\rangle$ and $q_2(t) \in \langle 0.0001, 1\rangle$ are bounded on the prescribed sectors then vector of the premise variables can be chosen as follows:

$$\boldsymbol{\theta}(t) = \begin{bmatrix} \theta_1(t) & \theta_2(t) \end{bmatrix} = \begin{bmatrix} q_2(t) & p(t) \end{bmatrix}. \quad (78)$$

Thus, the set of nonlinear sector functions as follows.

$$\begin{aligned} w_{11}(q_2(t)) &= \frac{b_1 - q_2(t)}{b_1 - b_2}, \\ w_{12}(q_2(t)) &= \frac{q_2(t) - b_2}{b_1 - b_2} = 1 - w_{11}(q_2(t)), \\ & \qquad b_1 = 0,\ b_2 = 1, \\ w_{21}(p(t)) &= \frac{c_1 - p(t)}{c_1 - c_2}, \\ w_{22}(p(t)) &= \frac{p(t) - c_2}{c_1 - c_2} = 1 - w_{21}(p(t)), \\ & \qquad c_1 = 105,\ c_2 = 300 \end{aligned} \quad (79)$$

implies the next set of normalized membership functions as follows:

$$\begin{aligned} h_1(q_2(t), p(t)) &= w_{11}(q_2(t))\, w_{21}(p(t)), \\ h_2(q_2(t), p(t)) &= w_{12}(q_2(t))\, w_{21}(p(t)), \\ h_3(q_2(t), p(t)) &= w_{11}(q_2(t))\, w_{22}(p(t)), \\ h_4(q_2(t), p(t)) &= w_{12}(q_2(t))\, w_{22}(p(t)). \end{aligned} \quad (80)$$

The transformation of nonlinear differential equation systems into a TS fuzzy system in standard form gives

$$\mathbf{A}_i = \begin{bmatrix} -a_{11} & 0 & 0 & 0 \\ 0 & -a_{22} & 0 & 0 \\ a_{31}c_k & 0 & -a_{31} & -a_{34}b_l \\ 0 & 0 & a_{43}b_l & -a_{44} \end{bmatrix}, \quad \mathbf{B} = \begin{bmatrix} a_{11} & 0 \\ 0 & b_{22} \\ 0 & 0 \\ 0 & 0 \end{bmatrix}, \quad \mathbf{C}^{T} = \begin{bmatrix} 0 & 0 \\ 1 & 0 \\ 0 & 1 \\ 0 & 0 \end{bmatrix} \quad (81)$$

with the associations

$$\begin{aligned} &i = 1 \longleftarrow (l = 1, k = 1) \quad i = 2 \longleftarrow (l = 2, k = 1) \\ &i = 3 \longleftarrow (l = 1, k = 2) \quad i = 4 \longleftarrow (l = 2, k = 2). \end{aligned} \quad (82)$$

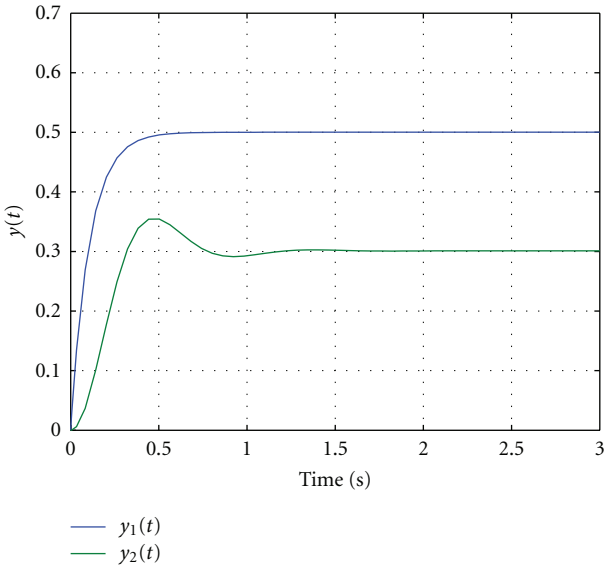

Figure 1: System output response.

Thus, solving (62), (63) with respect to the LMI matrix variables $\mathbf{T}$, $\mathbf{V}$, $\mathbf{N}_j$, $j = 1, 2, 3, 4$, and with $\delta = 9$ then, using Self-Dual-Minimization (SeDuMi) package for Matlab [25, 26], the feedback gain matrix design problem was feasible with the results

$$\mathbf{T} = \begin{bmatrix} 0.0017 & 0.0000 & -0.0223 & 0.0006 \\ 0.0000 & 0.9258 & 0.0000 & 0.0000 \\ -0.0223 & 0.0000 & 0.5679 & -0.1464 \\ 0.0006 & 0.0000 & -0.1464 & 1.7684 \end{bmatrix} > 0$$

$$\mathbf{V} = \begin{bmatrix} 0.0001 & 0.0000 & -0.0017 & -0.0001 \\ 0.0000 & 0.0481 & 0.0000 & -0.0000 \\ -0.0017 & 0.0000 & 0.0410 & -0.0253 \\ -0.0001 & 0.0000 & -0.0253 & 0.2027 \end{bmatrix} > 0 \tag{83}$$

$$\mathbf{K}_i = \begin{bmatrix} 0.0000 & 0.0002 \\ 0.0047 & 0.0000 \end{bmatrix}, \quad i = 1, 2, 3, 4$$

which rise up a stable set of closed-loop subsystems. It can be seen that with an enough precision the used design conditions imply the approximately equal control gain matrices. Comparing with design methods proposed in [17], the fuzzy control is so less conservative.

The conditions in simulations were specified for the system in the forced regime, where

$$\mathbf{u}(t) = \sum_{j=1}^{s} h_j(\boldsymbol{\theta}(t)) \left(-\mathbf{K}_j \mathbf{C}\mathbf{q}(t) + \mathbf{W}\mathbf{W}(t)\right),$$

$$\mathbf{W} = \begin{bmatrix} 0.0000 & 0.0002 \\ 0.0073 & 0.0000 \end{bmatrix}, \quad \mathbf{W}(t) = \begin{bmatrix} 0.5 \\ 0.3 \end{bmatrix}, \tag{84}$$

$$\mathbf{q}(0) = \mathbf{0}, \quad p(t) = 105.$$

Figure 1 shows the simulation result for the system with zero initial state.

6. Concluding Remarks

New approach for output feedback control design, taking into account the output matrix of the system model and the affine properties of the TS model structure, is presented in this paper. Applying the fuzzy output control scheme relating to the parallel distributed output compensators and introducing the slack matrices into an enhanced Lyapunov inequality, the method significantly reduces the conservativeness in the control design conditions. By the proposed procedure, strictly decoupling a Lyapunov matrix and the system parameter matrices in the LMIs, the control problem is parameterized in such LMI structure which admit more freedom in guaranteeing the output feedback control performances.

Sufficient conditions of the controller existence, manipulating the global stability of the system, imply the control structure which stabilizes the nonlinear system in the sense of Lyapunov, and the design of controller parameters directly from these conditions is a solved numerical problem. An additional benefit of the method is that controllers use minimum feedback information with respect to desired system output and the approach is flexible enough to allow the inclusion of additional design conditions such as fuzzy Lyapunov functions. The validity and applicability of the approach is demonstrated through a numerical design example.

Acknowledgments

The work presented in this paper was supported by VEGA, Grant Agency of Ministry of Education, and Academy of Science of Slovak Republic under Grant no. 1/0256/11. This support is very gratefully acknowledged.

References

[1] T. Takagi and M. Sugeno, "Fuzzy identification of systems and its applications to modeling and control," *IEEE Transactions on Systems, Man and Cybernetics*, vol. 15, no. 1, pp. 116–132, 1985.

[2] H. O. Wang, K. Tanaka, and M. F. Griffin, "An approach to fuzzy control of nonlinear systems: Stability and design issues," *IEEE Transactions on Fuzzy Systems*, vol. 4, no. 1, pp. 14–23, 1996.

[3] K. M. Passino and S. Yurkovich, *Fuzzy Control*, Addison-Wesley Longman, Berkeley, Calif, USA, 1998.

[4] M. Johansson, A. Rantzer, and K. E. Årzén, "Piecewise quadratic stability of fuzzy systems," *IEEE Transactions on Fuzzy Systems*, vol. 7, no. 6, pp. 713–722, 1999.

[5] K. Tanaka and H. O. Wang, *Fuzzy Control Systems Design and Analysis. A Linear Matrix Inequality Approach*, John Wiley & Sons, New York, NY, USA, 2001.

[6] F. Khaber, K. Zehar, and A. Hamzaoui, "State feedback controller design via Takagi-Sugeno fuzzy model: LMI approach," *International Journal of Computational Intelligence*, vol. 2, no. 3, pp. 148–153, 2005.

[7] K. Michels, F. Klawonn, R. Kruse, and A. Nurnberger, *Fuzzy Control. Fundamentals, Stability and Design of Fuzzy Controllers*, Springer, Berlin, Germany, 2006.

[8] I. Abdelmalek, N. Goléa, and M. L. Hadjili, "A new fuzzy Lyapunov approach to non-quadratic stabilization of Takagi-Sugeno fuzzy models," *International Journal of Applied Mathematics and Computer Science*, vol. 17, no. 1, pp. 39–51, 2007.

[9] D. Krokavec and A. Filasova, "Optimal fuzzy control for a class of nonlinear systems," *Mathematical Problems in Engineering*, vol. 2012, Article ID 481942, 29 pages, 2012.
[10] J. Pan, S. Fei, Y. Ni, and M. Xue, "New approaches to relaxed stabilization conditions and H_∞ control designs for T-S fuzzy systems," *Journal of Control Theory and Applications*, vol. 10, no. 1, pp. 82–91, 2012.
[11] M. P. A. Santim, M. C. M. Teixeira, W. A. de Souza, R. Cardim, and E. Assunao, "Design of a Takagi-Sugeno fuzzy regulator for a set of operation points," *Mathematical Problems in Engineering*, Article ID 731298, 17 pages, 2012.
[12] B. Boyd, L. El Ghaoui, E. Peron, and V. Balakrishnan, *Linear Matrix Inequalities in System and Control Theory*, SIAM Society for Industrial and Applied Mathematics, Philadelphia, Pa, USA, 1994.
[13] X. Liu and Q. Zhang, "New approaches to H_∞ controller designs based on fuzzy observers for T-S fuzzy systems via LMI," *Automatica*, vol. 39, no. 9, pp. 1571–1582, 2003.
[14] S. K. Nguang and P. Shi, "H_∞ fuzzy output feedback control design for nonlinear systems: an LMI approach," *IEEE Transactions on Fuzzy Systems*, vol. 11, no. 3, pp. 331–340, 2003.
[15] S. W. Kau, H. J. Lee, C. M. Yang, C. H. Lee, L. Hong, and C. H. Fang, "Robust H_∞ fuzzy static output feedback control of T-S fuzzy systems with parametric uncertainties," *Fuzzy Sets and Systems*, vol. 158, no. 2, pp. 135–146, 2007.
[16] B. S. Chen, C. S. Tseng, and H. J. Uang, "Mixed H_2/H_∞ fuzzy output feedback control design for nonlinear dynamic systems: an LMI approach," *IEEE Transactions on Fuzzy Systems*, vol. 8, no. 3, pp. 249–265, 2000.
[17] M. Chadli, D. Maquin, and J. Ragot, "Static output feedback for Takagi-Sugeno systems: an LMI approach," in *Proceedings of the 10th Mediterranean Conference on Control and Automation (MED '02)*, Lisbon, Portugal, July 2002.
[18] H. L. Jhi and C. S. Tseng, "Robust static output feedback fuzzy control design for nonlinear discrete-time systems with persistent bounded disturbances," *International Journal of Fuzzy Systems*, vol. 14, no. 1, pp. 131–140, 2012.
[19] E. S. Tognetti, R. C. L. F. Oliveira, and P. L. D. Peres, "Improved stabilization conditions for Takagi-Sugeno fuzzy systems via fuzzy integral Lyapunov functions," in *Proceedings of the American Control Conference (ACC '11)*, pp. 4970–4975, San Francisco, Calif, USA, June 2011.
[20] D. Krokavec and A. Filasova, "Stabilizing fuzzy static output control for a class of nonlinear systems," in *Proceedings of the 16th IEEE International Conference on Intelligent Engineering Systems (INES '12)*, pp. 285–290, Lisbon, Portugal, June 2012.
[21] D. Huang and S. K. Nguang, "Static output feedback controller design for fuzzy systems: an ILMI approach," *Information Sciences*, vol. 177, no. 14, pp. 3005–3015, 2007.
[22] W. M. Haddad and V. Chellaboina, *Nonlinear Dynamical Systems and Control. A Lyapunov-Based Approach*, Princeton University Press, Princeton, NJ, USA, 2008.
[23] E. Kim and H. Lee, "New approaches to relaxed quadratic stability condition of fuzzy control systems," *IEEE Transactions on Fuzzy Systems*, vol. 8, no. 5, pp. 523–534, 2000.
[24] P. Gerland, D. Groß, H. Schulte, and A. Kroll, "Robust adaptive fault detection using global state information and application to mobile working machines," in *Proceedings of the 1st Conference on Control and Fault-Tolerant Systems (SysTol '10)*, pp. 813–818, Nice, France, October 2010.
[25] D. Krokavec and A. Filasova, *Discrete-Time Systems*, Elfa, Kosice, Slovakia, 2008.
[26] D. Peaucelle, D. Henrion, Y. Labit, and K. Taitz, *USer's Guide for SeDuMi Interface 1. 04*, LAAS-CNRS, Toulouse, France, 2002.

Hindawi Publishing Corporation
Advances in Fuzzy Systems
Volume 2012, Article ID 927878, 9 pages
doi:10.1155/2012/927878

Research Article

Fuzzy Networked Control Systems Design Considering Scheduling Restrictions

H. Benítez-Pérez,[1,2] A. Benítez-Pérez,[2,3] J. Ortega-Arjona,[2,4] and O. Esquivel-Flores[1,2]

[1] *Departamento de Ingeniería de Sistemas Computacionales y Automatización, Instituto de Investigaciones en Matemáticas Aplicadas y en Sistemas, Universidad Nacional Autónoma de México, Apdo. Postal 20-726. Del. A. Obregón, 01000 México, DF, Mexico*
[2] *Posgrado en Ciencia e Ingeniería de la Computación, Universidad Nacional Autónoma de México, México, DF, Mexico*
[3] *Cecyt 11, Instituto Politecnico Nacional, Avenida de los Maestros S/N, México, DF, Mexico*
[4] *Departamento de Matemáticas, Facultad de Ciencias, Universidad Nacional Autónoma de México, DF, Mexico*

Correspondence should be addressed to H. Benítez-Pérez, hector@uxdea4.iimas.unam.mx

Received 23 May 2012; Revised 17 July 2012; Accepted 17 October 2012

Academic Editor: Sendren Sheng-Dong Xu

Nowadays network control systems present a common approximation when connectivity is the issue to be solved based on time delays coupling from external factors. However, this approach tends to be complex in terms of time delays. Therefore, it is necessary to study the behavior of the delays as well as the integration into differential equations of these bounded delays. The related time delays needs to be known a priory but from a dynamic real-time behavior. To do so, the use of priority dynamic Priority exchange scheduling is performed. The objective of this paper is to show a way to tackle multiple time delays that are bounded and the dynamic response from real-time scheduling approximation. The related control law is designed considering fuzzy logic approximation for nonlinear time delays coupling, where the main advantage is the integration of this behavior through extended state space representation keeping certain linear and bounded behavior and leading to a stable situation during events presentation by guaranteeing stability through Lyapunov.

1. Introduction

Nowadays real-time restrictions are the most certain definitions in terms of time delays where general considerations tend to be periodic and repeatable.

The control design and stability analysis of network-based control systems (NCSs) have been studied in recent years, based upon codesign strategy [1]. The main advantages of this kind of systems are their low cost, small volume of wiring, distributed processing, simple installation, maintenance, and reliability.

In a NCS, one of the key issues is the effect of network-induced delay in the system performance. The delay can be constant, time varying, or even random; this depends on the scheduler, network type, architecture, operating systems, and so forth. One strategy to be followed is the codesign since it takes both desired procedures to be followed. Nilsson analyzes several important facets of NCSs. Nilsson [2] introduces models for the delays in NCS, first as a fixed delay, afterward as an independently random, and finally like a Markov process. The author introduces optimal stochastic control theorems for NCSs based upon the independently random and Markovian delay models. In [3], Walsh et al. introduces static and dynamic scheduling policies for transmission of sensor data in a continuous-time LTI system. They introduce the notion of the *maximum allowable transfer interval* (*MATI*), which is the longest time after which a sensor should transmit a data. Walsh et al. [3] derived bounds of the MATI such that the NCS is stable. This MATI ensures that the Lyapunov function of the system under consideration is strictly decreasing at all times. In [4], Zhang et al. extend the work of Walsh, they developed a theorem which ensures the decrease of a Lyapunov function for a discrete-time LTI system at each sampling instant, using two different bounds. These results are less conservative than those of Walsh, because they do not require the system

Lyapunov function to be strictly decreasing at all time. Nevertheless, a number of different linear matrix inequality (LMI) tools for analyzing and designing optimal switched NCSs are introduced.

Alternatively Zhu [5] takes into consideration both the network-induced delay and the time delay in the plant a controller design method is proposed by using the delay-dependent approach. An appropriate Lyapunov functional candidate is utilized to obtain a memoryless feedback controller; this is derived by solving a set of Linear Matrix Inequalities (LMIs). In [6], Wang and Sun, model the network-induced delays of the NCSs as interval variables governed by a Markov chain. Using the upper and lower bounds of the delays, a discrete-time Markovian jump system with norm-bounded uncertainties is presented to model the NCSs. Based on this model, the H∞ state feedback controller can be constructed via a set of LMIs. Recently Fridman and Shaked [7] introduce a new (descriptor) model transformation for delay-dependent stability for systems with time-varying delays in terms of LMIs, and they also refine recent results on delay-dependent H∞ control and extend them to the case of time-varying delays. Based upon this review, this paper defines a model that integrates the time delays for a class of nonlinear system, therefore, this paper presents Fuzzy Control for NCSs [4, 8] considering time delay induced by the computer network as result of online reconfiguration the stability analysis is revised as well.

Since NCS is modified according to time delays, reconfiguration is a transition that modifies the structure of a system so it changes its representation of states. Here, it is used as a feasible approach for time delay modification.

In control systems, several modeling strategies for managing time delay within control laws have been studied by different research groups. Nilsson [2] proposes the use of a time delay scheme integrated to a reconfigurable control strategy, based on a stochastic methodology. Jiang and Zhao [9] describe how time delays are used as uncertainties, which modify pole placement of a robust control law. Izadi-Zamanabadi and Blanke [10] present an interesting case of fault tolerant control approach related to time delay coupling. Blanke et al. [11] study reconfigurable control from the point of view of structural modification, establishing a logical relation between dynamic variables and the respective faults. Finally, Thompson [12] and Benítez-Pérez and García-Nocetti [13] consider that reconfigurable control strategies perform a combined modification of system structure and dynamic response, and, thus, this approach has the advantage of bounded modifications over system response.

Normally, when a fault occurs during the operation of a system, a respective fault tolerance strategy is applied. However, applying such a fault tolerance strategy is not enough to maintain the performance of the system, since dynamic conditions are modified. Therefore, it is seems necessary to take into account current conditions in order to keep system performance, even degraded. Thus, this paper proposes a novel technique based on Fuzzy control and considering bounded variable time delays.

Table 1: First example for Priority Exchange.

Name	Consumption (in units)	Period (in units)
Task 1	2	9
Task 2	1	9
Task 3	2	10
Server	1	6

The objective of this paper is to present a reconfiguration control strategy developed from the time delay knowledge, following scheduling approximation where time delays are known and bounded according to used scheduling algorithm. The novelty of this approximation is to guarantee schedulability as well as stability in the presence of bounded time delays. This is feasible since time delays are bounded according to scheduler response.

2. Scheduling Approximation

Classical Earliest Deadline First plus Priority exchange (PE) algorithms are used to decompose time lines and the respective time delays when present. For instance, time delays are supervised as follows, for a number of tasks:

$$c_1 \longrightarrow c_n T_1 \longrightarrow T_n, \tag{1}$$

where priority is given as the well known Earliest Deadline First [14] algorithm which established as the process with the closest deadline has the most important priority. However, when a nonperiodic tasks appear it is necessary to deploy other algorithms to cope with concurrent conditions. To do so, Priority Exchange algorithm is pursuit in order to manage spare time from EDF algorithm. Priority exchange [15] algorithm uses a virtual server that deploys a periodic task with the highest priority in order to provide enough computing resources for aperiodic tasks. This simple procedure gives a proximity, deterministic, and dynamic behaviour within the group of included processes. In this case, time delays can be deterministic, and bounded. As an example, consider a group of tasks as shown in Table 1. In this case consumption time, as well as period, is given in terms of units that are entered. Remember that server task is the time given for an aperiodic task to take place on the system.

The result of the ordering based upon PE is presented in Figure 1.

Based upon this dynamic scheduling algorithm, time delays are given as current calculus in terms of task ordering. In this case, every time that scheduling algorithm takes place global time delays are modified in the short and long term. This behavior allows time delays to be known and bounded for different periods of time since current and future responses are established. On the other hand, if any aperiodic event would take place, this will be considered in terms of the server to be attended in a global periodic manner with the related time delay cost. For instance, follow next example where four tasks are settled and two aperiodic tasks take place at different times, giving different events with different time delays (see Table 2).

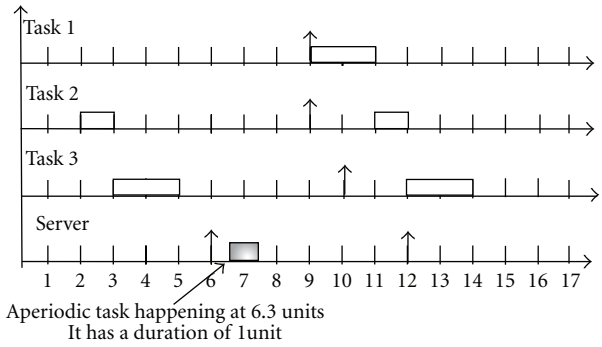

Figure 1: Related organization for PE with respect to Table 1.

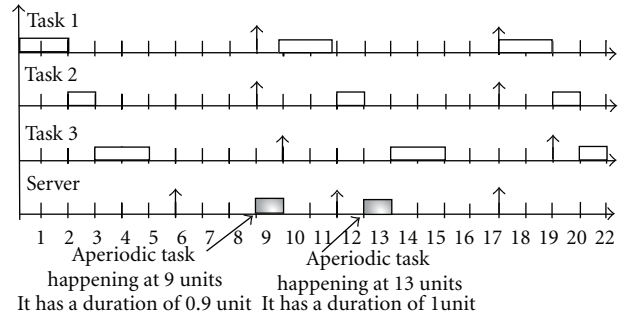

Figure 2: Task organization considering second example for PE.

Table 2: Second example of PE.

Name	Consumption (in units)	Period (in units)
Task 1	2	9
Task 2	1	9
Task 3	2	10
Server	1	6
Aperiodic task 1 (ap1)	0.9	It occurs at 9
Aperiodic task (ap2)	1.0	It occurs at 13

The following task ordering is shown in Figure 2, using PE algorithm where clearly time delays appear.

Now from this resulting ordering different tiny time delays are given for two scenarios as shown in Figure 3.

These two scenarios present two different local time delays that need to be taken into account beforehand in order to settle the related delays according to scheduling approach and control design. These time delays can be expressed in terms of local relations amongst dynamical systems. These relations are the actual and possible delays bounded as marked limit of possible and current scenarios. Then, delays may be expressed as local summations with a high degree of certainty for each specific scenario. In this case, if any new event takes place its response would be delayed until the server would place sometime for its requirements, giving the system a guarantee in terms of time delays and current response.

Now, in terms of this last example, during second scenario total delay is given as follows:

$$\begin{aligned}\text{Total delay} = {} & \text{consumption time delay aperiodic task1} \\ & + \text{consumption time delay task1} + \text{tsc2} \\ & + \text{consumption time delay task2} \\ & + \text{consumption time delay aperiodic task2} \\ & + \text{consumption time delay task3}.\end{aligned} \tag{2}$$

From this example l_p is equal to 2 and l_c is equal to 3. l_p and l_c are the total number of local delays within one scenario from sensor to control and from control to actuator respectively. Moreover, consumption_time_delay_task1, consumption_time_delay_task2, and consumption_time_delay_task3 are related to the actual time delays from Figure 3 when one particular scenario is presented. The same situation is presented with consumption_time_delay_aperiodic_task2. This simple example shows how total time delays play a key role in the dynamical system; however, these are no monolithic since are composed through different local and dynamic delays.

Since aperiodic as well as sporadic events are capable to be attended in terms of a virtual server per node involved on the network giving a bounded response, the resulting behaviour is only dependant on inherent bounded and systematic time delays that can be aggregated in laps. Now, the computer network is only dependant on the synchronization of the network, which is a topic that is out of the scope of this paper and to be reviewed in future work.

The important issue to be determined in this section is that communicating time delays are to be known and bounded even in sporadic situations. Since this modelling is possible, what is left is how to incorporate the aggregate delays (either local or global) onto the dynamic modelling of the system. This strategy is proposed thorough Fuzzy Control since this technique provides the necessary elements to guarantee current global stability even in conditions of sporadic time delays since these are bounded according to the use of virtual server.

3. Fuzzy Control Design Considering Time Delays

Having defined time delays as result of scheduling approximation, several scenarios are potentially presented following this time delay behavior since this is bounded. In fact, the number of scenarios is finite since the combinatorial formation is bounded. Therefore, any strategy, in order to design a control law, needs to take into account gain scheduling approximation. To do so, Fuzzy Control strategy is based upon Takagi-Sugeno. Therefore based upon Fuzzy Control systems [16] stays as

$$1 < i < m, \quad 1 < j < m, \quad \mu_{ij}(x_i(t)), \tag{3}$$

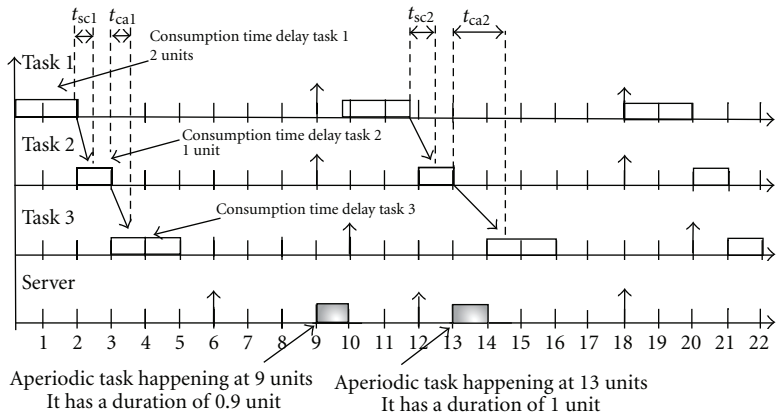

Figure 3: Related time delays are depicted according to both scenarios.

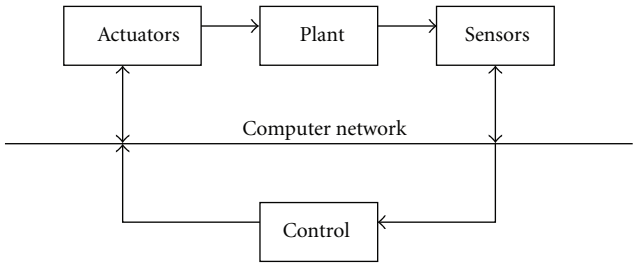

Figure 4: Network control system diagram.

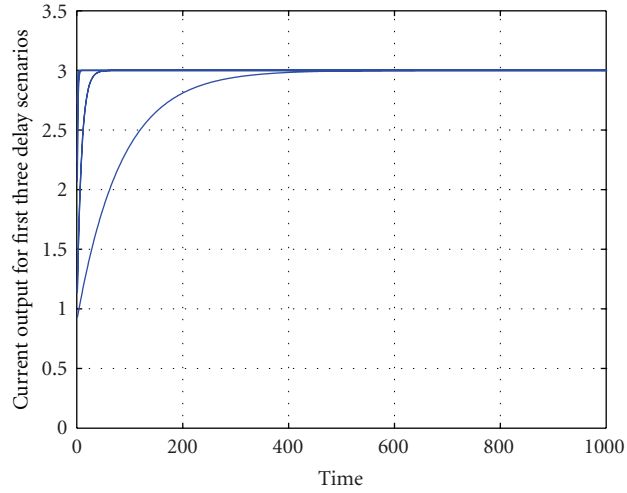

Figure 5: Systems response to those different time delay scenarios.

where x are the states, m is the number of inputs, and μ is the related membership function. One has

$$g_j = \prod_{i=1}^{m} \left\{ \mu_{ij}[x_i(k)] \right\}, \tag{4}$$

$$h_j = \frac{g_j}{\sum_{j=1}^{m} g_j}, \tag{5}$$

$$x(k+1) = \sum_{j=1}^{m} \left[h_j \left\{ A_j^p x(k) + B_j^p u(k) \right\} \right], \tag{6}$$

where $x(k)$ and $u(k)$ are the state and input vectors, and A_j^p and B_j^p are the plant representation per scenario according to current time delays following Figure 4.

Now, considering current time delays as t_{caj} which is current time delay from controller to actuator and t_{scj} which is current time delay from sensor to controller. In here, current time delays are local aggregations of current behavior from scheduling strategy in any condition regardless of the event as long as this is prevented onto virtual server processes. One has

$$\begin{aligned} x_p(k+1) &= \sum_{j=1}^{m} \left[h_j \left\{ A_j^p x_p(k) + B_j^p u_p\left(k - t_{caj}\right) \right\} \right], \\ x_c(k+1) &= \sum_{j=1}^{m} \left[h_j^p \left\{ A_j^c x_c(k) + B_j^c u_c\left(k - t_{scj}\right) \right\} \right], \end{aligned} \tag{7}$$

where A_j^c and B_j^c are the controller representation per scenario, $x_p(k+1)$ and $u_p(k+1)$ are state vector and input vector of the plant, and $x_c(k+1)$ and $u_c(k+1)$ are state vector and input vector of the controller.

From [17] remember that time delay representation in terms of discrete observe the following equations:

$$\begin{aligned} B_j^p &= \sum_{i=1}^{l_p} \left[\int_{t_i}^{t_{i+1}} B_j^c e^{A_j^c t} dt \right], \\ B_j^c &= \sum_{i=1}^{l_c} \left[\int_{t_i}^{t_{i+1}} B_j^p e^{A_j^c t} dt \right]. \end{aligned} \tag{8}$$

Remember that l_p and l_c are the total number of local time delays that appears per scenario. These are defined in last section as local time delays that can be aggregated as in (1) or they maybe presented as shown in (8). In any case final

result is shown in (10) and (11). One has

$$\begin{aligned} y_{p_i} &= c_p^i x_p(k), \\ y_{c_i} &= c_c^i x_c(k), \end{aligned} \tag{9}$$

where l_p and l_c are the number of local time delays; c_c^i and c_p^i are the gains related to observable states; the outputs are gathering as

$$y_p = \sum_{j=1}^{m} \left[h_j \left\{ c_p^j x_p(k) \right\} \right], \tag{10}$$

$$y_c = \sum_{j=1}^{m} \left[h_j \left\{ c_c^j x_c(k) \right\} \right], \tag{11}$$

$$u_p\left(k - t_{caj}\right) \longrightarrow y_c = c_c x_c(k), \tag{12}$$

$$u_c\left(k - t_{scj}\right) \longrightarrow y_p = c_p x_p(k), \tag{13}$$

$$x_p(k+1) = \sum_{j=1}^{m} \left[h_j \left\{ A_j^p x_p(k) + B_j^p u\left(k - t_{caj}\right) \right\} \right], \tag{14}$$

$$= \sum_{j=1}^{m} \left[h_j \left\{ A_j^p x_p(k) + B_j^p C_c x_c\left(k - t_{caj}\right) \right\} \right]. \tag{15}$$

From last equation, the related dynamics are expressed A_j^C as B_j^C and C_c^j where j is the index with respect to each scenario. These scenarios are the related events presented in last section and are the result of local time delays and possible use of virtual server. In any case, (16) shows the holistic representation of the plant in conditions of potential time delays as well as the current dynamic modifications result from each scenario. One has

$$x_p(k+1) = \sum_{j=1}^{m} \left[h_j \left\{ A_j^p x_p(k) + B_j^p \left\{ \sum_{i=1}^{m} h_j \left(c_c^i x_c(k - t_{cai}) \right) \right\} \right] \right] \tag{16}$$

from state of the controller

$$x_c(k+1) = \sum_{i=1}^{m} \left[h_i \{ A_i^c x_c(k) + B_i^c u_c(k - t_{sci}) \} \right],$$

$$x_c(k+1) = \sum_{i=1}^{m} \left[h_i \left\{ A_i^c x_c(k) + B_i^c \left(\sum_{j=1}^{m} h_j \left[c_p^j x_p\left(k - t_{scj}\right) \right] \right) \right\} \right] \tag{17}$$

and in terms of the plant x_p

$$x_p(k+1) = \sum_{j=1}^{m} \left[h_j \left\{ A_j^p x_p(k) + \sum_{i=1}^{m} h_i B_j^p \left(c_c^i x_c(k - t_{cai}) \right) \right\} \right],$$

$$x_p(k+1) = \sum_{j=1}^{m} \sum_{i=1}^{m} \left[h_j h_i \left[B_i^p \left(c_c^i x_c(k - t_{cai}) \right) \right] + h_j A_j^p x_p(k) \right]. \tag{18}$$

For x_c,

$$x_c(k+1) = \sum_{j=1}^{m} \left(h_j \left\{ A_j^c x_c(k) + h_i B_j^c \left(\sum_{j=1}^{m} h_j \left(c_p^i x_p\left(k - t_{scj}\right) \right) \right) \right\} \right),$$

$$x_c(k+1) = \sum_{j=1}^{m} \sum_{i=1}^{m} \left[h_j h_i \left[B_j^p \left(c_c^j x_c(k) + \sum_{i=1}^{m} h_i B_i^c \right) \right] \times \left(\sum_{j=1}^{m} h_j \left(c_p^i x_p\left(k - t_{scj}\right) \right) \right) \right],$$

$$x_c(k+1) = \sum_{j=1}^{m} \sum_{i=1}^{m} \left[h_j h_i B_j^c \left(c_p^i x_p(k - t_{sci}) \right) + h_j A_j^c x_c(h) \right], \tag{19}$$

where the t_{caj} is current time delay from controller to actuator and t_{scj} is current time delay from sensor to controller. Moreover, A_j^c is the related dynamic Matrix of Control law. Now, the second main point presented in this work is the following: since the delays are bounded and can be known it is possible to develop a dynamic representation by using augmented states in terms of current control law and the related state space representation.

$$X = \begin{bmatrix} x_c \\ x_p \end{bmatrix},$$

$$\begin{matrix} x_c(k+1) \\ x_p(k+1) \end{matrix} = \begin{cases} \sum_{j=1}^{m} \sum_{i=1}^{m} \left[h_j h_i \left[B_j^p \left(c_c^i x_c(k - t_{cai}) \right) \right] + h_j A_j^p x_p(k) \right] \\ \sum_{j=1}^{m} \sum_{i=1}^{m} \left[\left(h_j h_i B_j^c \left(C_p^i x_p(k - t_{sci}) \right) + h_j A_j^c x_c(k) \right) \right]. \end{cases} \tag{20}$$

Now, the delays (t_{cai}, t_{sci}) are independent based upon the time obtained from scheduling approximation. This condition is very important for two reasons; firstly time delays are strictly local and may be aggregated differently per scenario or event and secondly these are bounded to inherent sampling time of dynamic benchmarking. Therefore, any aggregation must be bounded as presented.

$$t_{ca1} + t_{sc1} < t_{ca2} + t_{sc2} < \cdots < t_{cam} + t_{scm} < T. \tag{21}$$

Now, in terms of the stability which is necessary to guarantee system response in several conditions, it is pursued the use of classical Lyapunov candidate since one the main conditions

is system bounded response as linear inherent behavior. Therefore, the derivative of a candidate Lyapunov function is expressed as

$$\Delta u(k) = V(k+1) - V(k), \tag{22}$$

and the related Lyapunov function is proposed as

$$V(k) = X(k)^T P X(k). \tag{23}$$

Now in terms of the augmented states and the related fuzzy rules

$$V(k) = \begin{bmatrix} x_c \\ x_p \end{bmatrix}^T P \begin{bmatrix} x_c \\ x_p \end{bmatrix}, \tag{24}$$

where each of the fuzzy rules is given as an expression of local delays (which are the results of local time delays that can be aggregate per event) from current condition from plant towards controller and vice verse. One has

$$\begin{bmatrix} x_c \\ x_p \end{bmatrix} = \begin{bmatrix} x_c(k) \\ x_c(k-t_{ca1}) \\ x_c(k-t_{ca2}) \\ \vdots \\ x_c(k-t_{cam}) \\ x_p(k) \\ x_p(k-t_{sc1}) \\ x_p(k-t_{sc2}) \\ x_p(k-t_{sc3}) \\ \vdots \\ x_p(k-t_{scm}) \end{bmatrix}. \tag{25}$$

Now for each rule, it exists a delay related to a particular condition (which is expressed as event in terms of Section 2) involving the plant and controller. This delay is unique on every specific time. In this case, these are associated to a particular relationship of last equation.

$$\begin{aligned} V(k+1) - V(k) &= \begin{bmatrix} x_c(k+1) \\ x_p(k+1) \end{bmatrix}^T P \begin{bmatrix} x_c(k+1) \\ x_p(k+1) \end{bmatrix} \\ &\quad - \begin{bmatrix} x_c(k) \\ x_p(k) \end{bmatrix}^T P \begin{bmatrix} x_c(k) \\ x_p(k) \end{bmatrix}, \\ V(k+1) - V(k) &= \begin{bmatrix} \sum_{j=1}^{m}\sum_{i=1}^{m}\left(h_j h_i\left(B_j^P\left(c_c^i x_c\left(k-t_{caj}\right)\right)\right) + h_j A_j^P x_p(k)\right) \\ \sum_{j=1}^{m}\sum_{i=1}^{m}\left(h_j h_i\left(B_j^c\left(c_p^i x_p\left(k-t_{scj}\right)\right)\right) + h_j A_j^c x_c(k)\right) \end{bmatrix}^T P \\ &\quad \times \begin{bmatrix} \sum_{j=1}^{m}\sum_{i=1}^{m}\left(h_j h_i\left(B_j^P\left(c_c^i x_c\left(k-t_{caj}\right)\right)\right) + h_j A_j^P x_p(k)\right) \\ \sum_{j=1}^{m}\sum_{i=1}^{m}\left(h_j h_i\left(B_j^c\left(c_p^i x_p\left(k-t_{scj}\right)\right)\right) + h_j A_j^c x_c(k)\right) \end{bmatrix} \\ &\quad - \begin{bmatrix} x_c(k) \\ x_p(k) \end{bmatrix}^T P \begin{bmatrix} x_c(k) \\ x_p(k) \end{bmatrix}. \end{aligned} \tag{26}$$

Remember h_j and h_i are defined following (5). Therefore

$$\begin{aligned} V(k+1) - V(k) &= \begin{bmatrix} x_c(k+1) \\ x_p(k+1) \end{bmatrix}^T P \begin{bmatrix} x_c(k+1) \\ x_p(k+1) \end{bmatrix} \\ &\quad - \begin{bmatrix} x_c(k) \\ x_c(k-t_{ca1}) \\ x_c(k-t_{ca2}) \\ \vdots \\ x_c(k-t_{cam}) \\ x_p(k) \\ x_p(k-t_{sc1}) \\ x_p(k-t_{sc2}) \\ x_p(k-t_{sc3}) \\ \vdots \\ x_p(k-t_{scm}) \end{bmatrix}^T \\ &\quad \times P \begin{bmatrix} x_c(k) \\ x_c(k-t_{ca1}) \\ x_c(k-t_{ca2}) \\ \vdots \\ x_c(k-t_{cam}) \\ x_p(k) \\ x_p(k-t_{sc1}) \\ x_p(k-t_{sc2}) \\ x_p(k-t_{sc3}) \\ \vdots \\ x_p(k-t_{scm}) \end{bmatrix}. \end{aligned} \tag{27}$$

Now considering the fuzzy system representation in terms of local time delays as well as local plants and control laws,

$$\begin{aligned} &V(k+1) - V(k) \\ &= \begin{bmatrix} \sum_{j=1}^{m}\sum_{i=1}^{m}\left(h_j h_i\left(B_j^P\left(c_c^i x_c\left(k-t_{caj}\right)\right)\right) + h_i A_i^P x_p(k)\right) \\ \sum_{j=1}^{m}\sum_{i=1}^{m}\left(h_j h_i\left(B_j^c\left(c_p^i x_p\left(k-t_{scj}\right)\right)\right) + h_i A_i^c x_c(k)\right) \end{bmatrix}^T \\ &\quad \times P \begin{bmatrix} \sum_{j=1}^{m}\sum_{i=1}^{m}\left(h_j h_i\left(B_j^P\left(c_c^i x_c\left(k-t_{caj}\right)\right)\right) + h_i A_i^P x_p(k)\right) \\ \sum_{j=1}^{m}\sum_{i=1}^{m}\left(h_j h_i\left(B_j^c\left(c_p^i x_p\left(k-t_{scj}\right)\right)\right) + h_i A_i^c x_c(k)\right) \end{bmatrix} \\ &\quad - \begin{bmatrix} x_c(k) \\ x_c(k-t_{ca1}) \\ x_c(k-t_{ca2}) \\ \vdots \\ x_c(k-t_{cam}) \\ x_p(k) \\ x_p(k-t_{sc1}) \\ x_p(k-t_{sc2}) \\ x_p(k-t_{sc3}) \\ \vdots \\ x_p(k-t_{scm}) \end{bmatrix}^T P \begin{bmatrix} x_c(k) \\ x_c(k-t_{ca1}) \\ x_c(k-t_{ca2}) \\ \vdots \\ x_c(k-t_{cam}) \\ x_p(k) \\ x_p(k-t_{sc1}) \\ x_p(k-t_{sc2}) \\ x_p(k-t_{sc3}) \\ \vdots \\ x_p(k-t_{scm}) \end{bmatrix}. \end{aligned} \tag{28}$$

Now if only one of the time delays is considered. This condition is possible since time delays are bounded and strictly less than sampling time of dynamic system. Therefore at any case following inequality is always kept true. One has

$$0 > \begin{bmatrix} x_c(k+1) \\ x_p(k+1) \end{bmatrix}^T P \begin{bmatrix} x_c(k+1) \\ x_p(k+1) \end{bmatrix} - \begin{bmatrix} x_c(k) \\ x_c\left(k - t_{caj}\right) \\ x_p(k) \\ x_p\left(k - t_{scj}\right) \end{bmatrix}^T P \begin{bmatrix} x_c(k) \\ x_c\left(k - t_{caj}\right) \\ x_p(k) \\ x_p\left(k - t_{scj}\right) \end{bmatrix}. \tag{29}$$

Therefore this may be expressed as follows:

$$\begin{aligned} 0 > & \left\{ \begin{bmatrix} h_j h_i\left(B_j^P(c_c^i)\right) & h_i A_i^P \ \ 0 \ \ 0 \\ 0 & 0 \ \ h_j h_i\left(B_j^c\left(c_p^i\right)\right) \ \ h_i A_i^c \end{bmatrix} \right. \\ & \left. \times \begin{bmatrix} x_c\left(k - t_{caj}\right) \\ x_p(k) \\ x_p\left(k - t_{scj}\right) \\ x_c(k) \end{bmatrix} \right\}^T \\ & \times P \begin{bmatrix} h_j h_i\left(B_j^P(c_c^i)\right) & h_i A_i^P \ \ 0 \ \ 0 \\ 0 & 0 \ \ h_j h_i\left(B_j^c\left(c_p^i\right)\right) \ \ h_i A_i^c \end{bmatrix} \\ & \times \begin{bmatrix} x_c\left(k - t_{caj}\right) \\ x_p(k) \\ x_p\left(k - t_{scj}\right) \\ x_c(k) \end{bmatrix} \\ & - \begin{bmatrix} x_c\left(k - t_{caj}\right) \\ x_p(k) \\ x_p\left(k - t_{scj}\right) \\ x_c(k) \end{bmatrix}^T P \begin{bmatrix} x_c\left(k - t_{caj}\right) \\ x_p(k) \\ x_p\left(k - t_{scj}\right) \\ x_c(k) \end{bmatrix}. \end{aligned} \tag{30}$$

and based upon this particular case, state representation may given as

$$\begin{aligned} 0 > & \begin{bmatrix} x_c\left(k - t_{caj}\right) \\ x_p(k) \\ x_p\left(k - t_{scj}\right) \\ x_c(k) \end{bmatrix}^T \\ & \times \left[\begin{bmatrix} h_j h_i\left(B_j^P(c_c^i)\right) & h_i A_i^P \ \ 0 \ \ 0 \\ 0 & 0 \ \ h_j h_i\left(B_j^c\left(c_p^i\right)\right) \ \ h_i A_i^c \end{bmatrix}^T \right. \\ & \left. \times P \begin{bmatrix} h_j h_i\left(B_j^P(c_c^i)\right) & h_i A_i^P \ \ 0 \ \ 0 \\ 0 & 0 \ \ h_j h_i\left(B_j^c\left(c_p^i\right)\right) \ \ h_i A_i^c \end{bmatrix} - P \right] \\ & \times \begin{bmatrix} x_c\left(k - t_{caj}\right) \\ x_p(k) \\ x_p\left(k - t_{scj}\right) \\ x_c(k) \end{bmatrix}. \end{aligned} \tag{31}$$

Because only one specific delay is possible on current time, only one state condition is available and is expressed as before following LMI conditions matrix; G_j^i.

$$G_j^i = \begin{bmatrix} h_j h_i\left(B_j^P(c_c^i)\right) & h_i A_i^P \ \ 0 \ \ 0 \\ 0 & 0 \ \ h_j h_i\left(B_j^c\left(c_p^i\right)\right) \ \ h_i A_i^c \end{bmatrix}. \tag{32}$$

The core of current representation is expressed as

$$\begin{aligned} 0 > & \left[\begin{bmatrix} h_j h_i\left(B_j^P(c_c^i)\right) & h_i A_i^P \ \ 0 \ \ 0 \\ 0 & 0 \ \ h_j h_i\left(B_j^c\left(c_p^i\right)\right) \ \ h_i A_i^c \end{bmatrix}^T \right. \\ & \left. \times P \begin{bmatrix} h_j h_i\left(B_j^P(c_c^i)\right) & h_i A_i^P \ \ 0 \ \ 0 \\ 0 & 0 \ \ h_j h_i\left(B_j^c\left(c_p^i\right)\right) \ \ h_i A_i^c \end{bmatrix} - P \right], \end{aligned} \tag{33}$$

$$0 > G_j^{i\,T} P G_j^i - P. \tag{34}$$

Remember that in terms of LMI this consideration should be globally stable in terms of index performance.

4. Experimental Setup

The following is a setup to demonstrate how achievable this combination to make a suitable approximation for time delays managements is. The number of periodic tasks is equal to 5 and the number of aperiodic tasks is 7. Following table presents tasks conditions.

Now based upon plant dynamics this is given as

$$\begin{aligned} A &= \begin{bmatrix} -0.3 & 0 & 3 \\ -4 & -2 & 0.1 \\ 0.1 & 0.3 & -1 \end{bmatrix}, \\ B &= \begin{bmatrix} 0.1 \\ 0.3 \\ 0.2 \end{bmatrix}, \\ \dot{x} &= Ax + Bu, \\ y &= cu. \end{aligned} \tag{35}$$

Time delays are determined per scenario with each local delay considered. The number of scenarios is 13 (as shown in Figure 6), where each columns is one scenario and the related time delays are amongst each sensor following (8). The given control design following (34) is expressed as follows, where time delays tend to be constant per scenario:

Time delays =[0.001 0.0000 0.0 0.00 0.0 0.0 0.0 0.0 0.0 0.0 0.0 0.0 0.0 0.0
0.0012 0.0001 0.0003 0.00075 0.0001 0.000101 0.00009 0.00002 0.00002 0.000012 0.00003 0.00001 0.000109
0.003 0.0002 0.001 0.0009 0.00018 0.0001601 0.000109 0.000102 0.0000222 0.0000212 0.000063 0.000061 0.000209
0.004 0.0012 0.00232 0.00101 0.00021 0.0020101 0.000209 0.000302 0.000062 0.0000412 0.000073 0.000101 0.000309
0.005 0.002 0.004 0.0013 0.00031 0.0030101 0.000609 0.000602 0.000082 0.0000712 0.000303 0.000201 0.000609
0.00611 0.00302 0.0055 0.00244 0.00041 0.0040101 0.000809 0.001002 0.000102 0.0000812 0.000503 0.001001 0.001009
0.007 0.006 0.0065 0.0033 0.00101 0.0050101 0.001009 0.003002 0.0001202 0.0005012 0.000703 0.002001 0.003009
0.00811 0.0072 0.0085 0.0044 0.00201 0.0060101 0.003009 0.004002 0.000402 0.0008012 0.000903 0.003001 0.004009
0.0095 0.008 0.0095 0.0066 0.00401 0.0070101 0.0039009 0.006002 0.000602 0.0020012 0.002003 0.005001 0.005009
0.0099 0.009 0.0099 0.008 0.00501 0.0080101 0.006009 0.007002 0.004002 0.0050012 0.005003 0.007001 0.009009
0.010 0.01 0.01000 0.01 0.00701 0.008990101 0.007009 0.030002 0.040002 0.0070012 0.010003 0.070001 0.090009]

Figure 6

$$k = \begin{bmatrix} 0.1 & 0.11 & 0.001 & 0.01 & 0.1 & 0.01 & -0.001 & -0.01 & 0.0 & -0.0 & -2.2 \\ -0.2 & -0.11 & 0.1 & -1.1 & -0.2 & -0.5 & -1.1 & -0.9 & 0.1 & -0.01 & -0.1 \\ -1.2 & -1.1 & -1.1 & -0.2 & -0.13 & -2.1 & -0.9 & -2.1 & -1.01 & -1.1 & -0.2 \end{bmatrix}. \quad (36)$$

Fuzzy variables as well as the number of rules are determined following Méndez-Monroy and Benítez-Pérez [16]; here final approximation is determined by similar error following time delay approach and the related system response. Now the response of system according to First output is shown in Figure 5.

5. Conclusions

Current time delays can be modeled using real-time dynamic scheduling algorithms; however the resulting delays are time varying and stationary, therefore related local control laws need to be designed according to this characteristic and time integration is the key global issue to be taken into consideration. Global stability is reached by the use of Takagi-Sugeno Fuzzy Control Design where nonlinear combination is followed by current situation of the states which are partially delayed due to communication behavior.

The main contribution on this paper is the capability to determine local time delays that can be aggregated per event since a scheduling algorithm contributes to bound time response. Therefore Fuzzy Control may be attractive to guarantee global stability since any condition is bounded to be less than sampling period at the worst case scenario with no loose of generality.

The use of dynamic scheduling approximation allows the system to be predictable and bounded; therefore, time delays can be modeled in these terms. Moreover, the resulting dynamic representation tackles the inherent switching per scenario. This approximation has the main drawback that context switch may be invoked every time a periodic task takes place and it is possible to be executed; in this case inherent time delays to this action are taken into account to be processed as uncertainties.

Acknowledgments

The authors acknowledge the support of UNAM-PAPIIT IN103310, ICyTDF PICCO 10-53, and Mr. Adrian Duran for his valuable help.

References

[1] H. Benítez-Pérez, "Real-time distributed control: a fuzzy and model predictive control approach for a nonlinear problem," *Nonlinear Analysis: Hybrid Systems*, vol. 2, no. 2, pp. 474–490, 2008.

[2] J. Nilsson, *Real-time control with delays [Ph.D. thesis]*, Department of Automatic Control, Lund Institute of Technology, Lund, Sweden, 1998.

[3] G. C. Walsh, H. Ye, and L. Bushnell, "Stability analysis of networked control systems," in *Proceedings of the American Control Conference (ACC '99)*, pp. 2876–2880, San Diego, Calif, USA, June 1999.

[4] H. Zhang, D. Yang, and T. Chai, "Guaranteed cost networked control for T-S fuzzy systems with time delays," *IEEE Transactions on Systems, Man and Cybernetics C*, vol. 37, no. 2, pp. 160–172, 2007.

[5] X. Zhu, C. Hua, and S. Wang, "State feedback controller design of networked control systems with time delay in the plant," *International Journal of Innovative Computing, Information and Control*, vol. 4, no. 2, pp. 283–290, 2008.

[6] Y. Wang and Z. Sun, "H∞ control of networked control systems via LMI approach," *International Journal of Innovative Computing, Information and Control*, vol. 3, no. 2, pp. 343–352, 2007.

[7] E. Fridman and U. Shaked, "Delay-dependent stability and H∞ control: constant and time-varying delays," *International Journal of Control*, vol. 76, no. 1, pp. 48–60, 2003.

[8] K. Tanaka and H. O. Wang, *Fuzzy Control Systems Design and Analysis: A Linear Matrix Inequality Approach*, John Wiley & Sons, New York, NY, USA, 2001.

[9] J. Jiang and Q. Zhao, "Reconfigurable control based on imprecise fault identification," in *Proceedings of the American Control Conference (ACC '99)*, vol. 1, pp. 114–118, San Diego, Calif, USA, June 1999.

[10] R. Izadi-Zamanabadi and M. Blanke, "A ship propulsion system as a benchmark for fault-tolerant control," *Control Engineering Practice*, vol. 7, no. 2, pp. 227–239, 1999.
[11] M. Blanke, M. Kinnaert, J. Lunze, and M. Staroswiecki, *Diagnosis and Fault Tolerant Control*, Springer, 2003.
[12] H. A. Thompson, "Wireless and internet communications technologies for monitoring and control," *Control Engineering Practice*, vol. 12, no. 6, pp. 781–791, 2004.
[13] H. Benítez-Pérez and F. García-Nocetti, *Reconfigurable Distributed Control*, Springer, 2005.
[14] Y. Liu, *Real Time Systems*, Wiley, 2000.
[15] Buttazzo, *Real Time Systems*, Springer, 2004.
[16] P. E. Méndez-Monroy and H. Benítez-Pérez, "Supervisory fuzzy control for networked control systems," *International Journal Innovative Computing, Information and Control Express Letters*, vol. 3, no. 2, pp. 233–240, 2009.
[17] H. Benitez-Pérez, J. Ortega-Arjona, F. Cardenas-Flores, and P. Quiñones-Reyes, "Reconfiguration control strategy using Takagi-Sugeno model predictive control for network control systems—a magnetic levitation case study," *Proceedings of the Institution of Mechanical Engineers I*, vol. 224, no. 8, pp. 1022–1032, 2010.

Hindawi Publishing Corporation
Advances in Fuzzy Systems
Volume 2012, Article ID 504368, 12 pages
doi:10.1155/2012/504368

Research Article

Application of a Data-Driven Fuzzy Control Design to a Wind Turbine Benchmark Model

Silvio Simani

Department of Engineering, University of Ferrara, 44122 Ferrara, Italy

Correspondence should be addressed to Silvio Simani, silvio.simani@unife.it

Received 1 August 2012; Accepted 2 November 2012

Academic Editor: Sendren Sheng-Dong Xu

In general, the modelling of wind turbines is a challenging task, since they are complex dynamic systems, whose aerodynamics are nonlinear and unsteady. Accurate models should contain many degrees of freedom, and their control algorithm design must account for these complexities. However, these algorithms must capture the most important turbine dynamics without being too complex and unwieldy, mainly when they have to be implemented in real-time applications. The first contribution of this work consists of providing an application example of the design and testing through simulations, of a data-driven fuzzy wind turbine control. In particular, the strategy is based on fuzzy modelling and identification approaches to model-based control design. Fuzzy modelling and identification can represent an alternative for developing experimental models of complex systems, directly derived directly from measured input-output data without detailed system assumptions. Regarding the controller design, this paper suggests again a fuzzy control approach for the adjustment of both the wind turbine blade pitch angle and the generator torque. The effectiveness of the proposed strategies is assessed on the data sequences acquired from the considered wind turbine benchmark. Several experiments provide the evidence of the advantages of the proposed regulator with respect to different control methods.

1. Introduction

Wind turbines are complex nonlinear dynamic systems forced by gravity and stochastic wind disturbance, which are affected by gravitational, centrifugal, and gyroscopic loads. Their aerodynamics are nonlinear and unsteady, whilst their rotors are subject to complicated turbulent wind inflow fields driving fatigue loading. Therefore, wind turbine modelling and control represent complex and challenging tasks [1, 2].

Accurate models have to contain many degrees of freedom in order to capture the most important dynamic effects. It is clear that the design of control algorithms for wind turbines has to take into account these complexities. On the other hand, control algorithms must capture the most important turbine dynamics, without being too complex and unwieldy [1, 3].

Today's wind turbines employ different control actuation and strategies to achieve the required goals and performances. Some turbines perform the control action through passive methods, such as in fixed-pitch, stall control machines. In these machines, the blades are designed so that the power is limited above rated wind speed through the blade stall. Thus, no pitch mechanism is needed [1]. On the other hand, below rated wind speed, the generator speed is fixed [4]. Rotors with adjustable pitch are often used in constant-speed machines to provide turbine power control better than the one achievable with blade stall [5]. Therefore, blade pitching can be regulated to provide constant power above rated wind speed. The pitch mechanisms have to be quite fast, in order to provide good power regulation in the presence of gusts and turbulence. In order to maximise the power output below the wind speed, the rotational speed of the turbine must vary with wind speed.

The control strategies for such machines are typically designed using simple classical control design techniques such as (Proportional Integral Derivative) PID control for blade pitch regulation, as shown for example, in [6]. Advanced controls can be used to improve the energy capture, for example through the generator torque control, as shown for example, in [7]. In the same situation,

Johnson et al. [8] proposed an adaptive control approach. Advanced multivariable control design methods, such as those based on state-space models, can be used to meet control objectives and use all the available actuators and sensors in a reduced number of control loops. In [9], a multivariable approach was used to design both an independent pitch controller to mitigate the effects of asymmetric wind disturbances. Even though two separate control loops were used for example, in [9], the multivariable control design approach can require fewer control loops compared to classical control design methods, as shown for example, in [10]. Therefore, the trade-off between wind turbine control algorithms' accuracy and their limited computational complexity represents the challenging point that motivates this study.

The first contribution of this work consists of providing an application example of the design, and testing through simulations, of a data-driven fuzzy wind turbine control. In particular, the strategy is based on fuzzy modelling and identification approaches to model-based control design. As stated above, since a mathematical model is a description of system behaviour, accurate modelling for a complex nonlinear system can be very difficult to achieve in practice. Thus, fuzzy modelling and identification can represent an alternative for developing experimental models of complex systems, such as wind turbine systems considered in this work. In contrast to pure nonlinear identification methods, fuzzy systems are capable of deriving nonlinear models directly from measured input-output data without detailed system assumptions [11]. Thus, it is suggested to describe the plant under investigation by a collection of local affine systems of the type of Takagi-Sugeno (TS) fuzzy prototypes [12], whose parameters are obtained by identification procedures. The proposed identification approach is motivated by previous works by the same author [13, 14].

Regarding the controller design, this paper suggests a fuzzy control approach for the adjustment of both the wind turbine blade pitch angle and the generator torque, with application to a wind turbine benchmark. This design is performed according to the following steps. Firstly, a PI regulator is devised using the classic Ziegler-Nichols method [15]. Then, the corresponding fuzzy (Proportional Integral) PI controller is built, by means of a suitable choice of the gains. The membership functions (MFs) and rules are derived directly from the identified TS fuzzy models. The effectiveness of the proposed fuzzy modelling and control strategy are assessed on the data sequences acquired from the considered benchmark. Several simulation experiments provide the evidence of the advantages of the proposed fuzzy PI regulator with respect to the switching control strategy developed in [16].

The capabilities of the proposed control strategy are compared with respect to the control strategy developed in [16], and with reference to different control methods based for example, on sliding mode or neural controllers [17, 18].

The next feature of the work is related with the impact evaluation of the modelling uncertainties, disturbance, and measurement errors on the designed control scheme. In particular, the paper proposes the use of extensive Monte-Carlo simulations for the analysis and the assessment of the design, the robustness, the stability, and its final performance evaluation. In fact, as in this case the wind turbine cannot be described by any analytical dynamic model, the Monte-Carlo tool represents the only method for evaluating the performances of the developed control scheme when applied to the monitored process.

The last key point of the paper concerns the assessment of the developed control algorithms through a hardware in the loop (HIL) facility, which has been developed to qualify the proposed approaches in the presence of experimental limitations closer to real situations.

Finally, the paper has the following structure. Section 2 provides an overview of the wind turbine system considered in this work. Section 3 recalls the fuzzy modelling and identification strategy exploited for the design of the fuzzy controller. This proposed fuzzy controller design, followed by a simple tuning strategy, are presented in Section 3.2. The achieved results and comparisons with different control strategies are summarised in Section 4, where the stability, the robustness analysis, and the capabilities of the developed control method with respect to measurement and modelling errors are investigated in simulation. Realistic simulations and comparisons with different control schemes relying on sliding mode and neural controller are also reported. Section 5 ends the paper by highlighting the main achievements of the work, providing some suggestions for possible further research topics.

2. Wind Turbine Benchmark Description

The three-blade horizontal axis turbine considered in this paper works according to the principle that the wind is acting on the blades, and thereby moving the rotor shaft. In order to up-scale the rotational speed to the needed one at the generator, a gear box is introduced. A more accurate description of the benchmark model can be found in [16, 19]. The diagram of the wind turbine model is sketched in Figure 1.

The rotational speed, and consequently the generated power, is regulated by means of two controlled inputs: the converter torque $\tau_g(t)$ and the pitch angle $\beta_r(t)$ of the turbine blades. From the wind turbine system, a number of measurements can be acquired. $\omega_r(t)$ is the rotor speed, $\omega_g(t)$ is the generator speed, and $\tau_g(t)$ is the torque of the generator controlled by the converter, which is provided with the torque reference, $\tau_r(t)$. The estimated aerodynamic torque is defined as $\tau_{\text{aero}}(t)$. This estimate clearly depends on the wind speed, which unfortunately is very difficult to measure correctly. A very uncertain measurement can be available as described in [16].

2.1. Model Description. This section recalls briefly the wind turbine model description in the continuous-time domain. It is subsequently approximated via identified discrete-time prototypes, as shown in Section 3.

The aerodynamic model is defined as in

$$\tau_{\text{aero}}(t) = \frac{\rho A C_p(\beta_r(t), \lambda(t))\, v^3(t)}{2\omega_r(t)}, \tag{1}$$

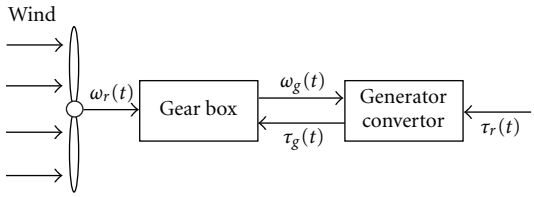

Figure 1: Logic diagram of the wind turbine, where only two of the three blades are shown.

where ρ is the density of the air, A is the area covered by the turbine blades in its rotation, $\beta_r(t)$ is the pitch angle of the blades, $v(t)$ is the wind speed, whilst $\lambda(t)$ is the tip-speed ratio of the blade, defined as

$$\lambda(t) = \frac{\omega_r(t)R}{v(t)} \tag{2}$$

with R the rotor radius. C_p represents the power coefficient, here described by means of a two-dimensional map (look up table) [16]. Equation (1) is used to estimate $\tau_{\text{aero}}(t)$ based on an assumed estimated $v(t)$, and measured $\beta_r(t)$ and $\omega_r(t)$. Due to the uncertainty of the wind speed, the estimate of $\tau_{\text{aero}}(t)$ is considered affected by an unknown measurement error, which motivates the approaches described in Section 3.

A simple one-body model is used to represent the drive train, as described in [19]. The generator torque $\tau_g(t)$ and the reference $\tau_r(t)$ are in this context transformed to the low speed side of the drive train (rotor side), whilst p_{gen} is the generator power coefficient. With these assumptions, the complete continuous-time description of the system under diagnosis has the form of

$$\begin{aligned} \dot{x}_c(t) &= f_c(x_c(t), u(t)), \\ y(t) &= x_c(t), \end{aligned} \tag{3}$$

where $u(t) = [\beta_r(t), \tau_g(t)]^T$ and $y(t) = x_c(t) = [P_g(t), \omega_g(t)]^T$ are the control inputs and the monitored output measurements, respectively. $f_c(\cdot)$ represents the continuous-time nonlinear function that will be approximated via discrete-time prototypes from N sampled data $u(k)$ and $y(k)$, with $k = 1, 2, \ldots, N$, presented in Section 3.

Regarding the input and output signals, $\omega_g(t)$ is the generator speed measurement, $P_g(t)$ is the generator power measurement, $\beta_r(t)$ is the pitch measurement, and $\tau_g(t)$ is generator torque measurement. Finally, the model parameters and the map $C_p(\beta, \lambda)$ are chosen in order to represent a realistic turbine, which is used as benchmark system in this study [16].

2.2. Wind Turbine Benchmark Control System. The controller for a wind turbine operates in principle in two main zones. Zone 1 is the power optimisation, whilst zone 2 corresponds to constant power production. The optimal power in zone 1 is obtained if the blade pitch angle β_r is equal 0 degrees, and if the tip speed ratio is constant at its optimal value λ_{opt}. The tip speed ratio, λ, as already described by (2), can be written as in (4), where R is the radius of the blades, v is the wind speed, and ω_r is the angular rotor speed:

$$\lambda = \frac{\omega_r R}{v}. \tag{4}$$

The optimal value of λ, which is denoted with λ_{opt}, is determined as the maximal value point in the power coefficient mapping of the wind turbine. This optimal value is achieved by setting the reference torque to the converter, $\tau_g = \tau_{gr}$. The reference torque τ_{gr} in this power optimisation zone can be written as

$$\tau_{gr} = K_{\text{opt}} \omega_r^2 \tag{5}$$

with:

$$K_{\text{opt}} = \frac{1}{2} \rho A R^3 \frac{C_{p_{\max}}}{\lambda_{\text{opt}}^3} \tag{6}$$

with ρ being the air density, A the area swept by the turbine blades, $C_{p_{\max}}$ the maximal value of C_p (i.e., the power coefficient map), related to the λ_{opt}, that is, the optimal tip-speed ratio.

When the power reference is achieved, the controller can be switched to control zone 2. In this zone the control objective consists of following the power reference, P_r, which is obtained by controlling β_r, such that the C_p is decreased. In a traditional industrial control scheme, usually a PI controller is used to keep ω_r at the prescribed value by changing β_r. The second control input is τ_g, whose value is computed by using (5).

The wind turbine benchmark controller considered in this study was implemented with a sample frequency at 100 Hz, that is, $T_s = 0.01$ s. The controller starts in zone 1. Therefore, the control mode should switch from zone 1 to zone 2 if the following conditions hold [16]:

$$P_g(k) \geq P_r(k), \qquad \omega_g(k) \geq \omega_{\text{nom}}, \tag{7}$$

where k indicates the acquired discrete-time measurements from the corresponding continuous-time signals, whilst ω_{nom} is the nominal turbine speed. On the other hand, the control switches from zone 2 to zone 1 if

$$\omega_g(k) < \omega_{\text{nom}} - \omega_\Delta, \tag{8}$$

where ω_Δ is a number that introduces hysteresis to ensure a minimum time between transitions. On the other hand, for the control zone 2:

$$\begin{aligned} \beta_r(k) &= \beta_r(k-1) + k_p e(k) + \left(k_i T_s - k_p\right) e(k-1), \\ e(k) &= \omega_g(k) - \omega_{\text{nom}} \end{aligned} \tag{9}$$

with $k = 1, 2, \ldots, N$. The parameters for this PI *speed controller* are $k_i = 0.5$ and $k_p = 3$, with sampling time $T_s = 0.01$ s., as described in [19].

Finally, regarding the control of the input τ_g, a second PI regulator is implemented, as the one of (9):

$$\begin{aligned} \tau_r(k) &= \tau_r(k-1) + k_p e(k) + \left(k_i T_s - k_p\right) e(k-1), \\ e(k) &= P_g(k) - P_r. \end{aligned} \tag{10}$$

The parameters for this second PI *power controller* are $k_i = 0.014$ and $k_p = 447 \times 10^{-6}$, according to [19].

3. Fuzzy Identification and Control Design

This section describes the comprehensive approach exploited for obtaining the fuzzy description of the wind turbine system and the control strategy used for the regulation of its input variables. In particular, the fuzzy modelling and identification scheme, which is recalled in Section 3.1, enhances the design procedure of the proposed fuzzy controller, as shown in Section 3.2.

3.1. Fuzzy Identification and Data Clustering. In order to generate fuzzy models automatically from measurements, a comprehensive methodology is used. This employs fuzzy clustering techniques to partition the available data into subsets characterised by a linear behaviour. The relationships between the presented identification method and linear regression are exploited, allowing for the combination of fuzzy logic techniques with system identification tools. In addition, the implementation in the Matlab toolbox of the Fuzzy Modelling and Identification (FMID) techniques presented in the following is available [20]. Fuzzy identification usually refers to methods and algorithms for constructing fuzzy models from data.

A large part of fuzzy modelling and identification algorithms (see, e.g., [11] and references therein) share a common two-step procedure, in which at first, the operating regions are determined using heuristics or data clustering techniques. Then, in the second stage, the identification of the parameters of each submodel is achieved using the identification algorithm in particular proposed by the author [13, 14], which can be seen as a generalisation of classical least-squares. From this perspective, fuzzy identification can be regarded as a search for a decomposition of a nonlinear system, which gives a desired balance between the complexity and the accuracy of the model, effectively exploring the fact that the complexity of systems is usually not uniform. A suitable class of fuzzy clustering algorithms can be thus used for this decomposition purpose, and in particular, the well-known Gustafson-Kessel (GK) fuzzy clustering [11] is exploited in this work, since already implemented and available in [20].

The fuzzy rule-based model suitable for the approximation of a large class of nonlinear systems was introduced by Takagi and Sugeno (TS) in [12]. In the TS fuzzy model, the rule consequents are crisp functions of the model inputs:

$$R_i : \textbf{IF } \mathbf{x}(k) \text{ is } A_i \text{ THEN } y_i = f_i(\mathbf{x}(k)), \tag{11}$$

where $i = 1, 2, \ldots, M$, $\mathbf{x}(k) \in \Re^p$ is the input (antecedent) variable and $y_i \in \Re$ is the output (consequent) variable. R_i denotes the ith rule, and M is the number of rules in the rule base. A_i is the antecedent fuzzy set of the ith rule, defined by a (multivariate) membership function. The consequent functions f_i are typically chosen as instances of a suitable parameterised function, whose structure remains equal in all the rules and only the parameters vary. A simple and practically useful parameterisation of the function f_i is the affine form:

$$y_i = \mathbf{a}_i \mathbf{x} + b_i, \tag{12}$$

where a_i is the parameter vector (regressand), and b_i is the scalar offset. $\mathbf{x} = \mathbf{x}(k)$ represents the regressor vector, which can contain delayed samples of $u(k)$ and $y(k)$. This model is referred to as *affine TS model*, and it can be written as [12]

$$y = \frac{\sum_{i=1}^{M} \mu_i(\mathbf{x}) y_i}{\sum_{i=1}^{M} \mu_i(\mathbf{x})}. \tag{13}$$

The *antecedent* fuzzy sets μ_i are extracted from the fuzzy partition matrix [11, 20]. The *consequent parameters* $\mathbf{a}_i$ and b_i are estimated from the data using the method developed by the author [13, 14] and recalled below. This identification scheme exploited for the estimation of the TS model parameters has been integrated into the FMID toolbox for Matlab by the author. This approach developed by the author is usually preferred when the TS model should serve as predictor, as it computes the consequent parameters by the so-called *Frisch scheme* [13, 14]. Therefore, after the clustering of the data has been obtained via the GK algorithm, the data subsets are processed according the Frisch scheme identification procedure [13, 14], in order to estimate the TS parameters for each affine submodels.

3.2. Fuzzy Controller Design. The proposed fuzzy logic controller is fed by the error signal $e(k)$, that is, the tracking error defined as the difference between the considered set-point $r(k)$ and the plant controlled output $y(k)$ at the sample k:

$$e(k) = r(k) - y(k). \tag{14}$$

The fuzzy PI controller uses a second input signal, defined as the sum of the system errors, which is computed using

$$\delta e(k) = \sum_{i=1}^{k} e(i). \tag{15}$$

It is known from the Digital Control Theory that the most frequently used digital PI control algorithm can be described as follows:

$$u(k) = k_p e(k) + k_i \delta e(k), \tag{16}$$

where $k_i = k_p(T_s/T_i)$, T_s is the sampling time, T_i is the integral time constant of the conventional controller, k_p is the proportional gain, and $u(k)$ is the output control action.

The structure of the control system with the proposed fuzzy controllers are based on Sugeno's fuzzy technique. The Sugeno's fuzzy rules into the fuzzy PI controller are in the generalised form of "IF-THEN" composition with a premise and an antecedent part to describe the control policy. The rule base comprises a collection of M rules, where the index j represents the rule number:

$$R_j : \textbf{IF } \mathbf{x}(k) \text{ is } A_j \text{ THEN}$$

$$f_u^{(j)}(k) = K_P^{(j)} e(k) + K_I^{(j)} \delta e(k) + b_j, \quad j = 1, 2, \ldots, M, \tag{17}$$

where $e(k)$ and $\delta e(k)$ are the input variables, with $k = 1,\ldots,N$. In this expression, a similarity between the expression of the conventional digital PI controller of (16) and the Sugeno's output function of (17) can be found. In this case, the fuzzy PI controller is considered as a collection of several local PI controllers, which are represented by the Sugeno's functions into the different fuzzy rules.

For a discrete universe with M quantisation levels in the fuzzy output, the control action $u = u_F$ is expressed as a weighted average of the Sugeno's output functions f_u, and their membership degrees μ_i of the quantisation levels, with $i = 1,\ldots,M$. Also in this case, before the output can be inferred, the degree of fulfilment of the antecedent denoted by $\mu_i(\mathbf{x})$ must be computed. Thus, the degree of fulfilment is simply equal to the membership degree of the given input $\mathbf{x}$, that is, $\mu_i = \mu_{A_i}(\mathbf{x})$. By recalling the identified TS model, the inference is reduced to a simple expression, similar to the fuzzy-mean defuzzification formula [11]:

$$u_F = \frac{\sum_{j=1}^{M} \mu_j(\mathbf{x}) f_u^{(j)}}{\sum_{j=1}^{M} \mu_j(\mathbf{x})} \tag{18}$$

or by substituting the expression of the fuzzy PI terms:

$$u_F(k) = \frac{\sum_{j=1}^{M} \mu_j(\mathbf{x}(k)) \left(K_P^{(j)} e(k) + K_I^{(j)} \delta e(k) + b_j\right)}{\sum_{j=1}^{M} \mu_j(\mathbf{x}(k))}, \tag{19}$$

where the time dependence at the instant k has been highlighted.

It is worth noting that the PI controller parameters $K_P^{(j)}$ and $K_I^{(j)}$ (with $j = 1,\ldots,M$) are settled according to the Ziegler-Nichols rules applied to the identified local linear TS submodels. Then, in order to obtain a quick reaction to set-point variations, gain scheduling of the fuzzy regulator parameters is performed depending on the error, as shown by (19).

In more detail, if for example the TS consequents are represented by second order discrete-time local linear dynamic models ($n = 2$) described in (12) by their identified parameters $\mathbf{a}_i = [\alpha_1^{(i)}, \alpha_2^{(i)}, \gamma_1^{(i)}, \gamma_2^{(i)}]$, and regressor $\mathbf{x}^T(k) = [-y(k-1), -y(k-2), u(k-1), u(k-2)]$, ($i = 1,\ldots,M$), the so-called critical gain $K_o^{(i)}$ and critical period of oscillations $T_o^{(i)}$ required by the Ziegler-Nichols method can be computed for example, as follows [15]:

$$K_o^{(i)} = \frac{\alpha_1^{(i)} - \alpha_2^{(i)} - 1}{\gamma_2^{(i)} - \gamma_1^{(i)}},$$
$$T_o^{(i)} = \frac{2\pi T_s}{\arccos \delta^{(i)}}, \quad \text{with } \delta^{(i)} = \frac{\alpha_2^{(i)} \gamma_1^{(i)} - \alpha_1^{(i)} \gamma_2^{(i)}}{2\gamma_2^{(i)}} \tag{20}$$

which holds if $|\delta^{(i)}| < 1$. Alternative formulas can also be used [15]. Equation (21) is thus used for calculating the parameters $K_P^{(i)}$ and $K_I^{(i)}$ of the (local) ith PI controller of (17):

$$K_P^{(i)} = 0.6 K_o^{(i)} \left(1 - \frac{T_s}{T_o^{(i)}}\right),$$
$$K_I^{(i)} = \frac{1.2 K_o^{(i)}}{K_P^{(i)} T_o^{(i)}}, \tag{21}$$

where T_s is the sampling time. As shown for example, in [15], TS consequents of orders n greater than 2 can be considered.

Once the fuzzy PI controller parameters have been computed, the second step consists of building the fuzzy controller of (19). The input MFs $\mu_j(\mathbf{x})$ can coincide with the ones of the identified TS model, as described for example, in [11]. The number of the input MFs determines the number of rules and output MFs. In this work, the optimal number of rules M is equal to the minimal number of clusters used to identify the nonlinear system, as described at the end of Section 3.1. Finally, the adopted fuzzy operators are the product as AND operator, the bounded sum as OR operator, MIN as implication method, and the Centre of Gravity (COG) as defuzzification method.

Section 4 will show the achieved results regarding the fuzzy PI controller parameter tuning using the data sequences from the wind turbine benchmark.

4. Simulation Results

This section describes the simulation results achieved with the method relying on both the fuzzy modelling techniques oriented to the design of the fuzzy controller.

Regarding the proposed control method, the GK clustering algorithm discussed in Section 3.1 with $M = 3$ clusters and a number of shifts $n = 2$ were applied to the estimation and validation sampled data sets $\{P_g(k), \omega_g(k), \beta_r(k)\}$, with $k = 1, 2, \ldots, N$ and $N = 440 \times 10^3$. On the other hand, a number of clusters $M = 3$ and $n = 2$ were considered for achieving a suitable clustering of the sampled data sets $\{P_g(k), \omega_g(k), \tau_g(k)\}$. After clustering, the TS model parameters for each output were estimated. Therefore, the ith output $y(t)$ of the wind turbine ($i = 1,\ldots,m$ and $m = 2$) continuous-time model of (3) is approximated by a TS fuzzy prototype (13). The relative mean square errors of the output estimations are 0.0254 for the first output and 0.0125 for the second one.

The fitting capabilities of the estimated fuzzy models can be expressed also in terms of the so-called Variance Accounted For (VAF) index [11]. In particular, the VAF value for first output was bigger than 90%, whilst bigger than 99% for the second one. Hence, the fuzzy multiple models seem to approximate the process under investigation quite accurately. As an example, Figure 2 represents simulated output values ω_g and P_g of the TS fuzzy model from the training of the wind turbine benchmark model by using FMID.

Using these identified TS fuzzy prototypes, the model-based approach for determining the fuzzy controller was exploited and applied to the considered wind turbine

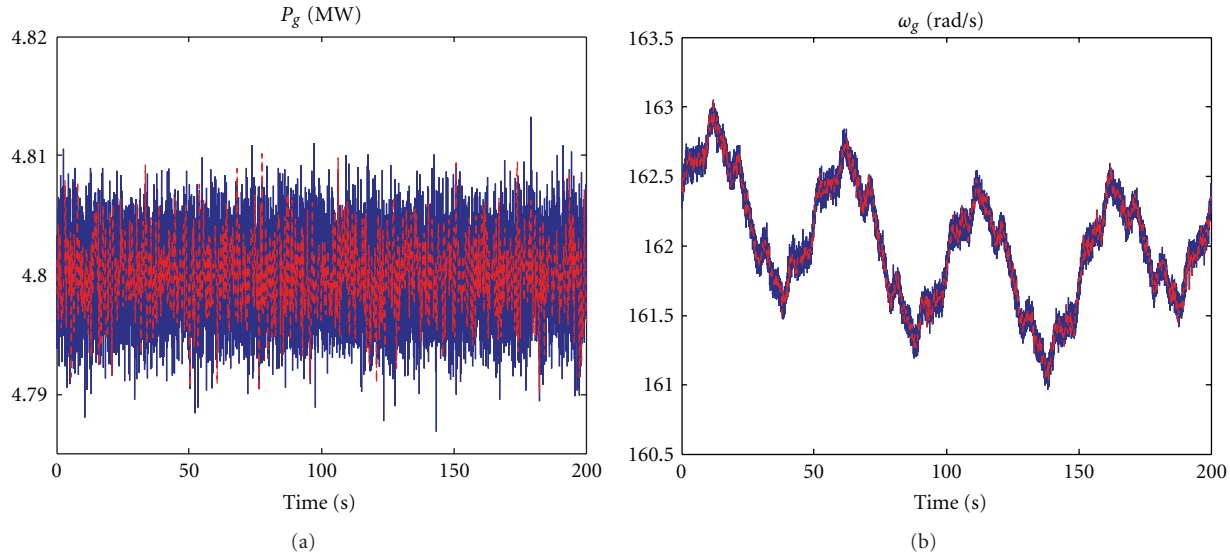

Figure 2: TS fuzzy model estimated outputs (red) compared with the measured ones (blue).

benchmark. According to Section 3.2, the parameters of the fuzzy PI controllers were computed.

In the following, the suggested fuzzy PI controllers and the original switching strategy described in Section 2 were implemented in the Matlab and Simulink environments.

The experimental setup employs 2 (Multiple-Input Single-Output) MISO fuzzy PI regulators used for the control of the blade pitch angles and the generator control torque, respectively. As an example, by using the previous (21), the following tuned parameter sets have been computed for the pitch angle control:

$$\begin{aligned} \left\{K_P^{(1)}, \ldots, K_P^{(3)}\right\} &= \{2.3, 3.1, 3.2\}, \\ \left\{K_I^{(1)}, \ldots, K_I^{(3)}\right\} &= \{0.2, 0.4, 0.5\}. \end{aligned} \tag{22}$$

In order to compare the advantages of the proposed fuzzy PI strategy, the obtained results were also compared with the ones achieved by using the original switching wind turbine benchmark regulator recalled in Section 2.

The controller capabilities were assessed in simulation by considering different data sequences. In Tables 1 and 2, the per cent Normalised Sum of Squared tracking Error (NSSE) values defined as

$$\text{NSSE\%} = 100\sqrt{\frac{\sum_{k=1}^{N}\left(r(k)-y(k)\right)^2}{\sum_{k=1}^{N} r^2(k)}} \tag{23}$$

are computed for the designed controllers.

It is worth noting that in *partial load operation* (zone 1), the performance is represented by the comparison between the power produced by the generator, P_g, with respect to the theoretical maximum power output, P_r, given the instant wind speed. On the other hand, in *full load operation* (zone 2), the performance depends on the generator speed, ω_g, with respect to the nominal one, ω_{nom}.

Table 1: Controllers in *partial load operation*: NSSE% values.

Data set	Benchmark controller	Fuzzy PI
Estimation data	39.34%	21.36%
Validation data	42.19%	22.17%

Table 2: Controllers in *full load operation*: NSSE% values.

Data set	Benchmark controller	Fuzzy PI
Estimation data	19.53%	11.57%
Validation data	21.01%	12.85%

According to these simulation results, the properties of the suggested fuzzy controllers appear better than the original switching regulator described in Section 2.2.

4.1. Robustness and Attraction Domain Evaluation. In this section, further experimental results were reported. They regard the performance evaluation of the developed control scheme with respect to modelling errors and measurement uncertainty. In particular, the simulation of different data sequences was performed by exploiting the wind turbine benchmark simulator and a Matlab Monte-Carlo analysis [21]. In fact, the Monte-Carlo tool is useful at this stage as the control strategy performances depend on the error magnitude due to the model approximation and uncertainty, as well as on input-output measurement errors [22].

In particular, the nonlinear wind turbine simulator originally developed in the Simulink environment [19] was modified by the author in order to vary the statistical properties of the signals used for modelling possible process parameter uncertainty and measurement errors. Therefore, in this case, the Monte-Carlo analysis represents a viable method for analysing some properties of the developed fuzzy

Table 3: Simulated wind turbine parameter uncertainties.

Variable	Nominal value	Min. error	Max. error
ρ	$1.225\,\text{kg/m}^3$	±0.1%	±20%
A	$6647.6\,\text{m}^2$	±0.1%	±20%
J	$7.794 \times 10^6\,\text{kg/m}^2$	±0.1%	±30%
p_{gen}	$98\,\text{s}^{-1}$	±0.1%	±20%
N_r	95	±0.1%	±20%
C_p	C_{p0}	±0.1%	±50%
u	u_0	±0.1%	±20%
y	y_0	±0.1%	±20%

Table 4: Monte-Carlo analysis for the fuzzy controller: NSSE% values.

Test case	Partial load	Full load
Best case	19.37%	9.57%
Average case	21.19%	11.94%
Worst case	23.19%	13.94%

control scheme, when applied to the considered process. Under this assumption, Table 3 reports the nominal values of the considered wind turbine model parameters with respect to their simulated uncertainty.

The Monte-Carlo analysis was performed by describing these variables as Gaussian stochastic processes, with zero-mean and standard deviations corresponding to minimal and maximal error values in Table 3.

Moreover, it is assumed that the input-output signals u and y and the power coefficient map C_p entries were affected by errors, expressed as per cent standard deviations of the corresponding nominal values u_0, y_0, and C_{p0} also reported in Table 3. These values can be motivated by the work from the same author [23], which suggests to provide a polynomial approximation of the map C_p via an identification procedure from the input-output u and y affected by measurement errors.

Therefore, for performance evaluation, reliability and robustness analysis of the fuzzy control scheme, the best, average, and worst values of the NSSE% index were computed, and experimentally evaluated with 500 Monte-Carlo runs [22]. The value of NSSE% is computed for several possible combinations of the parameter values reported in Table 3. Table 4 summarises the results obtained by considering the fuzzy control scheme in Section 3.

In particular, Table 4 summarises the values of the considered performance indices according to the best, worst, and average cases, with reference to the possible combinations of the parameters described in Table 3. Table 4 shows that the proposed fuzzy control scheme allows to maintain good control performances even in the presence of considerable error and uncertainty effects.

The robustness of the controller designs could be evaluated also on the basis of the Domain Of Attraction (DOA) analysis [24]. In fact, the stability of equilibrium points plays a fundamental role in dynamical systems. For nonlinear dynamical systems an investigation of the stability and robustness properties requires the characterisation of the DOA of an equilibrium point, that is, the set of initial conditions from which the trajectory of the controlled system converges to such a point. In this case, it is clear that estimating or controlling the DOA are very difficult problems because of the complex relationship of this set with the model of the wind turbine. Moreover, as shown in Section 2, the wind turbine system cannot be described as an analytic model. Therefore, the DOA analysis can be performed only in simulation using again the Monte-Carlo tool, which is used for providing random variations of wind turbine initial conditions, in a similar way of Table 3.

Figures 3 and 4 show an example of the results from a Monte-Carlo run, where the wind turbine monitored outputs, that is, the generator power P_g and the generator angular rate ω_g (red) are compared with their reference values (blue), thus assessing the equilibrium point stability, for a perturbed arbitrary initial condition.

In particular, Figure 3 shown that for an arbitrary initial condition randomly changed by the Monte-Carlo tool, the proposed fuzzy TS is able to maintain the stability of the wind turbine. However, the monitor process becomes unstable when controller by the benchmark PI regulator, as highlighted in Figure 4. The simulation results highlight that the benchmark regulator scheme stabilises the wind turbine up to 10% level of variation in its nominal initial conditions, whilst the proposed fuzzy TS control strategy tolerates ranges within 30% of the nominal initial values.

Finally, the results demonstrate that Monte-Carlo simulation is an effective tool for experimentally testing the design robustness, stability, and reliability of the proposed control method with respect to modelling uncertainty and disturbance.

4.2. Comparative Studies. This section provides some comparative results with respect to alternative control approaches, in particular relying on the sliding mode and neural network controllers.

In general, the sliding mode control can be designed on the basis of a linear or a nonlinear model [17]. In both cases, the design procedure is based on the selection of an appropriate switching manifold, and then on the determination of a control law, including a discontinuous term, that ensures the sliding motion in this manifold. However, sliding mode control design for the nonlinear case is generally applied to systems in the so-called *regular form*, which consists of two blocks: one depending on the control, with the same dimension of the control vector, and the other independent. Such regular form may be obtained by means of a nonlinear coordinate transformation. On the other hand, if a linear model is used, the transformation into the regular form and the design of the sliding mode dynamics are simpler, since known results from linear control techniques (i.e., pole placement, eigenstructure assignment, and optimal quadratic) are applicable. This design procedure can be therefore tolerant with respect to uncertainty and modelling errors, since these disturbances are decoupled from the sliding motion.

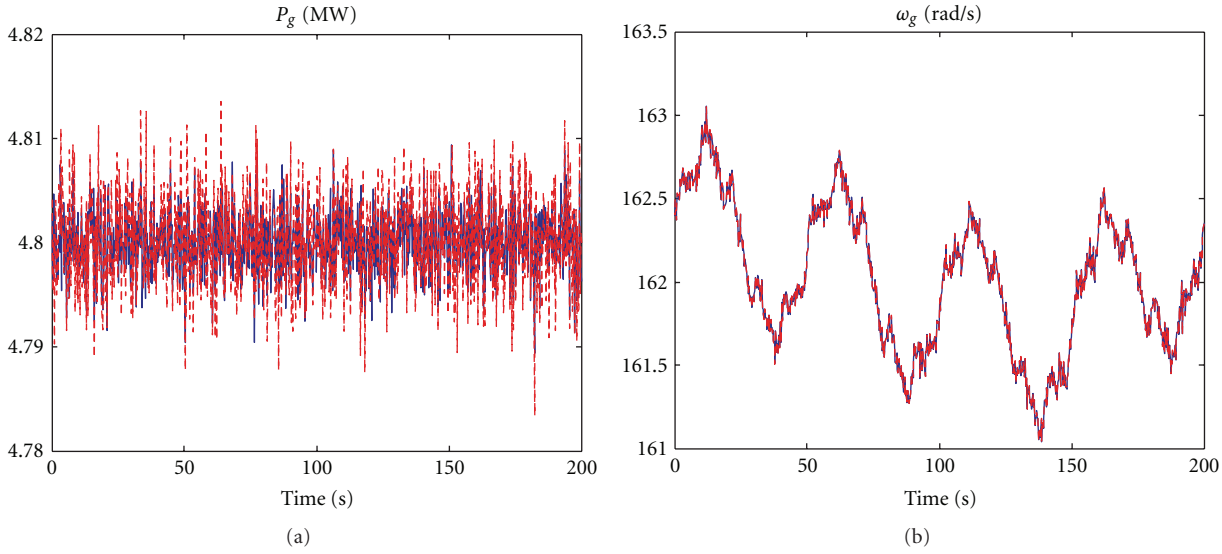

Figure 3: P_g and ω_g outputs with the fuzzy TS controller.

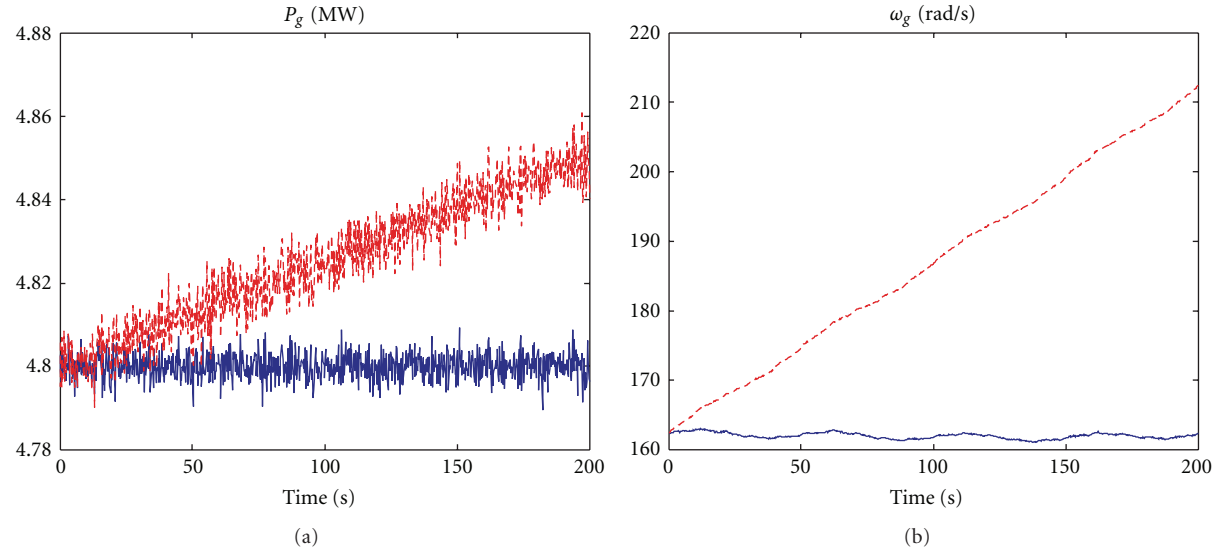

Figure 4: P_g and ω_g outputs with the PI benchmark regulator.

The second control scheme exploited for comparison purposes was developed by using the strategy relying on the Neural Network (NN) tool [18]. The NN controller was on a 2-inputs 2-outputs time-delayed three-layer Multi-Layer Perceptron (MLP) NN with 5 neurons in the input layer, 10 neurons in the hidden layer and 2 neurons in the output layer. The NN has been trained in order to provide the optimal reference tracking on the basis of the training patterns and target sequences [18].

In order to provide a brief but clear insight into the above-mentioned control technique, the comparison was performed in the same previous working conditions and based on the NSSE% index suggested at the beginning of Section 4.

It is worth noting that the schemes implemented via the sliding mode or neural controllers do not exploit any adaptation mechanism. In fact, the sliding mode control strategy is able to decouple the uncertainty via the sliding motion, whilst neural networks were designed to *passively tolerate* disturbance and modelling errors.

Tables 5 and 6 summarise the results obtained by comparing the sliding mode and NN techniques analysed in this subsection. It can be seen how the different schemes are able to tolerate uncertainty and errors, thus achieving graceful control performance degradation.

The comparison between Tables 5 and 6 shows that the scheme using the sliding mode controller allows to achieve better performances in terms of tracking error. However,

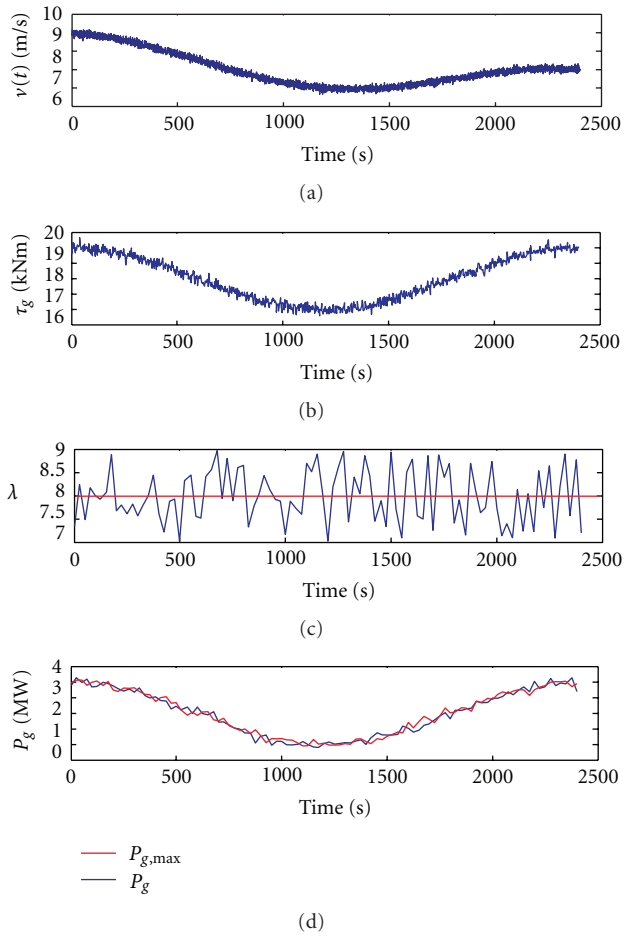

Figure 5: Simulations of the wind turbine benchmark working at partial load.

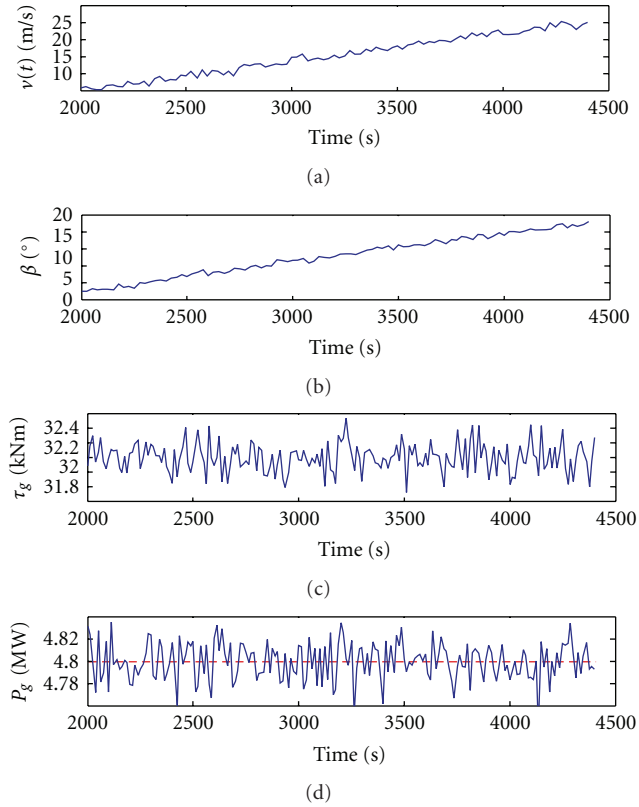

Figure 6: Simulations of the wind turbine benchmark operating at full load.

Table 5: Monte-Carlo analysis with the sliding mode controller.

Test case	Partial load	Full load
Best case	27.71%	26.55%
Average case	28.52%	27.72%
Worst case	29.19%	28.44%

Table 6: Monte-Carlo analysis with the NN controller.

Test case	Partial load	Full load
Best case	36.45%	35.57%
Average case	37.49%	37.94%
Worst case	41.19%	39.94%

the control input energy required by the sliding mode controller is bigger than the other cases. Moreover, the sliding mode controller can increase the computational time considerably with respect to the other solution.

Few further comments can be drawn here. When the modelling of the dynamic system can be perfectly obtained, in general model-based control strategies are preferred. On the other hand, when modelling errors and uncertainty are present, alternative control schemes relying on fuzzy control method can show interesting robustness properties in the presence of unmodeled disturbance, modelling mismatch, and measurement errors. With reference to the neural controller, in the case of a controlled system with modelling errors, the offline learning can lead to quite good results. Other explicit disturbance decoupling techniques can take advantage of their robustness capabilities, but with quite complicated and not straightforward design procedures. The NN-based scheme relies on the learning accumulated from offline simulations, but the training stage can be computationally heavy. Regarding the proposed method using the fuzzy tools, it seems rather simple and straightforward, even if optimisation stages can be required.

4.3. Stability Tests. The stability properties of the overall control strategy were checked again by means of a Monte-Carlo campaign based on the wind turbine benchmark simulator when controlled by means of the proposed regulators. In fact, as pointed out in Section 2, the wind turbine system contains the power coefficients map C_p that cannot be described by any analytical model obtained via first principles. Thus, the Monte-Carlo analysis represents the only method for estimating the stability of the developed fuzzy control scheme when applied to the monitored process.

Initial conditions were changed randomly and disturbance affecting the system was simulated during the transient related to the stability analysis.

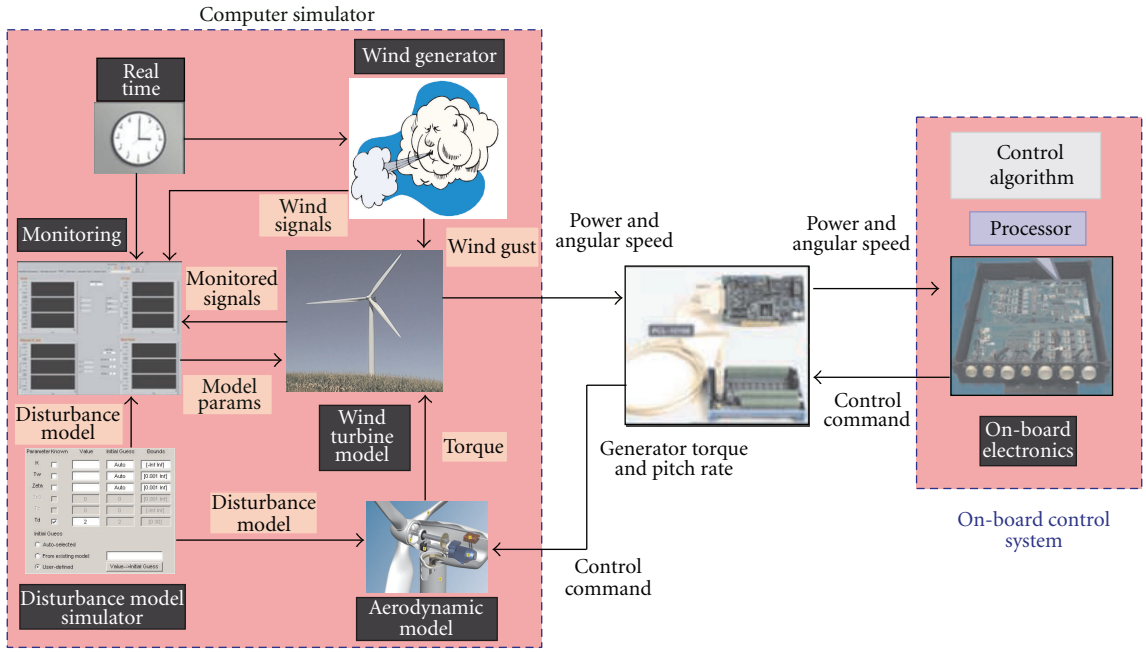

Figure 7: Main elements of the HIL test-bed.

All simulations were performed by considering noise signals modelled as band limited white processes, according to the standard deviations reported in Table 3.

As an example of a single Monte-Carlo run, Figure 5 highlighted that the main wind turbine model variables, such as the generator torque τ_g, the tip-speed-ratio λ, and the generator power P_g remain bounded around the reference values, proving the overall system stability in simulation, even in the presence of disturbance and uncertainty. These results refer to the case of partial load operation with the fuzzy controller, when the wind speed $v(t)$ is below 12 m/s.

Figure 5 highlights also that in the first part of the simulation the output power P_g becomes larger than the theoretical one $P_{g,\max}$, as the kinetic energy from the rotor shaft is converted into electrical energy produced by the generator. On the other hand, $P_{g,\max}$ can be above the generated power, since the inertia of the rotor is accelerated before $P_{g,\max}$ can be matched.

As further example of the Monte-Carlo run, the results achieved with the fuzzy controller above rated wind speed are reported in Figure 6.

Figure 6 depicts also the generator speed ω_g and the control input β_r. Also in this situation, the main wind turbine variables remain bounded around the reference values, thus assessing the overall system stability in simulation, even in the presence of modelling errors and noise signals.

It is worth noting that the fuzzy control design followed by the analysis procedures shown in Sections 4.1, 4.2, and 4.3 were developed using the Matlab and Simulink software tools, in order to automate the overall simulation process. These feasibility and reliability studies are of paramount importance for real application of control strategies once implemented to future wind turbine installations.

To this aim, Section 4.4 illustrates how the designed control algorithms are assessed through the hardware in the loop (HIL) test-bed to evaluate their capabilities in a more realistic experimental situation.

4.4. Hardware in the Loop Tests. In order to evaluate the potential of utilising the proposed control algorithms in real applications and investigate their capability to on-board implementation, this section presents the results of the hardware in the loop (HIL) tests. These experimental results serve to validate definitely the desired requirements attributed to the designed algorithms considering almost real conditions that the wind turbine may experiment with during its working situations. For this purpose, HIL test-bed is developed according to Figure 7, which provides the capabilities to validate the developed control algorithms in an almost real-time condition.

This laboratory facility includes the following three elements:

(i) *Computer simulator*: this simulator, which has been created in the Labview software from the Matlab and Simulink environments, provides the modelling of the wind turbine dynamics considering the factors such as uncertainty, disturbance, measurement errors, and wind turbine component models, as described in Section 2. This software tool allows to monitor the parameters related to the control algorithms and analyse their performance.

(ii) *On-board electronics*: the control algorithms have been implemented in this element. The electronic device utilised in this module is the AWC 500 system, which in addition satisfies standard wind turbine

Table 7: HIL results with the fuzzy controller: NSSE% values.

Partial load	Full load
22.81%	12.83%

technical specifications. This element also provides the flexibility to implement and evaluate the different control algorithms. As it can be seen from Figure 7, the on-board electronics receives the wind turbine power and generator angular rate as its inputs, and after the algorithm processing, generates the generator torque and pitch command output signals transmitted to the computer simulator. The generator torque and the pitch commands are generated by the proposed control algorithms and are applied to the wind turbine model simulator to guarantee its stability and the required specifications.

(iii) *Interface circuits*: they consist of the appropriately selected input-output cards, which receive the output signals from the computer simulator and transmit the output signals generated by the control algorithms.

The results achieved from one test are summarised in Table 7 for the proposed fuzzy controller.

Table 7 illustrates that there are some deviations between the achieved results, but consistent with the ones of Table 4 from the Monte-Carlo analysis. In fact, the performances in the simulation case are somehow better than the HIL experimental case, which is reasonable due to the issues detailed below.

(1) Accuracy of the float calculations in the on-board electronics processor is more restrictive than the CPU of the computer simulator.

(2) The major deviation between the results originates from the analog to digital and digital to analog conversions.

Since the data must be transferred between the on-board electronics and the computer simulator, a 16 bit conversion is inevitable, so this conversion error may lead to the deterioration of the experimental results. Note that, since the real situations do not need to transfer data between the on-board electronics and the computer, this error is not a problem and is consistent with the results already achieved via the Monte-Carlo tool. Moreover, although there are some deviations between the simulation and the experimental results, but due to the reasons stated above, these deviations are not critical, and the results obtained are accurate enough for real wind turbine applications.

5. Conclusion

The paper is focused on the control design problem for wind turbines, since they are complex nonlinear dynamic systems. Moreover, their aerodynamics are nonlinear, unsteady, and complex, and their modelling is thus challenging. Therefore, the design of control algorithms for wind turbines must account for these complexities. This paper showed how a fuzzy control design method can be suggested to improve classic control limitations, such as PI standard regulators. Therefore, the application example of a viable, simple, and straightforward control design was provided, through extensive simulations of a wind turbine prototype. Tests on the considered benchmark process and Monte-Carlo analysis represented the tools for assessing experimentally the properties of the proposed fuzzy control scheme, in the presence of modelling and measurement errors. The developed control method was also compared with other different approaches. To highlight the potential of the proposed control algorithms in real applications, hardware in the loop test facility was planned to study the digital implementation of the designed strategies. The test results showed again that the developed schemes maintained their desired performances, which validated their feasibility also in real-time implementations. Future works aim to perform sustainable and dependability analyses that are of paramount importance for real wind turbine applications.

References

[1] K. E. Johnson, L. Y. Pao, M. J. Balas, and L. J. Fingersh, "Control of variable-speed wind turbines: standard and adaptive techniques for maximizing energy capture," *IEEE Control Systems Magazine*, vol. 26, no. 3, pp. 70–81, 2006.

[2] P. F. Odgaard, C. Damgaard, and R. Nielsen, "On-line estimation of wind turbine power coefficients using unknown input observers," in *Proceedings of the 17th World Congress, International Federation of Automatic Control (IFAC '08)*, Seoul, Korea, July 2008.

[3] Z. Hameeda, Y. Honga, Y. Choa, S. Ahnb, and C. Song, "Condition monitoring and fault detection of wind turbines and related algorithms: a review," *Renewable and Sustainable Energy Reviews*, vol. 13, no. 1, pp. 1–39, 2009.

[4] X. F. Zhang, D. P. Xu, and Y. B. Liu, "Adaptive optimal fuzzy control for variable speed fixed pitch wind turbines," in *Proceedings of the 5fth World Congress on Intelligent Control and Automation, Conference Proceedings (WCICA '04)*, pp. 2481–2485, June 2004.

[5] R. Sakamoto, T. Senjyu, T. Kinjo, N. Urasaki, and T. Funabashi, "Output power leveling of wind turbine generator by pitch angle control using adaptive control method," in *Proceedings of the International Conference on Power System Technology (POWERCON '04)*, pp. 834–839, November 2004.

[6] E. A. Bossanyi, "Developments in closed loop controller design for wind turbines," in *Proceedings of the 19th ASME Wind Energy Conference (ASME '00)*, pp. 64–74, ASME, Reno, Nev, USA, 2000.

[7] L. J. Fingersh and K. E. Johnson, "Baseline results and future plans for the NREL controls advanced research turbine," in *Proceedings of the 23rd ASME Wind Energy Conference*, pp. 87–93, ASME, Reno, Nev, USA, January 2004.

[8] K. E. Johnson, L. J. Fingersh, M. J. Balas, and L. Y. Pao, "Methods for increasing region 2 power capture on a variable-speed wind turbine," *Journal of Solar Energy Engineering*, vol. 126, no. 4, pp. 1092–1100, 2004.

[9] M. Geyler and P. Caselitz, "Individual blade pitch control design for load reduction on wind turbines," in *Proceedings of the European Wind Energy Conference and Exhibition*, pp. 7–10, Milan, Italy, May 2007.

[10] A. D. Wright, L. J. Fingersh, and M. J. Balas, "Testing state-space controls for the controls advanced research turbine," *Journal of Solar Energy Engineering*, vol. 128, no. 4, pp. 506–515, 2006.

[11] R. Babuška, *Fuzzy Modeling for Control*, Kluwer Academic Publishers, 1998.

[12] T. Takagi and M. Sugeno, "Fuzzy identification of systems and its applications to modeling and control," *IEEE Transactions on Systems, Man and Cybernetics*, vol. 15, no. 1, pp. 116–132, 1985.

[13] S. Simani, C. Fantuzzi, R. Rovatti, and S. Beghelli, "Noise rejection in parameters identification for piecewise linear fuzzy models," in *Proceedings of the IEEE International Conference on Fuzzy Systems Part 2 (of 2)*, pp. 378–383, May 1998.

[14] S. Simani, C. Fantuzzi, R. Rovatti, and S. Beghelli, "Parameter identification for piecewise-affine fuzzy models in noisy environment," *International Journal of Approximate Reasoning*, vol. 22, no. 1, pp. 149–167, 1999.

[15] V. Bobál, J. Böhm, J. Fessl, and J. Machácek, *Digital Self-Tuning Controllers: Algorithms, Implementation and Applications. Advanced Textbooks in Control and Signal Processing*, Springer, 1st edition, 2005.

[16] P. F. Odgaard, J. Stoustrup, and M. Kinnaert, "Fault tolerant control of wind turbines—a benchmark model," in *Proceedings of the 7th IFAC Symposium on Fault Detection, Supervision and Safety of Technical Processes*, vol. 1, pp. 155–160, Barcelona, Spain, July 2009.

[17] C. Edwards and S. Spurgeon, *Sliding Mode Control: Theory and Applications*, Taylor & Francis, London, UK, 1st edition, 1998.

[18] J. Korbicz, J. M. Koscielny, Z. Kowalczuk, and W. Cholewa, Eds., *Fault Diagnosis: Models, Artificial Intelligence, Applications*, Springer, 1st edition, 2004.

[19] P. F. Odgaard and J. Stoustrup, "Unknown input observer based scheme for detecting faults in a wind turbine converter," in *Proceedings of the 7th IFAC Symposium on Fault Detection, Supervision and Safety of Technical Processes*, vol. 1, Elsevier, Barcelona, Spain, June 2009.

[20] R. Babuška, *Fuzzy Modelling and Identification Toolbox*, Control Engineering Laboratory, Faculty of Information Technology and Systems, Delft University of Technology, Delft, The Netherlands, 2000.

[21] A. Doucet, N. de Freitas, and N. Gordon, Eds., *Sequential Monte Carlo Methods in Practice. Statistics for Engineering and Information Science*, Springer, New York, NY, USA, 2001.

[22] D. Lieber, A. Nemirovskii, and R. Y. Rubinstein, "A fast Monte Carlo method for evaluating reliability indexes," *IEEE Transactions on Reliability*, vol. 48, no. 3, pp. 256–261, 1999.

[23] S. Simani and P. Castaldi, "Estimation of the power coefficient map for a wind turbine system," in *Proceedings of the 9th European Workshop on Advanced Control and Diagnosis (ACD '11)*, Budapest University of Technology and Economics, Ed., no. paper 13, pp. 1–7, MTA SZTAKI Computer and Automation Research Institute, Hungarian Academy of Sciences, and BME Budapest University of Technology and Economics, BME Budapest University of Technology and Economics, Budapest, Hungary, November 2011.

[24] H. K. Khalil, *Nonlinear Systems*, Prentice Hall, 3rd edition, 2001.

Hindawi Publishing Corporation
Advances in Fuzzy Systems
Volume 2012, Article ID 801650, 8 pages
doi:10.1155/2012/801650

Research Article

Proper Fuzzification of Prime Ideals of a Hemiring

H. V. Kumbhojkar

403 Poorvarang Apartments, 13th Lane, Kolhapur 416008, Maharashtra, India

Correspondence should be addressed to H. V. Kumbhojkar, hvk_maths@yahoo.co.in

Received 26 April 2012; Accepted 8 October 2012

Academic Editor: Sendren Sheng-Dong Xu

Prime fuzzy ideals, prime fuzzy k-ideals, and prime fuzzy h-ideals are roped in one condition. It is shown that this way better fuzzification is achieved. Other major results of the paper are: every fuzzy ideal (resp., k-ideal, h-ideal) is contained in a prime fuzzy ideal (resp., k-ideal, h-ideal). Prime radicals and nil radicals of a fuzzy ideal are defined; their relationship is established. The nil radical of a fuzzy k-ideal (resp., an h-ideal) is proved to be a fuzzy k-ideal (resp., h-ideal). The correspondence theorems for different types of fuzzy ideals of hemirings are established. The concept of primary fuzzy ideal is introduced. Minimum imperative for proper fuzzification is suggested and it is shown that the fuzzifications introduced in this paper are proper fuzzifications.

1. Introduction

This paper is, in some sense, an extended version of the article "On Fuzzification of Prime Ideals with Special Reference to Semirings" in SciTopics and something more.

Several attempts have been made to fuzzify the concepts of prime ideals/k-ideals/h-ideals of a semiring [1–7], prime ideals of a ring [8–15], and prime ideals of a semigroup [16–18]. We have discussed elsewhere [6], in detail, the deficiencies in the definition of a prime fuzzy h-ideal proposed in [7]. The definition suffers from three major drawbacks. First, it is very restrictive in the sense that the fuzzy h-ideals, which are prime according to the definition, are 2-valued function. Secondly, since one of the two values is always 1 (the greatest element of the lattice), the function is determined by only one value, thus, severely curtailing its fuzziness. Third, when the zero element of the valuation lattice is not a prime element (and this happens in many important lattices), even the characteristic function of a prime ideal fails to be a prime fuzzy ideal. The technique adopted for the fuzzification by Zhan and Dudek in [7] and by others in [1–3, 5] is identical. Therefore, their prime fuzzy ideals inherit the same drawbacks. In [6] we have redefined prime fuzzy left h-ideal so that these deficiencies are completely removed. (It should be thankfully mentioned that one of the referees of the present paper has pointed out that in [4] two similar definitions of prime fuzzy ideal are stated. However, while proving major results of the paper, only 2-valued prime fuzzy ideals are used.) In this paper, we show that the problem of fuzzification of left ideal, left k-ideal, and left h-ideal need not be tackled separately. One single condition governs all the three. We also "refine" our definitions so that they look more compact, elegant, and easy for application. We prove that every proper fuzzy ideal (resp., k-ideal, h-ideal) is contained in a prime fuzzy ideal (resp., k-ideal, h-ideal). We introduce the concepts of fuzzy prime radical (or to be more precise, prime radical of a fuzzy ideal) and fuzzy nil radical (or nil radical of a fuzzy ideal), and fuzzy primary ideal. The prime and the nil radicals of a fuzzy k-ideal coincide when the valuation lattice is linearly ordered (e.g., when it is $[0, 1]$). An analogous result holds for fuzzy h-ideals. We establish a correspondence between fuzzy ideals (resp., k-ideals, h-ideals) of a hemiring and those of its homomorphic image. The correspondence preserves prime, semiprime, and primary fuzzy ideals/k-ideals/h-ideals. Fuzzifications introduced in this paper can be labeled as "proper fuzzifications".

2. Preliminaries

2.1. Ideals of a Semiring. In the following discussion, $(S, +, \cdot)$ stands for a semiring. That is, $(S, +)$ is a commutative monoid having identity element 0 and $(S, \cdot)$ is a semigroup satisfying the following identities: $a(b + c) = ab + ac$, $(a + b)c = ac + bc$, and $0 \cdot x = 0 = x \cdot 0$. A commutative semiring with unity is a semiring $(S, +, \cdot)$ such that $(S, \cdot)$ is

a commutative monoid. We denote the identity element of $(S, \cdot)$ by 1. With abuse of notation, we denote $(S, +, \cdot)$ by S. A left ideal A of S is a nonempty set A which is closed under the addition of S and is such that, for all $x \in S$ and $a \in A$ we have $xa \in A$. A left ideal A of S is called a left k-ideal, if for all $x \in S$, $x + a \in A$, and $a \in A \Rightarrow x \in A$. It is called a left h-ideal, if for all $x, z \in S$, $x + a + z = b + z$, and $a, b \in A \Rightarrow x \in A$. A right ideal (resp., k-ideal, h-ideal) is similarly defined. Whenever a statement is made about left ideals, it is to be understood that the analogous statement is made about right ideals. An ideal is one, which is both right and left ideal. A left ideal P is called prime left ideal, if it satisfies the following conditions:

(i) $P \neq S$ and

(ii) for all left ideals A & B of S, we have

$$AB \subseteq P \Longrightarrow \text{either } A \subseteq P \text{ or } B \subseteq P. \tag{I}$$

It is natural to call P a k-prime (resp., h-prime) left ideal, if the condition (I) holds for left k-ideals (resp., h-ideals) A and B.

Clearly, every prime left ideal is k-prime and every k-prime left ideal is h-prime. However, as will be seen in Example 1, the reverse implications, in general, are not true.

Example 1. (a) If $S = \{0, \alpha, \beta, 1\}$ is the Boolean lattice of four elements, then 0 is not a k-prime ideal, as the condition (I) fails for k-ideals $A = \{0, \alpha\}$ and $B = \{0, \beta\}$. However, S being the only h-ideal of S, 0 is h-prime. Clearly, 0 is neither prime nor an h-ideal.

(b) Consider the semiring $S = \{0, 1, 2, 3\}$, where the binary operations $\oplus$ and $\otimes$ are defined as follows: $a \oplus b = \text{Min}\{a + b, 3\}$ and $a \otimes b = \text{Min}\{ab, 3\}$. One can easily see that S has only three proper ideals, namely, 0, $A = \{0, 2, 3\}$, and $B = \{0, 3\}$. Since we have $AA \subseteq B$ and $A \not\subseteq B$, B is not a prime ideal. However, 0 and S being the only k-ideals of S, one can see that B is a k-prime ideal. Again, B is neither prime nor a k-ideal.

We shall soon see that the concepts of primeness and k-primeness (resp., h-primeness) coincide for k-ideals (resp., h-ideals).

Proposition 2 (see [5, 7]). *If S is a semiring and A and B are left ideals of S, then $k(AB) = k(k(A)k(B))$ and $h(AB) = h(h(A)h(B))$, where $k(A)$ and $h(A)$, respectively, denote k-closure and h-closure of A.*

Using Proposition 2 we get the following.

Theorem 3. *Let P be a proper left k-ideal (resp., h-ideal) of a semiring S. The following statements are equivalent.*

(a) *P is prime.*

(b) *P is k-prime (resp., h-prime).*

(c) *For all $a, b \in S$, $aSb \subseteq P$ implies $a \in P$ or $b \in P$.*

Proof. We prove the statement: "(b) implies (c)", for h-ideals.

Suppose P is a proper h-prime left h-ideal such that $aSb \subseteq P$ for $a, b \in S$. Clearly, we have $SaSb \subseteq P$. Our first claim is that for $A = h(Sa)$ and $B = h(Sb)$, where $h(I)$ stands for the h-closure of a left ideal I of S, we have $AB \subseteq P$. Suppose we have $x \in A$ and $y \in B$. Then for some s, t, u, v, z, z', in S, we have $x + sa + z = ta + z$ and $y + ub + z' = vb + z'$ and, therefore, the equalities: $ay + aub + az' = avb + az'$, and $xy + say + zy = tay + zy$. As aub and avb are elements of P and P is an h-ideal, ay is in P. Therefore, say, tay and consequently, xy are in P. It, then, follows that $AB \subseteq P$ and, P being h-prime, we have either $A \subseteq P$ or $B \subseteq P$. Suppose $A \subseteq P$. If $\langle a \rangle$ is the left ideal generated by a, then we have $\langle a \rangle \langle a \rangle \subseteq Sa$ and hence, $h(\langle a \rangle) h(\langle a \rangle) \subseteq h(h(\langle a \rangle) h(\langle a \rangle)) = h(\langle a \rangle \langle a \rangle) \subseteq h(Sa) = A \subseteq P$. Since P is h-prime, we have $h(\langle a \rangle) \subseteq P$ and consequently, $a \in P$. □

Using Zorn's Lemma one can prove the following.

Theorem 4. *Every proper ideal (resp., k-ideal, h-ideal) of a commutative hemiring S with unity is contained in a prime ideal (resp., k-ideal, h-ideal) of S.*

Theorem 5. *If T is a multiplicatively closed set in a commutative hemiring S with unity, disjoint from an ideal (resp., k-ideal, h-ideal) I of S, then there exists a prime ideal (resp., k-ideal, h-ideal) P of S such that $I \subseteq P$ and $P \cap T = \emptyset$.*

2.2. Prime Ideals of $\mathbf{N}$. In the hemiring $\mathbf{N}$ of nonnegative integers, obviously, an ideal $\mathbf{I}$ is a k-ideal if and only if it is an h-ideal. Moreover, $\mathbf{I}$ is a k-ideal if and only if $\mathbf{I} = n\mathbf{N}$ for some $n \in \mathbf{N}$. The prime k-ideals of $\mathbf{N}$ are either $p\mathbf{N}$ where p is a prime number in $\mathbf{N}$ or the zero ideal. For each prime p the ideal $p\mathbf{N}$ is a maximal k-ideal [19]. Clearly, $p\mathbf{N}$ is not a maximal ideal of $\mathbf{N}$.

Proposition 6. *Let p be a prime integer in $\mathbf{N}$ and $\mathbf{P} = \mathbf{N} \sim \{1\}$. There is no prime ideal $\mathbf{I}$ of $\mathbf{N}$ such that $p\mathbf{N} \subset \mathbf{I} \subset \mathbf{P}$.*

Proof. We first prove that the proposition holds for $p = 2$. Assuming the contrary, let $\mathbf{I}$ be a prime ideal such that $2\mathbf{N} \subset \mathbf{I} \subset \mathbf{P}$. Let x be the smallest element of $\mathbf{I} \sim 2\mathbf{N}$. Then $x = 2n + 1$ for some positive integer n. Let $\mathbf{J} = \{z \in \mathbf{N} \mid z \geq 2n\} \cup \{0\}$. Since $2, 2n$ and $2n + 1$ are in $\mathbf{I}$ and $\mathbf{I}$ is closed under addition, we have $\mathbf{J} \subset \mathbf{I}$. Clearly, if $n = 1$, then $\mathbf{J} = \mathbf{P}$. Therefore, we have $n \neq 1$ and $x \geq 5$. Consider $y = 3$. For sufficiently large value of s, we have y^s is in $\mathbf{J}$ and hence, in $\mathbf{I}$. Since $\mathbf{I}$ is a prime ideal, we have $y \in \mathbf{I}$. This contradicts the assumption that x is the smallest element of $\mathbf{I} \sim 2\mathbf{N}$. Therefore, $\mathbf{I}$ is not a prime ideal.

Consider a prime integer $p \geq 3$ and a prime ideal $\mathbf{I}$ such that $p\mathbf{N} \subset \mathbf{I} \subset \mathbf{P}$. Let x be the smallest element of $\mathbf{I} \sim p\mathbf{N}$. Then, $x = pn + r$ for some $n \in \mathbf{N}$ and $r = 1, 2, \ldots, p - 1$. Consider $x = pn + 1$. Clearly, $n \neq 0$ and thus, we have $x \geq 4$. Let $\mathbf{J} = \{z \in \mathbf{N} \mid z \geq (p - 1)pn\} \cup \{0\}$. Observe that for all $r = 1, 2, \ldots, p - 1$ we have $(p - 1)pn + r = (p - (r + 1))pn + r(pn + 1)$. Therefore $(p - 1)pn + r \in I$. However, $\mathbf{I}$ contains $p\mathbf{N}$ and therefore, $\mathbf{J}$. Now set $y = 2$. Since we assume $\mathbf{I}$ to be a prime ideal, we get $y \in \mathbf{I} \sim p\mathbf{N}$. This contradicts the choice of x as the smallest element in $\mathbf{I} \sim p\mathbf{N}$. Therefore, $x \neq pn + 1$. Consider $x = pn + r$ for $1 < r \leq p - 1$. Then, clearly, we have

$x \geq 2$. We claim that $x \neq 2$. If $x = 2$, then $2\mathbf{N} \subseteq \mathbf{I}$. Obviously, we have $2\mathbf{N} \not\subset \mathbf{I}$. On the other hand, if $2\mathbf{N} = \mathbf{I}$, then, we get the absurd result that $p\mathbf{N} \subseteq 2\mathbf{N}$ for $p \neq 2$. Now set, as before, $y = 2$ to get the contradiction to the assumption that x is the smallest element of $\mathbf{I} \sim p\mathbf{N}$ and complete the proof. □

Theorem 7. $\mathbf{P} = \mathbf{N} \sim \{1\}$ *is the only prime ideal of* $\mathbf{N}$ *which is not a k- ideal (resp., an h-ideal).*

Proof. One easily observes that $\mathbf{P}$ is a prime ideal and is not a k-deal. Let $\mathbf{I}$ be any other ideal of $\mathbf{N}$, which is not a k-ideal. Clearly, then, we have $0 \subset \mathbf{I} \subset \mathbf{P}$. Therefore, there exist $x \in \mathbf{I}$ such that $0 \neq x \neq 1$. Let $x = p_1^{\alpha 1}, \ldots, p_n^{\alpha n}$ be the prime factorization of x. If $\mathbf{I}$ is prime, there is at least one prime integer p in $\mathbf{I}$. Therefore, we have $p\mathbf{N} \subseteq \mathbf{I} \subset \mathbf{P}$. As $\mathbf{I}$ is not a k-ideal we have $p\mathbf{N} \neq \mathbf{I}$. On the other hand, by Proposition 6 we cannot have a prime ideal $\mathbf{I}$ such that $p\mathbf{N} \subset \mathbf{I} \subset \mathbf{P}$. Therefore, $\mathbf{I}$ is not a prime ideal. □

2.3. Fuzzy Ideals of a Semiring. Throughout this paper L stands for a complete Heyting algebra, that is, a complete lattice such that for all subsets T of L and all $b \in L$, $\vee\{a \wedge b \mid a \in T\} = (\vee\{a \mid a \in T\}) \wedge b$ and $\wedge\{a \vee b \mid a \in T\} = (\wedge\{a \mid a \in T\}) \vee b$. An L-fuzzy subset (or simply an L-fuzzy set) A of a set X is a function $A : X \to L$; a fuzzy set is an L-fuzzy set when L is the unit interval $[0, 1]$. If $\alpha \in L$, then the set $\{x \in X \mid A(x) \geq \alpha\}$ is called α-level cut or in short α-cut of A and is denoted by A_α. The strict α-level cut of A is the set $A_{\alpha+} = \{x \in X \mid A(x) > \alpha\}$. An L-fuzzy left ideal J of S is an L-fuzzy set $J : S \to L$ such that for all $a, b \in S$ the following conditions are satisfied: (i) $J(a+b) \geq J(a) \wedge J(b)$, (ii)$J(ab) \geq J(b)$. An L-fuzzy left ideal J of S is called an L-fuzzy left k-ideal, if the following condition is satisfied: $x + a = b \Rightarrow J(x) \geq J(a) \wedge J(b)$ for all $x, a, b, \in S$. It is an L-fuzzy left h-ideal, if $x + a + z = b + z \Rightarrow J(x) \geq J(a) \wedge J(b)$ for all $x, a, b, z \in S$. An L-fuzzy right ideal (resp., k-ideal, h-ideal) is similarly defined. Whenever a statement is made about L-fuzzy left ideals, it is to be understood that the analogous statement is made about an L-fuzzy right ideals. An L-fuzzy ideal is one, which is both L-fuzzy right and L-fuzzy left ideal.

3. Prime Fuzzy Ideals

We defined L-fuzzy prime h-ideal in [6]. We extend the definition to L-fuzzy ideals and k-ideals.

Definition 8. An L-fuzzy left ideal (resp., k-ideal, h-ideal) P of S is called a prime L-fuzzy left ideal (resp., k-ideal, h-ideal), if it is nonconstant and, for all $a, b \in S$ and $\alpha \in L$, the following condition is satisfied:

$$P(asb) \geq \alpha, \quad \forall s \in S \Longrightarrow P(a) \geq \alpha \text{ or } P(b) \geq \alpha. \tag{1}$$

Proposition 9. *A nonconstant L-fuzzy left ideal (resp., k-ideal, h-ideal) P of S is prime if and only if its every nonempty level cut of P is either a prime left ideal (resp., k-ideal, h-ideal) of S or S itself.*

Corollary 10. *A left ideal (resp., k-ideal, h-ideal)* $\mathbf{P}$ *of S is prime if and only if its characteristic function* χ_P *is an L-fuzzy prime left ideal (resp., k-ideal, h-ideal) for every complete Heyting algebra L.*

Proposition 9 is proved for L-fuzzy left h-ideal in [6].

Let P be an L-fuzzy prime (two sided) ideal of S. Then $P(asb) \geq P(a) \vee P(b)$ for all $s \in S$ and, therefore, $\wedge\{P(asb) \mid s \in S\} \geq P(a) \vee P(b)$. On the other hand, for $\wedge\{P(asb) \mid s \in S\} = \alpha$, we have:

$$\begin{aligned} &P(asb) \geq \alpha, \quad \forall s \in S \Longrightarrow P(a) \geq \alpha \text{ or } P(b) \geq \alpha \\ &\Longrightarrow P(a) \vee P(b) \geq \alpha = \wedge\{P(asb) \mid s \in S\}. \end{aligned} \tag{2}$$

Therefore, $\wedge\{P(asb) \mid s \in S\} = P(a) \vee P(b)$.

Let, further, $P(a) \geq \alpha$. Then, $P(a) \geq \alpha = \wedge\{P(asb) \mid s \in S\} \geq \{P(a) \vee P(b)\} \geq P(b)$.

Thus, $P(S)$ is totally ordered.

Conversely, let $P(S)$ be totally ordered and $\wedge\{P(asb) \mid s \in S\} = P(a) \vee P(b)$. Then,

$$\begin{aligned} &P(asb) \geq \alpha, \quad \forall s \in S \Longrightarrow P(a) \vee P(b) = \wedge\{P(asb) \mid s \in S\} \\ &\geq \alpha \Longrightarrow P(a) \geq \alpha \text{ or } P(b) \geq \alpha. \end{aligned} \tag{3}$$

Therefore, P is a prime L-fuzzy ideal.

This leads to the following elegant characterizations of prime fuzzy ideals.

Proposition 11. *Let P be a nonconstant L-fuzzy ideal (resp., k- ideal, h- ideal) of S, and* $a, b \in S$.

(1) *P is prime if and only if* $\wedge\{P(asb) \mid s \in S\} = P(a) \vee P(b)$ *and* $P(S)$ *is totally ordered.*

(2) *Let S be commutative hemiring with unity. P is prime if and only if* $P(ab) = P(a) \vee P(b)$ *and* $P(S)$ *is totally ordered.*

(3) *A nonconstant fuzzy ideal (resp., k- ideal, h- ideal) P is prime if and only if* $\text{Inf}\{P(asb) \mid s \in S\} = \text{Max}\{P(a), P(b)\}$.

(4) *Let S be commutative hemiring with unity. A nonconstant fuzzy ideal (resp., k- ideal, h- ideal) P is prime if and only if* $P(ab) = \text{Max}\{P(a), P(b)\}$.

The following example shows that the condition that $P(S)$ is totally ordered is necessary for P to be prime.

Example 12. Let $L = \{0, \alpha, \beta, 1\}$ be the Boolean algebra of four elements. Consider the L-fuzzy ideal $J : \mathbf{N} \to L$ defined as follows:

$$\begin{aligned} J(x) &= 1 \quad \text{if } x \in 6\mathbf{N}, \\ &= \alpha \quad \text{if } x \in 2\mathbf{N} \sim 6\mathbf{N}, \\ &= \beta \quad \text{if } x \in 3\mathbf{N} \sim 6\mathbf{N}, \\ &= 0 \quad \text{everywhere else.} \end{aligned} \tag{4}$$

Clearly, the L-fuzzy h-ideal J is not prime, though $P(ab) = P(a) \vee P(b)$ holds for all $a, b \in \mathbf{N}$.

Remark 13. While fuzzifying the condition (I) of "primeness" stated in §2.1 three types of products of fuzzy left ideals A and B of S, are used in the literature: namely, AoB, Ao_kB, and Ao_hB [1–3, 5, 7]. They are defined as follows:

$$\begin{aligned} AoB(x) &= \operatorname{Sup}\{\operatorname{Min}\{A(a), B(b)\} \mid x = ab,\ a, b \in S\}, \\ Ao_kB(x) &= \operatorname{Sup}\{\operatorname{Min}\{A(a), B(b), A(a'), B(b')\} \mid x + ab \\ &\qquad = a'b';\ a, b, a', b' \in S\}, \\ Ao_hB(x) &= \operatorname{Sup}\{\operatorname{Min}\{A(a), B(b), A(a'), B(b')\} \mid x + ab + z \\ &\qquad = a'b' + z;\ a, b, a', b', z \in S\}, \quad \forall x \in S. \end{aligned} \tag{5}$$

This was needed, because the problem of fuzzification of left ideals, left k-ideals, and left h-ideals were treated as three separate problems. Theorem 3 allows us to rope all the three in one and leads us to a compact characterization of primeness given in Proposition 11.

A semiprime fuzzy ideal, now defines itself.

Definition 14. An L-fuzzy left h-ideal J of S is called semiprime, if J is nonconstant and, for all $a \in S$ and $\alpha \in L$, the following condition is satisfied:

$$J(asa) \geq \alpha, \quad \forall s \in S \Longrightarrow J(a) \geq \alpha. \tag{6}$$

It follows that a nonconstant L-fuzzy ideal (resp., k-ideal, h-ideal) I of S is semiprime if and only if $\wedge\{I(asa) \mid s \in S\} = I(a)$ for all $s \in S$. In case S is commutative hemiring with unity, the above equation is further simplified to $I(a^2) = I(a)$. Analogues of Proposition 9 and Corollary 10 can easily be proved.

Theorem 15. *Every nonconstant fuzzy ideal (resp., k-ideal, h-ideal) of a commutative ring with unity is contained in a minimal prime fuzzy ideal (resp., k-ideal, h-ideal).*

Proof. As usual we prove the result for fuzzy h-ideals. Let J be a nonconstant fuzzy h-ideal of a commutative ring S with unity and $\mathbf{J} = \{x \in S \mid J(x) > J(1)\}$. Let $\mathbf{P}$ be a prime h-ideal containing $\mathbf{J}$. Define a fuzzy ideal $P : S \to [0, 1]$ by

$$\begin{aligned} P(x) &= 1 \quad \text{if } x \in \mathbf{P} \\ &= J(1) \quad \text{if } x \notin \mathbf{P}. \end{aligned} \tag{7}$$

Clearly, P is a prime fuzzy h-ideal containing J and, thus, the class C of all prime fuzzy h-ideals containing J is nonempty. We partially order C by reverse containment, that is, we define $P \leq P'$ if and only if $P' \subseteq P$ for all $P, P' \in C$, and consider a totally ordered subset $\{P^\lambda \mid \lambda \in \Lambda\}$ of C. Then, the set $\{P^\lambda_\alpha \mid \lambda \in \Lambda\}$ of the α-level cuts of P^λ is a totally ordered set consisting of prime h-ideals (and possibly of S) for each $\alpha \in [0, 1]$. Therefore, $\cap\{P^\lambda_\alpha \mid \lambda \in \Lambda\}$ is either a prime h-ideal of S or S itself. By Proposition 9, $\cap\{P^\lambda \mid \lambda \in \Lambda\}$ is a prime fuzzy h-ideal containing J. Since $\cap\{P^\lambda \mid \lambda \in \Lambda\}$ is an upper bound of the family $\{P^\lambda \mid \lambda \in L\}$, C has a maximal element which, clearly, is a minimal prime fuzzy h-ideal containing J. □

Remark 16. Example 12 will testify that Theorem 15 is not valid when $L \neq [0, 1]$, in general.

4. Prime Radicals of a Fuzzy Ideal

In this section, we assume S to be a commutative hemiring with unity.

Definition 17. If J is an L-fuzzy ideal of S, then the intersection of all prime L-fuzzy ideals (resp., k-ideals, h-ideals) of S containing J is called the *prime* (resp., *k-prime*, *h-prime*) *radical* of J. We denote it by $r(J)$ (resp., $r_k(J)$, $r_h(J)$). If the set of prime L-fuzzy ideals (resp., k-ideals, h-ideals) of S containing J is empty, we define $r(J)$ (resp., $r_k(J)$, $r_h(J)$) to be χ_S.

Note that $r(J)$, (resp., $r_k(J)$, $r_h(J)$) is a semiprime fuzzy ideal (resp., k-ideal, h-ideal) containing J. Clearly $r(J) \subseteq r_h(J) \subseteq r_k(J)$. However, the following examples show that strict containment holds.

Example 18. Let p be a prime integer. Consider $\alpha, \beta \in [0, 1]$ and $\beta < \alpha$. Define a fuzzy set $P : \mathbf{N} \to [0, 1]$ by

$$\begin{aligned} P(x) &= 1 \quad \text{if } x = 0, \\ &= \alpha \quad \text{if } x \in p\mathbf{N} \sim \{0\}, \\ &= \beta \quad \text{if } x \notin p\mathbf{N}. \end{aligned} \tag{8}$$

By Proposition 9, P is a prime fuzzy ideal (also k-ideal and h-ideal), for all $0 \leq \beta < \alpha \leq 1$. We will call the fuzzy ideal P a prime fuzzy k-ideal induced by the prime number p and denote it by $(p\mathbf{N})^{\alpha\beta}$.

Example 19. Suppose $\alpha, \beta, \gamma \in [0, 1]$ and $\gamma < \beta < \alpha$. Define a fuzzy set $Q : \mathbf{N} \to [0, 1]$ by

$$\begin{aligned} Q(x) &= 1 \quad \text{if } x = 0, \\ &= \alpha \quad \text{if } x \in p\mathbf{N} \sim \{0\}, \\ &= \beta \quad \text{if } x \in \mathbf{N} \sim (p\mathbf{N} \cup \{1\}), \\ &= \gamma \quad \text{if } x = 1. \end{aligned} \tag{9}$$

By Proposition 9, Q is a prime fuzzy ideal which is neither a fuzzy k-ideal nor a fuzzy h-ideal, for all $0 \leq \gamma < \beta < \alpha \leq 1$. We will call the fuzzy ideal Q a prime fuzzy ideal induced by the prime integer p and denote it by $(p\mathbf{N})^{\alpha\beta\gamma}$. Note that, in the light of Theorem 7, these are the only prime fuzzy ideals of $\mathbf{N}$ which are not fuzzy k-ideals.

Example 20. Consider a fuzzy ideal defined by $J : \mathbf{N} \to [0, 1]$:

$$\begin{aligned} J(x) &= 1 \quad \text{if } x = 0, \\ &= 0.5 \quad \text{if } x \geq 3, \\ &= 0 \quad \text{if } x = 1 \text{ or } 2. \end{aligned} \tag{10}$$

Let $0 \le \alpha < 1$ and O^α be the fuzzy k-ideal defined by $O^\alpha : \mathbf{N} \to [0,1]$:

$$\begin{aligned} O^\alpha(x) &= 1 \quad \text{if } x = 0, \\ &= \alpha \quad \text{if } x \neq 0. \end{aligned} \tag{11}$$

Let $X = \{O^\alpha \mid 0.5 \le \alpha < 1\} \cup \{(p\mathbf{N})^{\alpha\beta} \mid p \text{ is prime}, 0.5 \le \beta < \alpha \le 1\}$ and $Y = \{(p\mathbf{N})^{\alpha\beta\gamma} \mid 0 \le \gamma \le 0.5 < \beta \le \alpha \le 1, p \text{ is prime}\}$. Clearly, X is the set of all prime fuzzy k-ideals of $\mathbf{N}$ containing J and Y is the set of all those prime fuzzy ideals containing J, which are not fuzzy k-ideals. Since $r_h(J) = r_k(J) = \cap\{P \mid P \in X\}$ and $r(J) = \cap\{P \mid P \in X \cup Y\}$, it is mundane to verify that $r_h(J) = r_k(J) = O^{0.5}$ and $r(J)$ is the fuzzy ideal defined by $r(J) : \mathbf{N} \to [0,1]$:

$$\begin{aligned} &r(J)(x) = 1 \quad \text{if } x = 0, \\ &r(J)(x) = 0.5 \quad \text{for } x \ge 2, \\ &r(J)(x) = 0 \quad \text{if } x = 1. \end{aligned} \tag{12}$$

Clearly, $r(J) \subset r_k(J) = r_h(J)$.

Example 21. Let $S = \{0, \alpha, \beta, 1\}$ be the Boolean algebra of four elements. Consider the prime fuzzy ideal defined by $J : S \to [0,1]$ $J(0) = 1 = J(\alpha)$ and $J(\beta) = J(1) = 0.5$. Then, J being a prime fuzzy k-ideal $r_k(J) = J$. Since all the fuzzy ideals of S are fuzzy k-ideals, we have $r(J) = r_k(J)$. Since the set of fuzzy h-ideals of S is empty, $r_h(J) = \chi_S$.

Clearly, $r(J) = r_k(J) \subset r_h(J)$.

5. Nil Radicals of a Fuzzy Ideal

In this section, we assume S to be a commutative hemiring with unity.

Recall that if I is an ideal of S, then its radical (also called nil radical) is defined as $\sqrt{I} = \{x \in S \mid x^n \in I, \text{ for some integer } n > 0\}$.

We define the fuzzy analogue of nil radical as follows.

Definition 22. If J is an L-fuzzy ideal of S, then the L-fuzzy set $\sqrt{J} : S \to L$ defined by $\sqrt{J}(x) = \vee\{J(x^n) \mid n > 0\}$ is called the *L-fuzzy (nil) radical* of J.

Through series of propositions we prove that, when L is totally ordered and J is a fuzzy k-ideal (resp., h-ideal) of S, so is $\sqrt{J}$.

The following results are the direct consequences of Definition 22.

Proposition 23. *If I is an ideal of S, then $\sqrt{(\chi_I)} = \chi_{\sqrt{I}}$, where χ_I and $\chi_{\sqrt{I}}$ are the characteristic functions of I and $\sqrt{I}$, respectively.*

Proposition 24. *If P is a prime L-fuzzy ideal, then $\sqrt{P} = P$.*

Proposition 25. *If J and K are L-fuzzy ideals of a hemiring, then, the following statements hold.*

(a) $\sqrt{(\sqrt{J})} = \sqrt{J}$.

(b) *If $J \subseteq K$, then $\sqrt{J} \subseteq \sqrt{K}$.*

(c) $\sqrt{(J \cap K)} = \sqrt{J} \cap \sqrt{K}$.

Proposition 26. *Let J be an L- fuzzy ideals of S and $0 \le \alpha < 1$. Then, the following statements hold.*

(i) $\sqrt{(J_\alpha)} \subseteq (\sqrt{J})_\alpha$.

(ii) *If L is a totally-ordered set, then $(\sqrt{J})_{\alpha+} = \sqrt{(J_{\alpha+})}$, where $J_{\alpha+}$ and $(\sqrt{J})_{\alpha+}$ are strict level cuts.*

Proof. We prove only (ii):

$$\begin{aligned} x \in (\sqrt{J})_{\alpha+} &\iff \sqrt{J}(x) > \alpha \\ &\iff \vee\{J(x^n) \mid n > 0\} > \alpha \\ &\iff J(x^n) > \alpha \quad \text{for some } n > 0 \\ &\iff x^n \in J_{\alpha+} \quad \text{for some } n > 0 \\ &\iff x \in \sqrt{(J_{\alpha+})}. \end{aligned} \tag{13}$$

□

The following example shows that the set inclusion in Proposition 26(i) can be strict.

Example 27. Let $\mathbf{N}$ be the hemiring of non-negative integers, $L = [0,1]$, and $p \in \mathbf{N}$ a prime number. Let $\langle p^n \rangle$ denote the ideal of $\mathbf{N}$ generated by p^n.

Define a fuzzy ideal as follows:

$$\begin{aligned} &J : \mathbf{N} \longrightarrow L \\ &J(x) = 0, \quad \text{if } x \notin \langle p \rangle, \\ &J(x) = \frac{n}{n+1}, \quad \text{if } x \in \langle p^n \rangle \sim \langle p^{n+1} \rangle,\ n = 1, 2, \ldots \\ &J(0) = 1. \end{aligned} \tag{14}$$

Since $\sqrt{J}(p) = \sup\{n/(n+1) \mid n = 1, \ldots\} = 1$, we have $p \in (\sqrt{J})_1$. On the other hand, for each n, $J(p^n) = (n/(n+1)) < 1$ and thus, $p^n \notin J_1$, for any n. Consequently, we have $p \notin \sqrt{J_1}$.

Theorem 28. *If L is totally ordered and J an L-fuzzy k-ideal (resp., h-ideal) of S, then $\sqrt{J}$ coincides with $r_k(J)$ (resp., $r_h(J)$).*

Proof. As usual we restrict our discussion to h-ideals**.** If P is an L-fuzzy prime h-ideal containing J, then, by Proposition 26, we have $(\sqrt{J})_{\alpha+} = \sqrt{(J_{\alpha+})} = r_h(J_{\alpha+})$, where $r_h(J_{\alpha+})$ is the h-prime radical of the (scrisp) ideal $J_{\alpha+}$. On the other hand, for any $x \in S$ and $n > 0$, we have $J(x^n) \le P(x^n) = P(x)$ and therefore, we have $\sqrt{J} \subseteq r_h(J)$.

Suppose $\sqrt{J} \neq r_h(J)$. Then, there exists $a \in S$, such that $(\sqrt{J})(a) < r_h(J)(a)$. Let $(\sqrt{J})(a) = \alpha$. Since $a \notin r_h(J_{\alpha+})$, there exists a prime h-ideal say $\mathbf{P}$ such that $J_{\alpha+} \subseteq \mathbf{P}$ and $a \notin \mathbf{P}$.

Consider the following prime L-fuzzy h-ideal:

$$\begin{aligned} &P : S \longrightarrow L \\ &P(x) = 1, \quad \text{if } x \in \mathbf{P}, \\ &\quad = \alpha, \quad \text{if } x \notin \mathbf{P}. \end{aligned} \tag{15}$$

Clearly, if $x \in \mathbf{P}$, then we have $J(x) \leq P(x)$. On the other hand, if $x \notin \mathbf{P}$, then we have $x \notin J_{\alpha+}$ and $J(x) \leq \alpha = P(x)$. Thus, we get $J \subseteq P$ and consequently, $r_h(J) \subseteq P$.

However, this leads to the following contradiction, $\sqrt{J}(a) < r_h(J)(a) \leq P(a) = \alpha = \sqrt{J}(a)$.

Hence, we have $\sqrt{J} = r_h(J)$. □

Corollary 29. *Let L be a totally ordered set. If J is an L-fuzzy k-ideal (resp., h-ideal) of S, then, so is $\sqrt{J}$.*

6. Correspondence Theorems

In this section, $f : S \to S'$ is a homomorphism of hemirings, J is an L-fuzzy left ideal of S, and J' is an L-fuzzy left ideal of S'.

In [20, Proposition 3.11], Zhan claims that if J is an L-fuzzy h-ideal with sup property, then $f(J)$ is an L-fuzzy h-ideal of $f(S)$. The following example does not substantiate the claim.

Example 30. Let S be the hemiring given in Example 1 (b), $\mathbf{N}$ be the hemiring of non-negative integers, and $f : \mathbf{N} \to S$ be the epimorphism given by $f(x) = \min\{x, 3\}$ for all $x \in \mathbf{N}$.

Define a mapping $J : \mathbf{N} \to [0, 1]$ by

$$\begin{aligned} J(x) &= 1 \quad \text{if } x = 0, \\ &= \frac{1}{2} \quad \text{if } x = 2n \neq 0, \\ &= 0 \quad \text{if } x = 2n + 1, \quad \forall n \in \mathbf{N}. \end{aligned} \tag{16}$$

Since $f(x) = x$ for all $x \leq 3$ and $f(x) = 3$ for all $x \geq 3$, it can be verified that $f(J)(0) = 1$, $f(J)(2) = f(J)(3) = 1/2$, and $f(J)(1) = 0$.

One can readily see that J is an L-fuzzy h-ideal with sup property; but $f(J)$ is not an L-fuzzy h-ideal. For, we have $1 \oplus 2 \oplus 3 = 0 \oplus 3$ and $f(J)(2) \wedge f(J)(0) \not\leq f(J)(1)$.

Example 30 raises a natural question: What are the sufficient conditions for a homomorphic image of an h-ideal (resp., k-ideal) to be an h-ideal (resp., k-ideal)? In order to answer this question, we introduce the following definition.

Definition 31. Let $f : S \to S'$ be a homomorphism of hemirings. An L-fuzzy left ideal J of S is called *f-compatible* if, for all $x, a, b, z \in S$, $f(x + a + z) = f(b + z) \Rightarrow J(x) \geq J(a) \wedge J(b)$.

Recall that J is f-invariant, if $f(a) = f(b)$ implies $J(a) = J(b)$. We leave it to the reader to prove that an f-compatible fuzzy left ideal is f-invariant.

Proposition 32. *Let $f : S \to S'$ be a homomorphism of hemirings and J and J' L-fuzzy left ideals of S and S', respectively. Then, the following statements hold.*

(1) *$f^{-1}(J')$ is an f-invariant L-fuzzy left ideal of S.*

(2) *If J' is an L-fuzzy left k-ideal, then so is $f^{-1}(J')$.*

(3) *If J' is an L-fuzzy left h-ideal, then $f^{-1}(J')$ is an f-compatible L-fuzzy left h-ideal of S.*

(4) *If J is f-invariant (in particular if J is f-compatible), then $f(J)f(x) = J(x)$ and therefore, $f^{-1}(f(J)) = J$.*

(5) *If f is an epimorphism, $f(f^{-1}(J')) = J'$.*

Proof. We prove (4) and (5). If J is f-invariant and $x \in S$, then it is obvious that $f(J)f(x) = \vee\{J(z) \mid f(z) = f(x)\} = J(x)$. This proves (4). Moreover, if $x' = f(x)$, then $f(f^{-1}(J'))(x') = f^{-1}(J')(x) = J'(f(x)) = J'(x')$. It, then, follows that if f is an epimorphism, then $f(f^{-1}(J')) = J'$. □

This leads to the following correspondence theorem for L-fuzzy left k-ideals and h-ideals.

Theorem 33. *Let $f : S \to S'$ be an epimorphism of hemirings.*

(1) *There is one-to-one correspondence between the set of L-fuzzy left ideals (resp., k-ideals) of S' and that of f-invariant L-fuzzy left ideals (resp., k-ideals) of S.*

(2) *There is one-to-one correspondence between the set of L-fuzzy left h-ideals of S' and that of f-compatible L-fuzzy left h-ideals of S.*

The above correspondence preserves prime and semiprime L-fuzzy left ideals (resp., k-ideals, h-ideals).

Proof. Suppose $J$and J' are L-fuzzy left ideals of S and S'. By Proposition 32, the correspondence is given by $J \leftrightarrow f(J)$ and $J' \leftrightarrow f^{-1}(J')$. We only need to verify that, when J is an L-fuzzy left ideal (resp., k-ideals, h-ideal), then so is $f(J)$, under the conditions specified for J. A reader may easily prove that, when J is f-invariant, $f(J)$ is an L-fuzzy left ideal. Let, moreover, J be an L-fuzzy k-ideal, $x' + a' = b'$, $f(x) = x'$, $f(a) = a'$, and $f(b) = b'$. Then $f(x + a) = f(b)$ and therefore, we have $J(x + a) = J(b)$. Let $\alpha = J(a) \wedge J(b)$ and consider J_α. Clearly, $a, b \in J_\alpha$. Since $J(x + a) = J(b)$, we have $x + a \in J_\alpha$ and J_α being a k-ideal $x \in J_\alpha$. Therefore, $J(x) \geq J(a) \wedge J(b)$. But, by Proposition 32 (4), this inequality is equivalent to $f(J)(x') \geq f(J)(a') \wedge f(J)(b')$. Thus, $f(J)$ is an L-fuzzy left k-ideal.

On similar lines, one can prove that, when J is an f-compatible L-fuzzy left h-ideal of S, $f(J)$ is an L-fuzzy left h-ideal of S'. □

7. Primary Fuzzy Ideals

In this section, we assume that S is a commutative hemiring with unity.

Recall that an ideal $\mathbf{Q}$ of a hemiring S is *primary*, if (i) $\mathbf{Q} \neq S$ and (ii) $xy \in \mathbf{Q} \Rightarrow x \in \mathbf{Q}$ or $y^n \in \mathbf{Q}$ for some positive integer n.

We define primary fuzzy ideal as follows.

Definition 34. A nonconstant L-fuzzy ideal/k-ideal/h-ideal Q of S is *primary*, if $Q(xy) = Q(x)$ or $Q(xy) \leq Q(y^n)$ for some positive integer n.

The following propositions are immediate consequences of Definition 34.

Proposition 35. *A nonconstant L-fuzzy ideal of S is a primary L-fuzzy ideal (resp., k-ideal, h-ideal) if and only if each of its nonempty level cuts is either a primary ideal (resp., k-ideal, h-ideal) of S or S itself.*

Proposition 36. *Let* $\mathbf{Q}$ *be an ideal of S. The characteristic function* $\chi_{\mathbf{Q}}$ *is a primary L-fuzzy ideal (resp., k-ideal, h-ideal) of S if and only if* $\mathbf{Q}$ *is primary ideal (resp., k-ideal, h-ideal), for every complete Heyting algebra L.*

Proposition 37. *Every prime L- fuzzy ideal (resp., k-ideal, h-ideal) is a primary L-fuzzy ideal (resp., k- ideal, h-ideal).*

The fuzzy ideal J in Example 27 is primary but not prime, as every nonempty, proper level-cut of the fuzzy ideal is primary but not prime.

The proof of the following proposition is straightforward.

Proposition 38. *Let* $f : S \to S'$ *be a homomorphism of hemirings and Q and Q′ L-fuzzy ideals of S and S′, respectively.*

(a) *If* Q' *is primary, then* $f^{-1}(Q')$ *is primary f-invariant.*

(b) *Let* f *be an epimorphism and Q be f-invariant. If Q is a primary, then* $f(Q)$ *is primary.*

(c) *If* f *is an epimorphism and Q is an f-compatible primary fuzzy h-ideal, then* $f(Q)$ *is a primary L-fuzzy h-ideal.*

Thus, the correspondence theorems in the previous section preserve primary fuzzy ideals as well.

8. Minimum Imperative for Fuzzification

In this paper, we fuzzified the concepts of prime ideal, semiprime ideal, and primary ideal of a hemiring. Some of these concepts have been fuzzified earlier in different ways. Therefore, it is pertinent to ask: What constitutes "proper fuzzification" of a concept? Our answer is the following:

Suppose I is a (crisp) ideal with property p of a hemiring S and $\widetilde{I}$ is its fuzzification which inherits property $\widetilde{p}$. If it is the best fuzzification, it should satisfy the following properties.

(1) For every Heyting algebras L, the characteristic function of I satisfies the property $\widetilde{p}$ if and only if I has property p.

(2) $\widetilde{I}$ satisfies the property $\widetilde{p}$, whenever every nonempty levelcut of $\widetilde{I}$ different from S satisfies the property p and conversely.

(3) The set $\widetilde{I}(S)$ has more than two elements.
Let $f : S \to S'$ be a homomorphism of hemirings.

(4) If an L-fuzzy ideal J' of S' has property $\widetilde{p}$, then $f^{-1}(J')$, as an L-fuzzy ideal of S, has property $\widetilde{p}$.

(5) If L-fuzzy ideal J of S has property $\widetilde{p}$, then $f(J)$ is an L-fuzzy ideal of $f(S)$ with property $\widetilde{p}$, under some preassigned condition(s). The condition(s) is (are) suggested by the corresponding crisp situation.

The last sentence needs some elaboration. If $\mathbf{I}$ is a (crisp) ideal of S, $f(\mathbf{I})$ is an ideal of $f(S)$ provided that it satisfies the condition: $f(x) = f(y)$ and $y \in \mathbf{I}$ implies $x \in \mathbf{I}$. The f-invariance of J stated above is a "fuzzification" of the condition on the crisp ideal $\mathbf{I}$. If $\mathbf{I}$ is an h-ideal, then $f(\mathbf{I})$ is an h-ideal of $f(S)$ provided that it satisfies the condition: $f(x + a + z) = f(b + z)$ and $a, b \in \mathbf{I}$ implies $x \in \mathbf{I}$. The f-compatibility is a "fuzzification" of the condition on the ideal $\mathbf{I}$.

As proved earlier, the different types of prime, semiprime, and primary L-fuzzy ideals defined in this paper fulfill the above five conditions and, therefore, they are the best fuzzifications of the concepts.

Acknowledgments

The author expresses his deep sense of gratitude to the Editorial Board in general, and Editor-in-Chief in particular, of the journal "Advances in Fuzzy Systems". This paper may not have come out in the present form, if the author has not been invited by them to write it within a specified time limit. He is also grateful to the referees for their useful suggestions.

References

[1] J. Ahsan, K. Saifullah, and M. F. Khan, "Fuzzy semirings," *Fuzzy Sets and Systems*, vol. 60, no. 3, pp. 309–320, 1993.

[2] T. K. Datta and B. K. Biswas, "Fuzzy k-ideals of semirings," *Bulletin of Calcutta Mathematical Society*, vol. 87, pp. 91–96, 1995.

[3] P. Dheena and S. Coumaressane, "Fuzzy 2-(0- or 1-)prime ideals in semirings," *Bulletin of the Korean Mathematical Society*, vol. 43, no. 3, pp. 559–573, 2006.

[4] W. A. Dudek, M. Shabir, and R. Anjum, "Characterizations of hemirings by their h-ideals," *Computers and Mathematics with Applications*, vol. 59, no. 9, pp. 3167–3179, 2010.

[5] S. Ghosh, "Fuzzy k-ideals of semirings," *Fuzzy Sets and Systems*, vol. 95, no. 1, pp. 103–108, 1998.

[6] H. V. Kumbhojkar, "Spectrum of prime L-fuzzy h-ideals of a hemiring," *Fuzzy Sets and Systems*, vol. 161, no. 12, pp. 1740–1749, 2010.

[7] J. Zhan and W. A. Dudek, "Fuzzy h-ideals of hemirings," *Information Sciences*, vol. 177, no. 3, pp. 876–886, 2007.

[8] H. V. Kumbhojkar and M. S. Bapat, "Correspondence theorem for fuzzy ideals," *Fuzzy Sets and Systems*, vol. 41, no. 2, pp. 213–219, 1991.

[9] H. V. Kumbhojkar and M. S. Bapat, "On prime and primary fuzzy ideals and their radicals," *Fuzzy Sets and Systems*, vol. 53, no. 2, pp. 203–216, 1993.

[10] H. V. Kumbhojkar and M. S. Bapat, "On semiprime fuzzy ideals," *Fuzzy Sets and Systems*, vol. 60, no. 2, pp. 219–223, 1993.

[11] D. S. Malik and J. N. Mordeson, "Fuzzy prime ideals of a ring," *Fuzzy Sets and Systems*, vol. 37, no. 1, pp. 93–98, 1990.

[12] J. N. Mordeson, "Generating properties of fuzzy algebraic structures," *Fuzzy Sets and Systems*, vol. 55, no. 1, pp. 107–120, 1993.

[13] J. N. Mordeson and P. S. Nair, *Fuzzy Matehmatics*, Physica, Warsaw, Poland, 1998.

[14] T. K. Mukherjee and M. K. Sen, "On fuzzy ideals of a ring I," *Fuzzy Sets and Systems*, vol. 21, no. 1, pp. 99–104, 1987.

[15] U. M. Swamy and K. L. N. Swamy, "Fuzzy prime ideals of rings," *Journal of Mathematical Analysis and Applications*, vol. 134, no. 1, pp. 94–103, 1988.

[16] J. Ahsan and K. Saifullah, "Semigroups characterized by their fuzzy ideals," Tech. Rep. 147, King Fahd University of Petroleum and Minerals, Dhahran, Saudi Arabia , 1993.

[17] H.V. Kumbhojkar, "On prime fuzzy ideals of a semigroup," in *Proceedings of the 26th Annual Iranian Mathematics Conference*, pp. 193–199, 1995.

[18] N. Kuroki, "Fuzzy semiprime ideals in semigroups," *Fuzzy Sets and Systems*, vol. 8, no. 1, pp. 71–79, 1982.

[19] M. K. Sen and M. R. Adhikari, "On maximal k-ideals of semirings," *Proceedings of the American Mathematical Society*, vol. 118, pp. 699–703, 1993.

[20] J. Zhan, "On properties of fuzzy left h-ideals in hemirings with t-norms," *International Journal of Mathematics and Mathematical Sciences*, vol. 2005, no. 19, pp. 3127–3144, 2005.